

PETROLOGY AND CHEMISTRY OF SOME  
DIABASE SILLS IN CENTRAL ARIZONA

by

James Allen Fouts

---

A Dissertation Submitted to the Faculty of the

DEPARTMENT OF GEOSCIENCES

In Partial Fulfillment of the Requirements  
For the Degree of

DOCTOR OF PHILOSOPHY

In the Graduate College

THE UNIVERSITY OF ARIZONA

1 9 7 4

THE UNIVERSITY OF ARIZONA

GRADUATE COLLEGE

I hereby recommend that this dissertation prepared under my  
direction by James Allen Fouts  
entitled PETROLOGY AND CHEMISTRY OF SOME DIABASE  
SILLS IN CENTRAL ARIZONA  
be accepted as fulfilling the dissertation requirement of the  
degree of Doctor of Philosophy

*J. K. ...*  
Dissertation Director

July 29, 1974  
Date

After inspection of the final copy of the dissertation, the  
following members of the Final Examination Committee concur in  
its approval and recommend its acceptance:\*

<u><i>John W. ...</i></u>	<u>August 6, 1974</u>
<u><i>Donald C. Livingston</i></u>	<u>August 8, 1974</u>
<u><i>Donald L. Bryant</i></u>	<u>August 24, 1974</u>
<u> </u>	<u> </u>
<u> </u>	<u> </u>

\*This approval and acceptance is contingent on the candidate's adequate performance and defense of this dissertation at the final oral examination. The inclusion of this sheet bound into the library copy of the dissertation is evidence of satisfactory performance at the final examination.

STATEMENT BY AUTHOR

This dissertation has been submitted in partial fulfillment of requirements for an advanced degree at The University of Arizona and is deposited in the University Library to be made available to borrowers under rules of the Library.

Brief quotations from this dissertation are allowable without special permission, provided that accurate acknowledgment of source is made. Requests for permission for extended quotation from or reproduction of this manuscript in whole or in part may be granted by the head of the major department or the Dean of the Graduate College when in his judgment the proposed use of the material is in the interests of scholarship. In all other instances, however, permission must be obtained from the author.

SIGNED:

James A. Fouts

## ACKNOWLEDGMENTS

Dr. B. E. Nordlie first suggested the Arizona diabases as a possible dissertation topic and served as director of the study. Dr. D. E. Livingston assisted with the x-ray fluorescence analyses and permitted the use of his computer programs for data reduction. Drs. Nordlie, Livingston, J. W. Anthony, and D. L. Bryant all read the manuscript and provided constructive criticism.

The assistance of several fellow graduate students is also gratefully acknowledged. John Hoelle helped with the Rb and Sr analyses. Much of the initial work in perfecting the ferrous iron determination method was done by John Delaney and Michael Fellows.

TABLE OF CONTENTS

	Page
LIST OF TABLES . . . . .	vi
LIST OF ILLUSTRATIONS . . . . .	ix
ABSTRACT . . . . .	xi
INTRODUCTION . . . . .	1
Purpose of the Investigation . . . . .	1
Method of Investigation . . . . .	1
Previous Work . . . . .	3
AGE OF THE DIABASE . . . . .	4
DISTRIBUTION AND STRATIGRAPHIC POSITION OF DIABASE . . . . .	8
SALT RIVER CANYON COMPLEX . . . . .	12
Petrography of the Diabase . . . . .	14
Chemistry . . . . .	20
Albitite Dike . . . . .	28
Petrogenesis . . . . .	28
ROOSEVELT DAM SILL . . . . .	38
Petrography . . . . .	38
Chemistry . . . . .	41
Petrogenesis . . . . .	46
GLOBE COMPLEX . . . . .	49
Petrography . . . . .	50
Chemistry . . . . .	53
Petrogenesis . . . . .	57
LOOKOUT MOUNTAIN SILLS . . . . .	58
Petrography of the Small Sill . . . . .	60
Chemistry of the Small Sill . . . . .	62

## TABLE OF CONTENTS (Continued)

	Page
Petrography of the Large Sill . . . . .	67
Chemistry of the Large Sill . . . . .	71
Petrogenesis of the Lookout Mountain Sills . . . . .	77
Petrography and Chemistry of the Alaskite . . . . .	84
SANTA CATALINA MOUNTAINS SILL . . . . .	91
Petrography . . . . .	91
Chemistry . . . . .	92
PETROGRAPHIC TYPES IN THE DIABASE PROVINCE . . . . .	96
DIABASIC MAGMA TYPES . . . . .	98
CHEMISTRY OF THE DIABASE PROVINCE . . . . .	109
DISCUSSION OF THE TRACE ELEMENT DATA . . . . .	121
Copper . . . . .	121
Strontium . . . . .	123
Rubidium . . . . .	124
DIFFERENTIATION TRENDS . . . . .	130
GENESIS OF THE DIABASE . . . . .	135
SUMMARY AND CONCLUSIONS . . . . .	139
APPENDIX I: ANALYTICAL METHODS . . . . .	142
Atomic Absorption Analyses . . . . .	142
Ferrous Iron Analyses . . . . .	146
X-Ray Fluorescence Analyses . . . . .	150
REFERENCES . . . . .	152

LIST OF TABLES

Table	Page
1. Isotopic ages reported for diabase from south central Arizona . . . . .	6
2. Description and location of samples from the Salt River Canyon Complex . . . . .	15
3. Chemical analyses of samples from the Salt River Canyon Complex . . . . .	21
4. Trace element concentrations and elemental ratios in samples from the Salt River Canyon Complex . . . . .	22
5. Norms for samples from the Salt River Canyon Complex . . . . .	23
6. Viscosities and densities calculated from the analyses of sample SRD-5 . . . . .	33
7. Description and location of samples from the Roosevelt Dam sill . . . . .	39
8. Chemical analyses of samples from the Roosevelt Dam sill . . . . .	42
9. Trace element concentrations and elemental ratios in samples from the Roosevelt Dam sill . . . . .	43
10. Norms for samples from the Roosevelt Dam sill . . . . .	44
11. Description and location of samples from the Globe Complex . . . . .	51
12. Chemical analyses of samples from the Globe Complex . . . . .	54
13. Trace element concentrations and elemental ratios in samples from the Globe Complex . . . . .	55

## LIST OF TABLES (Continued)

Table	Page
14. Norms for samples from the Globe Complex . . . . .	56
15. Description and location of samples from the small Lookout Mountain sill . . . . .	61
16. Chemical analyses of samples from the small Lookout Mountain sill . . . . .	63
17. Trace element concentrations and elemental ratios in samples from the small Lookout Mountain sill . . . . .	64
18. Norms for samples from small Lookout Mountain sill . . . . .	65
19. Description and location of samples from the large Lookout Mountain sill . . . . .	68
20. Modal analyses of samples from the large Lookout Mountain sill . . . . .	69
21. Chemical analyses of samples from the large Lookout Mountain sill . . . . .	72
22. Trace element concentrations and elemental ratios in samples from the large Lookout Mountain sill . . . . .	73
23. Norms for samples from the large Lookout Mountain sill . . . . .	74
24. Chemical analyses of alaskite . . . . .	86
25. Chemical analyses and norms for samples from the Santa Catalina Mountains sill . . . . .	93
26. Trace element concentrations and elemental ratios in samples from the Santa Catalina Mountains sill . . . . .	94
27. Comparison of Arizona quartz tholeiites with some other tholeiites . . . . .	107

## LIST OF TABLES (Continued)

Table	Page
28. Comparison of Arizona alkali basalts with some other alkali and high-alumina basalts . . . . .	108
29. Compilation of replicate analyses of BCR-1 . . . . .	147
30. Compilation of replicate analyses of W-1 . . . . .	151

LIST OF ILLUSTRATIONS

Figure	Page
1. Map of south central Arizona showing principal diabase outcrops and locations of sills described in this study . . . . .	9
2. Geologic map of the northern part of the Salt River Canyon near Arizona highway 77 showing sample locations . . . . .	13
3. Chemical variations through the Salt River Canyon Complex . . . . .	25
4. Variations in average plagioclase grain size and the ratio $MgO/FeO+Fe_2O_3$ through the Salt River Canyon Complex . . . . .	30
5. A M F diagram of Salt River Canyon diabases . . . . .	31
6. Chemical variations through the Roosevelt Dam sill . . . . .	45
7. Geologic map of the Lookout Mountain area . . . . .	59
8. Chemical variations through the small Lookout Mountain sill . . . . .	66
9. Modal variations through the large Lookout Mountain sill . . . . .	70
10. Chemical variations through the large Lookout Mountain sill . . . . .	76
11. A M F diagram of the Lookout Mountain diabases . . . . .	82
12. Chemical analyses of alaskite shown as bar graphs . . . . .	87

## LIST OF ILLUSTRATIONS (Continued)

Figure	Page
13. Relationship between $\text{SiO}_2$ and alkalis for the analysed rocks . . . . .	99
14. Relationship between $\text{Al}_2\text{O}_3$ and $\text{SiO}_2$ for the analysed rocks . . . . .	103
15. Relationship between $\text{Al}_2\text{O}_3$ and alkalis for rocks containing more than 15 per cent $\text{Al}_2\text{O}_3$ and between 47.51 and 50.00 per cent $\text{SiO}_2$ . . . . .	104
16. Relationship between $\text{K}_2\text{O}$ , $\text{Na}_2\text{O}$ , and $\text{CaO}$ for the analysed rocks . . . . .	112
17. Relationship between $\text{TiO}_2$ and the ratio $\text{Rb}/\text{Sr}$ for the analysed rocks . . . . .	113
18. Relationship between $\text{K}$ and the ratio $\text{Ca}/\text{Sr}$ for the analysed rocks . . . . .	114
19. Relationship between $\text{Rb}$ and $\text{Sr}$ for the analysed rocks . . . . .	116
20. Diagram of $\text{Rb}$ versus the ratio $\text{Rb}/\text{Sr}$ . . . . .	117
21. Relationship between $\text{K}$ and the ratio $\text{K}/\text{Rb}$ for the analysed rocks . . . . .	118
22. Relationship between $\text{SiO}_2$ and $\text{Cu}$ for the analysed rocks . . . . .	119
23. Comparison of $\text{K}/\text{Rb}$ ratio in the Arizona diabases with those in some other basaltic rocks in the western United States . . . . .	128
24. A M F diagram for the Arizona diabases . . . . .	131
25. A M F diagram showing trends for some basaltic rocks . . . . .	132
26. Diagram of $\text{SiO}_2$ versus the ratio $\text{FeO}+\text{Fe}_2\text{O}_3/\text{FeO}+\text{Fe}_2\text{O}_3+\text{MgO}$ . . . . .	134

## ABSTRACT

Six diabase bodies occurring along an approximately north south line from the Santa Catalina Mountains to the Salt River Canyon were studied in order to define the petrology and chemistry of the Precambrian central Arizona diabase province. Samples collected from the bottom to the top of each sheet were examined petrographically and analysed for major oxides, Rb, Sr, and Cu.

The two northernmost occurrences (Salt River Canyon and Roosevelt Dam diabases) contain variable amounts of olivine and no quartz or potassium feldspar. Both of these bodies are multiple sills. Compared to the other bodies these rocks are low in  $\text{SiO}_2$ , Rb, and Cu and high in  $\text{Al}_2\text{O}_3$ ,  $\text{TiO}_2$ ,  $\text{Na}_2\text{O}$ , and Sr. The most common rock type in the Globe complex is quartz-bearing diabase, however, the lower part of the body contains no quartz and is chemically similar to the Salt River Canyon and Roosevelt Dam diabases. Field relationships suggest that this body is also a multiple sill.

Two sills occurring in Putnam Wash on the south side of Lookout Mountain contain quartz and orthoclase and are enriched in  $\text{SiO}_2$ , Rb, and Cu and depleted in  $\text{Al}_2\text{O}_3$ ,  $\text{TiO}_2$ ,  $\text{Na}_2\text{O}$ , and Sr relative to the Salt River Canyon and

Roosevelt Dam diabases. A small sill in the Santa Catalina Mountains contains quartz and is chemically similar to the Lookout Mountain rocks.

On the basis of their chemistries and normative mineralogies the Santa Catalina, Lookout Mountain, and quartz-bearing Globe diabase are quartz tholeiites. The Salt River Canyon and Roosevelt Dam diabases are alkali olivine basalts or olivine tholeiites, depending on the method of classification. The results of this study and published descriptions of other diabase occurrences suggest that the two types are concentrated in the southern and northern parts of the province respectively. The two distinct diabase types can be related if the magma which gave rise to the quartz tholeiites underwent a period of low pressure fractionation before final emplacement.

The diabasic magmas followed an iron-enrichment differentiation trend although highly differentiated phases are generally absent. The most highly differentiated rocks occur within a pegmatitic zone in the large Lookout Mountain sill whereas quartz-bearing diabase in the Globe Complex is more highly differentiated than most other bodies. A small albitite dike in the Salt River Canyon Complex formed from late stage low temperature fluids during the final stages of consolidation.

Alaskite at the contact with a diabase sill shows some chemical changes when compared with alaskite away from the sill. The contact rock and a xenolith are enriched in those elements more abundant in the diabase indicating some chemical exchanges with the diabasic magma.

## INTRODUCTION

### Purpose of the Investigation

The Arizona diabase province has been well known for many years but has received surprisingly little attention. Most of the few published descriptions of diabases occur in papers dealing with copper or uranium deposits and discuss only those aspects of the diabase that directly bear upon these deposits. Little is known about the chemistry and petrology of the diabase.

The present study was undertaken to define the chemical and petrologic types of diabase present and to determine differentiation trends of the diabase magmas. The results of this study should contribute to the understanding of the Arizona diabase province and provide a framework for future investigators. In addition, much of the existing data related to the chemistry of basaltic rocks are for younger rocks. Therefore older basaltic rocks such as the Arizona diabases are of interest in studies of basaltic magmatism throughout geologic time.

### Method of Investigation

The initial phase of the investigation involved visiting many different localities in order to choose

areas for detailed study. Published maps served to locate these areas. Several criteria were used in selecting areas for further study. Diabase is very susceptible to weathering so that the nature of the initial rock may be partially destroyed; several of the bodies examined had to be rejected for this reason. Areas of intense hydrothermal alteration were also avoided. Fresh rocks were found to be mostly restricted to recent road cuts and the walls of canyons or deep washes. Once several relatively unaltered bodies had been located, the final selection was made on the basis of the type of diabase present and the geographic location, in an effort to include a range of magma types and locations within the diabase province.

The six bodies sampled in detail include two olivine-bearing diabases, two quartz-bearing diabases and one quartz-bearing diabase with abundant hornblende. The sixth occurrence, a sill located on the north side of the Santa Catalina Mountains, was chosen mainly on the basis of its location in the southern part of the province.

Samples were collected across each sill, and from the adjacent country rock in one area. The samples are along traverses normal to the contacts as much as field conditions allowed. Thin sections were made from each sample and a representative part of each hand sample was prepared for chemical analyses. Chemical analyses were

made using atomic absorption, x-ray fluorescence, and wet chemical techniques. A detailed description of the analytical methods is given in the Appendix.

#### Previous Work

Much of the published information on the central Arizona diabases appears in papers dealing with copper and uranium deposits in the area. Ransome (1903, 1919), Peterson, Gilbert and Quick (1951), and Creasey (1965, 1967) gave brief descriptions of diabase in the Globe-Miami and San Manuel areas. Williams (1957), Neuerburg and Granger (1960), and Granger and Raup (1969) described diabase related to uranium deposits in central Arizona and listed a few chemical analyses. Smith (1969, 1970) and Nehru and Prinz (1970) gave more detailed data on the petrology and chemistry of the large Sierra Ancha complex, located in the northernmost part of the province.

Shride (1967) gave a detailed account of the field relations of younger Precambrian rocks, including diabase, in south central Arizona. A few workers have investigated the age of the diabase and their work is discussed in more detail in a later section.

## AGE OF THE DIABASE

The age of the diabase in south central Arizona has been the subject of some controversy for many years. Ransome (1903) assigned a Mesozoic age to diabase in the Globe area. In a later paper, Ransome (1919) suggested a late Paleozoic or early Mesozoic age for diabase at Ray and Miami. Darton (1925) concluded that the diabase in the Mescal Mountains was pre-Devonian. Peterson and others (1951) presented evidence for the existence of post-Pennsylvanian diabase in the Castle Dome area and concluded that intrusion was along faults that displaced the Pennsylvanian Naco Limestone. Sharp (1956) suggested that the large diabase sheets in the Sierra Ancha are Tertiary (?) in age. Granger and Raup (1969), however, have questioned Sharp's interpretation of the field relationships. Creasey (1965) stated that at least two ages of diabase are present in the San Manuel area. He assigned a Precambrian age to the older diabase and stated that ". . . some diabase dikes near Red Hill cut the granodiorite porphyry which is of Cretaceous (?) age. . . . (p. 8). Shride (1967) contended that no diabase postdates any of the Paleozoic rocks in south central Arizona.

Recently, several isotopic age determinations have become available. These are summarized in Table 1 and would seem to establish a Precambrian age for these diabases. The 841 my age reported by Balla (1972) is considerably younger than the other reported ages. He states that there is no field or petrographic evidence for a thermal event that might have reset the "isotopic clocks" but concludes that since other Precambrian rocks from the same area also gave anomalously young ages, some reheating has probably occurred. In view of this, the 841 my date is questionable.

If a Precambrian age is accepted for all the diabase within the province, the reasons for so many investigators proposing younger ages requires explanation. Part of the problem may have resulted by confusing the Troy Quartzite (Precambrian) with the Bolsa Quartzite (Cambrian) as suggested by Granger and Raup (1969). Shride (1967) has pointed out that some supposed intrusive contacts between diabase and Paleozoic limestones are actually depositional contacts since fine-grained diabase is absent at these contacts and the limestones show no evidence of metamorphism. The occurrence of other fine-grained dark rocks in the same general area as diabase occurrences has undoubtedly added to the confusion. Small dikes that appear similar to the fine-grained varieties of the diabase clearly cut Paleozoic

Table 1. Isotopic ages reported for diabase from south central Arizona.

Location	Method	Sample	Age (my)	Reference
Sierra Ancha	Pb-Pb	Zircon	1075±50	Silver, 1960
Sierra Ancha	K-Ar	Biotite	1140±40	Damon, Livingston and Erickson, 1962
Near Miami	K-Ar	Biotite	1040±30	Banks, Cornwall and Marvin, 1972
Sacaton Mountains	K-Ar	Whole Rock	841	Balla, 1972

limestones in the Winkelman area. However, in thin section, these rocks are very different from the diabase and are actually andesites. Since some of the younger ages were proposed from studies of mineralized areas, where hydrothermal alteration is intense and faulting has disrupted the stratigraphic sequence, it is easy to understand how such fine-grained intrusive rocks might be mistaken for diabase. The possibility remains, however, that diabase younger than Precambrian may occur in Arizona; especially in areas where basaltic volcanism has occurred. The sills studied in detail in this investigation are assumed to be Precambrian in age. No relationships were observed that are inconsistent with this interpretation.

DISTRIBUTION AND STRATIGRAPHIC  
POSITION OF DIABASE

Shride (1967) gave a detailed discussion of the distribution and field relationships of the younger Precambrian rocks, including diabase, in south central Arizona. Figure 1, modified from Shride (1967), shows the distribution of the larger diabase masses in the area. The largest masses are exposed in the Sierra Ancha and Salt River Canyon areas. Smaller occurrences are in most of the mountain ranges where younger Precambrian rocks are exposed.

The most common hosts for the diabase are the sedimentary rocks of the Apache Group, although extensive bodies also occur in the Troy Quartzite and in older Precambrian rocks. In the Colorado Plateau most of the sills are horizontal, whereas in the Basin and Range region they are tilted at various angles along with the enclosing sedimentary rocks. Most of the diabase apparently was emplaced in the form of concordant sills, although some dikes do occur. According to Shride (1967), dikes are insignificant in volume when compared to sills. The thickness of individual sills is variable, ranging from a few inches to 1200 feet; dikes are rarely more than a few tens of feet

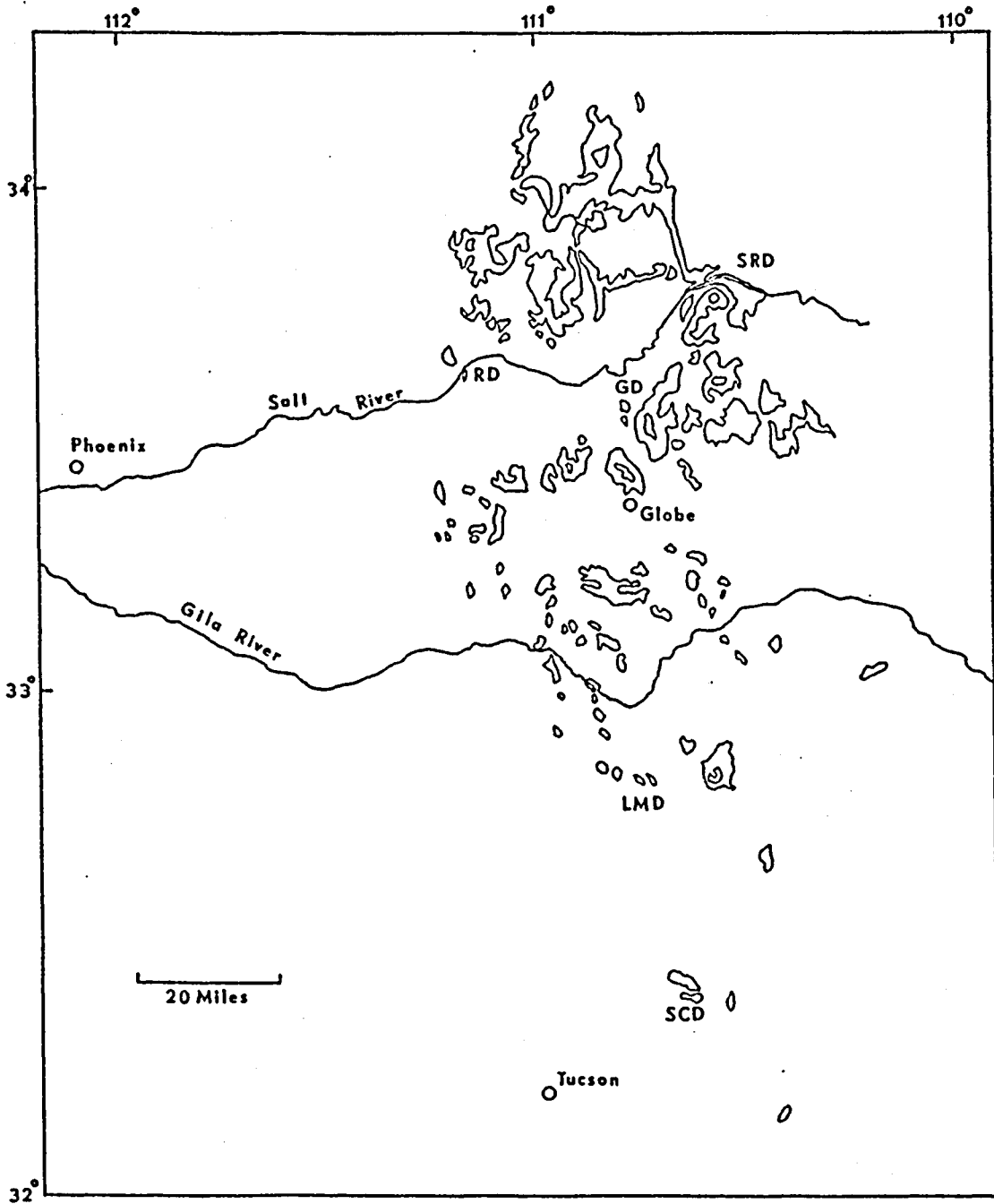


Figure 1. Map of south central Arizona showing principal diabase outcrops and locations of sills described in this study.

Modified from Shride, 1967.

thick. In general the sills are very persistent laterally; however, Basin and Range faulting has obscured relationships in most areas south of the Salt River Canyon. Most small sills represent single intrusions but multiple intrusions have been described in several areas (Shride, 1967; Nehru and Prinz, 1970; Schmidt, 1971). Apparently, intrusion occurred in some areas over an extended period of time because some members of the multiple sills show chilled contacts against coarser grained diabase, indicating that the earlier intrusion had cooled before the next magma was emplaced. Emplacement of the diabase in the entire province may have occurred over a fairly long time span.

Emplacement was controlled to some extent by the physical properties of the country rocks. Shride (1967) noted that sills are most common and most persistent where they separate layers of markedly different competencies. An apparent relationship exists between depth and diabase abundance. Diabase is most abundant in the sedimentary rocks of the Apache Group. However, in many areas the older Precambrian rocks underlying the Apache Group contain diabase. In general, the amount of diabase decreases with distance below the base of the Apache Group and Shride (1967) stated that "at depths of more than 500 feet below the base of the Apache Group extensive diabase intrusions

are practically nonexistent" (p. 56). Schmidt (1971) also noted that diabase bodies in the Oracle Granite are more extensive and thickest just below the base of the Apache Group. Thickness and abundance both decrease with depth.

The six diabase occurrences studied in detail will be discussed individually in the following sections, beginning with the northernmost sill and progressing to the south. The location of each occurrence is shown in Figure 1 where SRD, RD, GD, LMD, and SCD refer to the Salt River Canyon complex, Roosevelt Dam sill, Globe complex, Lookout Mountain and Santa Catalina Mountains sills respectively.

## SALT RIVER CANYON COMPLEX

A large multiple sill is well exposed in the walls of the Salt River Canyon near Arizona Highway 77. Good exposures exist on both canyon walls; however, relationships are clearer in the north wall and the samples studied are from this part of the complex. All samples were collected along the highway because of the exceptional freshness of the rock, the ready access, and the good control of sample locations. Field relationships are shown in Figure 2.

The total exposed thickness of diabase is approximately 920 ft. The diabase overlies the Mescal Limestone and, in turn is unconformably overlain by the Devonian Martin Formation. Thus, an unknown amount of diabase has been removed by erosion and the original thickness of the complex is unknown. The upper 80 ft of the complex is deeply weathered, apparently resulting from surficial exposure prior to the deposition of the Martin Formation.

A short distance west of Highway 77 the diabase complex consists of at least two separate sills separated by a thin sliver of Mescal Limestone which appears to be little disturbed. The limestone pinches out toward the east so that the two sills are in contact, forming a thick multiple sill. This contact is marked by a zone of

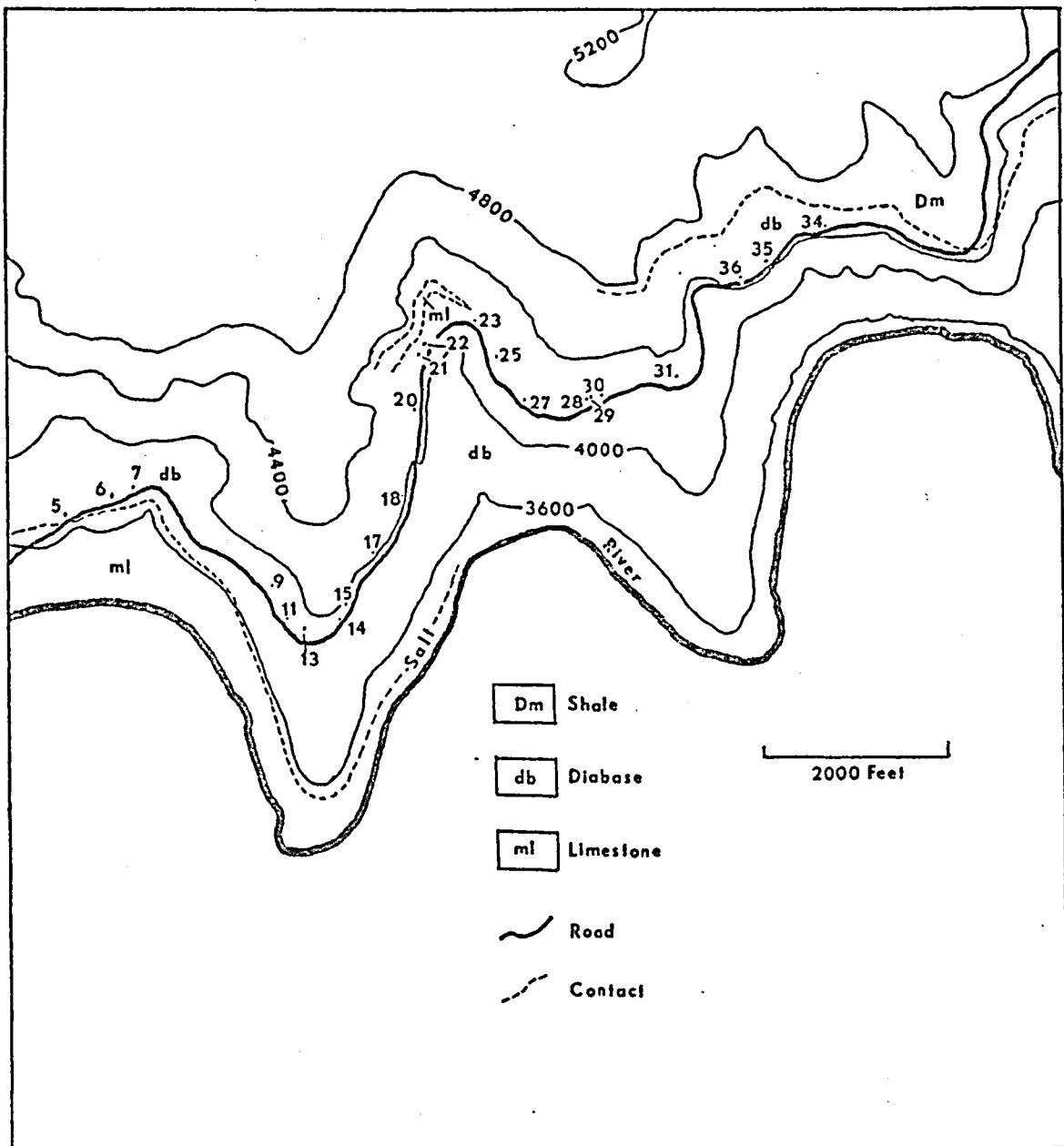


Figure 2. Geologic map of the northern part of the Salt River Canyon near Arizona highway 77 showing sample locations.

fine-grained diabase, presumably representing a chilled zone, and suggesting that the lower sill crystallized before the upper sill was emplaced. This interpretation is supported by the presence of several thin (2 in to 1.5 ft) veins of fine-grained diabase which cut the coarse-grained diabase of the lower sill just below the major fine-grained chill zone. The time interval between the two intrusions is unknown. The lower sill is approximately 670 ft thick and the remaining part of the upper sill is about 250 ft thick.

#### Petrography of the Diabase

Plagioclase and augite compose the essential mineralogy of all samples from the Salt River Canyon Complex. Magnetite is ubiquitous and olivine is abundant enough for the body as a whole to be characterized as olivine diabase. Textures are ophitic to subophitic with variable grain sizes (Table 2).

The lower 30 to 35 ft of the complex consists of ophitic, fine-grained diabase. Plagioclase ( $An_{57}$ ) laths average about 0.5 mm in length; however, a few larger crystals are present which usually occur as clusters. These clusters are up to 4 mm in diameter with individual crystals up to 1.0 mm in length. All plagioclase shows some degree of normal zoning. Pale green augite is the

Table 2. Description and location of samples from the Salt River Canyon Complex.

Sample Number	Rock Type	Distance Above Base
SRD-5	Fine-grained olivine diabase.	25'
SRD-6A	Medium-grained diabase.	83'
SRD-7	Medium-grained olivine diabase. Altered.	110'
SRD-9	Medium-grained olivine diabase.	245'
SRD-11	Medium-grained olivine diabase.	270'
SRD-13	Albitite dike.	280'
SRD-14	Medium-grained olivine diabase.	300'
SRD-15	Medium-grained diabase.	310'
SRD-17	Medium-grained altered diabase.	380'
SRD-18	Medium-grained olivine diabase.	395'
SRD-20	Medium-grained olivine diabase.	440'
SRD-21	Medium-grained diabase. Coarser grained than above samples.	500'
SRD-22	Pegmatitic diabase.	507'
SRD-23	Medium-grained altered diabase.	525'
SRD-25	Medium-grained diabase with traces of olivine.	580'

Table 2. (Continued)

Sample Number	Rock Type	Distance Above Base
SRD-27	Medium-grained diabase.	600'
SRD-28	Fine-grained diabase vein.	640'
SRD-29	Medium-grained diabase.	642'
SRD-30	Fine-grained diabase.	670'
SRD-31	Medium-grained olivine diabase.	710'
SRD-36	Medium-grained diabase.	830'
SRD-35	Medium-grained diabase.	840'
SRD-34	Medium-grained diabase.	860'

second most abundant mineral having an average diameter of about 0.5 mm with a few crystals as large as 1.0 mm. Thin marginal zones with slightly higher birefringence are present in some grains indicating compositional zoning. Olivine totals 5 to 10 percent of the rock, occurring as roughly spherical grains with an average diameter of approximately 0.25 mm. The optical properties of olivine indicate a composition in the range  $Fa_{10-20}$ . A few larger grains of olivine are present, some with diameters as large as 1.0 mm. Fine-grained magnetite is fairly abundant.

Above this fine-grained zone is a zone of generally homogeneous medium-grained diabase about 400 ft in thickness. Within this zone plagioclase laths average about 1.5 mm in length but are slightly larger near the center of the zone, decreasing slightly at the top. All plagioclase shows some normal zoning with cores ranging from  $An_{53}$  to  $An_{55}$  and margins averaging  $An_{39}$ . Augite remains an important constituent throughout this part of the sill. It is intimately intergrown with plagioclase to form a well developed ophitic texture. Several pyroxene grains that appear to be completely separated in thin section are in optical continuity; this indicates that the grains are connected in the third dimension and are grains with diameters of a few millimeters that contain numerous inclusions of

plagioclase. Most augite is a very light tan color, bi-axial (+) with a  $2V$  of 40-50 degrees.

Olivine is more abundant in this zone than in any other part of the complex, but never composes more than 10 per cent of the rock. Most olivines are less than about 1 mm in diameter but a few samples from near the bottom of this zone contain somewhat coarser grained olivines. Spherical grains of olivine are disseminated throughout the rock and are sometimes completely enclosed by augite.

Magnetite is fairly abundant in most samples. Pyrite is also present in many samples, commonly is very fine-grained, and occurs with chlorite and other alteration products of augite. A few samples from the lower part of this zone contain coarser grained pyrite as irregularly shaped grains up to 2 mm in diameter. How much, if any, pyrite is primary is difficult to determine. In one case pyrite fills a small fracture, suggesting that it is secondary.

Above this zone is a generally coarser grained zone that extends upward to more fine-grained diabase, a distance of 230 ft. Plagioclase laths in this zone average near 3 mm in length and have compositions similar to those below. Augite is also coarser grained and the ophitic texture is retained. Almost no olivine is present in this zone. Magnetite is generally more abundant in this zone

than in the lower part of the complex. Within this zone numerous pods, lenses, and veins of pegmatitic diabase occur. These are all small with the veins all being less than 2 in in width. In these pegmatitic rocks plagioclase averages about 3.5 mm in length with augite grains as large as 8 mm. The ophitic texture, so characteristic of the normal diabase, is very poorly developed. Magnetite grains up to 1.5 mm are abundant and some biotite is present.

Above this zone is a zone of finer grained diabase that marks the base of the upper sill. This grades upward into medium-grained diabase generally similar to the lower part of the lower sill. Olivine is present in small amounts or is absent in these rocks and biotite and uralitic hornblende are more abundant than in the lower sill.

Almost all samples from the Salt River Canyon complex show some deuteric alteration. Olivine has been affected more than the other minerals and in a few samples it is difficult to determine if olivine was initially present. Alteration products of olivine and augite are serpentine, talc, saponite, and chlorite. Dark green uralitic hornblende is present in several samples and is more abundant in the upper unit. Plagioclase is altered to fine-grained white mica; it usually occurs in localized

patches on plagioclase grains but is more pervasive in a few samples.

### Chemistry

Twenty two samples of diabase from the Salt River Canyon complex were analysed for 10 major oxides, Sr, Rb, and Cu (Tables 3 and 4). Relative to most of the other sills studied, the Salt River Canyon rocks are low in  $\text{SiO}_2$ , and relatively high in  $\text{TiO}_2$ ,  $\text{Al}_2\text{O}_3$ ,  $\text{Na}_2\text{O}$ , and Sr. Overall, the complex has the characteristics of alkali or high-alumina basalts (Table 5).

Figure 3 shows the chemical variations from the bottom to the top of the complex. Although there are considerable fluctuations in oxide percentages through the complex, some trends are apparent. Silica is slightly higher in the basal fine-grained zone than throughout most of the lower part of the lower unit where it is fairly constant. Pegmatitic veins and pods near the top of the lower sill are markedly higher in  $\text{SiO}_2$  (sample SRD-22). Alumina averages about 15.50 per cent throughout the lower 150 ft of the complex, then increases to over 17 per cent and remains fairly constant up to the upper part of the lower unit, where it drops to about 14 per cent in the pegmatitic diabase and enclosing coarse-grained diabase. Fine- to medium-grained diabase interpreted as the base of

Table 3. Chemical analyses of samples from the Salt River Canyon Complex.

	SiO <sub>2</sub>	TiO <sub>2</sub>	Al <sub>2</sub> O <sub>3</sub>	Fe <sub>2</sub> O <sub>3</sub>	FeO	MnO	MgO	CaO	Na <sub>2</sub> O	K <sub>2</sub> O	Total
SRD-5	48.66	1.45	15.78	2.29	9.36	0.18	6.63	9.82	2.42	1.09	97.68
SRD-6A	47.21	2.15	15.77	3.37	10.41	0.20	5.83	7.45	3.10	1.75	97.24
SRD-7	48.07	2.18	15.18	2.54	10.11	0.22	6.22	6.76	4.09	0.47	95.84
SRD-9	46.31	1.59	17.30	3.44	8.83	0.17	6.87	7.73	3.03	1.56	96.83
SRD-11	47.29	1.52	17.88	2.41	9.29	0.17	7.04	8.98	2.69	1.06	98.33
SRD-13	58.30	0.39	15.82	1.02	0.69	0.06	1.21	7.01	9.24	0.10	93.84
SRD-14	47.97	1.68	17.27	3.12	8.91	0.16	7.38	9.47	2.72	0.75	99.43
SRD-15	47.42	1.88	16.75	2.56	9.92	0.18	6.92	9.22	2.71	0.72	98.28
SRD-17	47.18	1.70	17.66	2.77	9.85	0.19	6.45	6.45	3.09	1.59	96.93
SRD-18	48.47	1.12	16.93	1.99	9.76	0.18	8.27	9.89	2.37	0.74	99.72
SRD-20	47.93	1.75	18.27	2.58	8.72	0.17	5.32	8.66	3.08	1.16	97.64
SRD-21	44.88	2.90	13.98	4.64	11.87	0.21	6.37	8.84	2.43	1.24	97.36
SRD-22	49.82	2.18	14.25	2.60	10.21	0.20	4.64	8.04	4.24	1.02	97.20
SRD-23	48.43	2.81	14.02	2.67	11.95	0.25	5.24	6.91	3.92	1.04	97.24
SRD-25	48.08	1.74	17.39	2.04	10.22	0.17	5.69	7.96	3.25	0.98	97.52
SRD-27	44.86	2.75	14.55	3.53	12.66	0.23	5.97	8.33	2.80	1.07	96.75
SRD-28	46.27	2.79	16.70	2.25	10.46	0.20	6.52	6.85	3.24	1.44	96.72
SRD-29	47.85	2.42	14.97	3.39	10.99	0.24	5.55	6.96	3.56	1.31	97.24
SRD-30	46.30	2.63	16.72	3.00	9.77	0.21	6.43	7.41	3.19	1.29	96.95
SRD-31	46.42	2.42	16.99	2.54	9.71	0.19	6.90	8.27	3.02	1.12	97.58
SRD-36	45.75	2.57	16.93	2.55	9.82	0.19	6.79	8.00	3.16	1.18	96.94
SRD-35	45.18	2.46	16.98	2.10	10.42	0.18	7.01	7.33	2.96	1.38	96.00
SRD-34	46.29	2.63	17.01	2.55	10.00	0.19	6.94	6.29	3.13	1.97	97.00

Table 4. Trace element concentrations and elemental ratios in samples from the Salt River Canyon Complex.

Sample	Cu (ppm)	Sr (ppm)	Rb (ppm)	Rb/Sr	K/Rb	Ca/Sr
SRD-5	132	269.4	25.4	0.0942	354	261
SRD-6A	71	434.4	41.7	0.0960	348	123
SRD-7	68	402.3	4.2	0.0104	929	120
SRD-9	--	423.0	40.3	0.0952	323	131
SRD-11	51	487.0	20.5	0.0420	429	132
SRD-13	26	78.5	N.D.	--	--	638
SRD-14	47	476.8	19.0	0.0252	517	142
SRD-15	--	455.2	8.9	0.0196	614	145
SRD-17	56	407.5	43.9	0.1077	301	113
SRD-18	117	195.9	16.9	0.0864	361	361
SRD-20	60	476.6	29.9	0.0627	321	130
SRD-21	--	359.4	28.2	0.0786	365	176
SRD-22	99	277.4	23.5	0.0849	362	207
SRD-23	53	276.0	22.4	0.0812	384	179
SRD-25	47	436.6	19.5	0.0448	415	130
SRD-27	186	368.1	21.3	0.0579	418	162
SRD-28	47	506.6	35.0	0.0692	343	97
SRD-29	58	410.7	37.8	0.0919	288	121
SRD-30	42	539.7	28.3	0.0524	378	98
SRD-31	--	582.6	19.3	0.0332	482	101
SRD-36	36	615.1	22.5	0.0365	436	93
SRD-35	--	541.3	28.3	0.0523	406	97
SRD-34	38	457.4	41.7	0.0912	393	98

Table 5. Norms for samples from the Salt River Canyon Complex.

	SRD-5	SRD-6A	SRD-7	SRD-9	SRD-11	SRD-14	SRD-15	SRD-17
Quartz	--	--	--	--	--	--	--	--
Orthoclase	6.66	10.78	2.91	9.54	6.39	4.48	4.37	9.74
Albite	22.48	29.02	38.49	27.19	24.66	24.70	24.98	28.77
Anorthite	29.98	24.98	22.73	30.04	34.30	33.08	32.27	30.73
Nepheline	--	--	--	0.59	--	--	--	--
Wollastonite	--	--	--	--	--	--	--	--
Diopside	16.33	10.85	9.94	7.74	8.95	11.55	11.76	1.96
Hypersthene	13.87	2.56	6.63	--	5.36	9.43	9.78	6.87
Olivine	6.12	15.02	13.33	18.87	15.61	11.09	11.41	16.48
Magnetite	2.48	3.67	2.78	3.72	2.57	3.30	2.75	3.00
Ilmenite	2.09	3.12	3.18	2.29	2.16	2.37	2.69	2.46
Hematite	--	--	--	--	--	--	--	--
	SRD-18	SRD-20	SRD-21	SRD-22	SRD-23	SRD-25	SRD-27	SRD-28
Quartz	--	--	--	--	--	--	--	--
Orthoclase	4.40	7.07	7.74	6.27	6.43	5.98	6.70	8.86
Albite	21.40	28.53	23.05	39.60	36.18	30.14	26.63	30.30
Anorthite	33.57	33.64	24.92	17.53	18.41	30.97	25.40	27.90
Nepheline	--	--	--	--	--	--	--	--
Wollastonite	--	--	--	--	--	--	--	--
Diopside	12.62	8.54	17.13	19.18	13.97	7.86	14.70	6.00
Hypersthene	10.81	6.37	5.86	0.35	5.03	7.34	1.78	0.96
Olivine	13.55	10.56	11.92	11.09	12.33	13.00	16.82	19.48
Magnetite	2.09	2.78	5.12	2.83	2.92	2.20	3.91	2.45
Ilmenite	1.57	2.51	4.27	3.16	4.09	2.50	4.06	4.05
Hematite	--	--	--	--	--	--	--	--

Table 5. (Continued)

	SRD-29	SRD-30	SRD-31	SRD-36	SRD-35	SRD-34
Quartz	--	--	--	--	--	--
Orthoclase	8.08	7.93	6.82	7.23	8.53	12.05
Albite	33.39	29.80	27.96	27.49	26.63	28.34
Anorthite	21.95	28.62	30.42	29.60	30.34	27.50
Nepheline	--	--	--	1.16	0.72	0.46
Wollastonite	--	--	--	--	--	--
Diopside	11.30	7.71	9.51	9.26	6.19	3.85
Hypersthene	5.76	2.32	1.04	--	--	--
Olivine	12.29	16.54	18.04	18.78	21.71	21.24
Magnetite	3.70	3.26	2.74	2.77	2.30	2.76
Ilmenite	3.52	3.81	3.48	3.71	3.59	3.79
Hematite	--	--	--	--	--	--

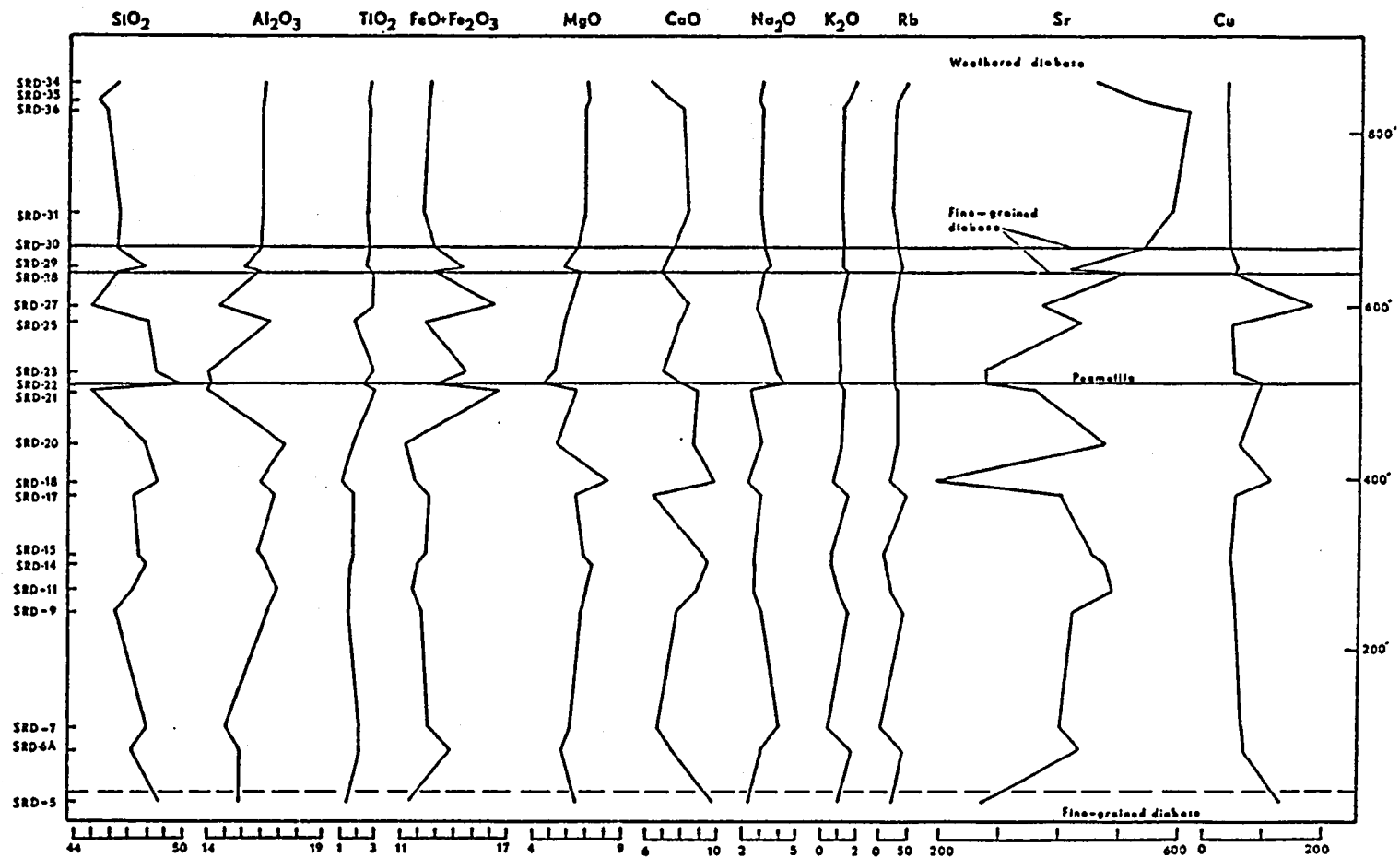


Figure 3. Chemical variations through the Salt River Canyon Complex.  
 Oxides in per cent, trace elements in ppm.

the upper sill, as well as three samples from above this fine-grained zone all contain about 17 per cent  $\text{Al}_2\text{O}_3$ .

Total iron and  $\text{TiO}_2$  show the same distribution pattern. Both increase just above the basal fine-grained zone, then decrease and remain fairly constant throughout the central part of the lower unit. The highest values for both elements occur in the upper coarser grained zone of the lower unit (samples SRD-21, SRD-22, SRD-23, and SRD-27). The ratio  $\text{FeO}/\text{FeO}+\text{Fe}_2\text{O}_3$  is generally constant throughout the complex. Magnesium is slightly enriched in the lower one-half of the lower unit and depleted in the coarser-grained rocks near the top of this unit. Calcium distribution is similar to that of  $\text{MgO}$ , but somewhat more erratic. Sodium is fairly constant at about 3 per cent but is enriched in the pegmatitic diabase. Potassium shows some fluctuations but averages slightly more than one per cent. Rubidium distribution is almost identical to that of  $\text{K}_2\text{O}$  and ranges from 4 to 44 ppm. Potassium to rubidium ratios are generally higher than in the other sills investigated. Strontium contents fluctuate markedly from a low of 196 ppm to over 600 ppm but average concentrations are higher than in the other sills resulting in very low Rb/Sr ratios. Most of the samples analysed for copper contain about 50 ppm; however, a few samples have considerably higher concentrations.

Some of the chemical variations shown in Figure 3 are related to deuteric alteration. Samples SRD-7, SRD-17, and SRD-23 are highly altered and all three are anomalously low in CaO and somewhat enriched in Na<sub>2</sub>O. Other chemical variations can be related to differences in primary mineralogy. Samples SRD-21, SRD-23, and SRD-27 are all enriched in total iron and TiO<sub>2</sub> which is consistent with their higher content of opaque minerals. The lower SiO<sub>2</sub> content of SRD-21 and SRD-27 is probably also because of their higher content of oxide minerals. Magnesium is enriched in SRD-18, which is the most olivine-rich sample.

In general, the lower 450 ft of the medium-grained diabase is fairly homogeneous with CaO being an exception. Coarser grained diabase in the upper 230 feet of the lower unit shows larger variations from one sample to the next for most elements. The remaining part of the upper unit is remarkably constant in composition with only K<sub>2</sub>O and Rb, which increase upward, and CaO and Sr, which decrease showing any significant variations. Fine- to medium-grained diabases (SRD-28 and SRD-30) interpreted as representing the base of the upper sill, are chemically similar to each other and to overlying medium-grained rocks. These similarities support field and petrographic evidence for placing the contact between the two units at this position.

### Albitite Dike

An unusual rock occurs as a 6 in dike, exposed in a vertical face about 280 ft above the base of the complex. This light colored dike, which could not be traced away from this outcrop, has very sharp contacts with the diabase. The rock is composed largely of fine- to medium-grained albite, varying amounts of calcite, and minor epidote, chlorite, and apatite. The albite is subhedral to anhedral and exhibits complex "chessboard" twinning. Calcite is present throughout the dike but is more abundant near the margins where it makes up 10 to 15 per cent of the rock. The chemistry (Table 3, sample SRD-13) reflects the unusual mineralogy with high  $\text{Na}_2\text{O}$ ,  $\text{CaO}$ ,  $\text{Al}_2\text{O}_3$ , and  $\text{SiO}_2$  concentrations.

### Petrogenesis

No strongly differentiated phases are present within the area studied. The pegmatitic veins and pods near the top of the lower unit probably represent the most highly differentiated diabase. The occurrence of these rocks indicates that they crystallized after the surrounding diabases. These rocks are enriched in  $\text{SiO}_2$  and  $\text{Na}_2\text{O}$  and depleted in  $\text{MgO}$  relative to the other diabase samples. Total iron and  $\text{TiO}_2$  are more abundant in the coarser grained upper zone of the lower unit as well as in the pegmatitic diabase.

Standard indices used to indicate differentiation trends are not too useful for the Salt River Canyon rocks because of their similar chemistry. This is especially true for indices using  $\text{SiO}_2$  and alkalis. The most useful index for these rocks is the ratio  $\text{MgO}/\text{FeO}+\text{Fe}_2\text{O}_3$ . Figure 4 is a plot of this ratio versus position within the complex. Also shown in Figure 4 is a plot of average plagioclase lath length versus position in the complex. It is clear from this figure that rocks in the upper coarser grained zone of the lower unit are more highly differentiated than other rocks in the complex. The most mafic rocks occur within the upper part of the lower medium-grained zone. Fine to medium-grained rocks at the base of the upper unit are much less differentiated than the coarser grained rocks underneath.

Figure 5 is a standard A M F plot of the Salt River Canyon samples. A fairly strong iron enrichment trend is indicated. Two samples of coarser grained diabase (SRD-21, and SRD-27) show more extreme iron enrichment and plot off the main trend. The pegmatitic diabase (SRD-22) shows more enrichment in alkalis mostly  $\text{Na}_2\text{O}$ . This may indicate the involvement of a late stage sodium-rich volatile phase. This is also suggested by the higher  $\text{Na}_2\text{O}$  content of samples showing extreme deuteric alteration. Although highly differentiated diabase is absent, some mechanism appears to

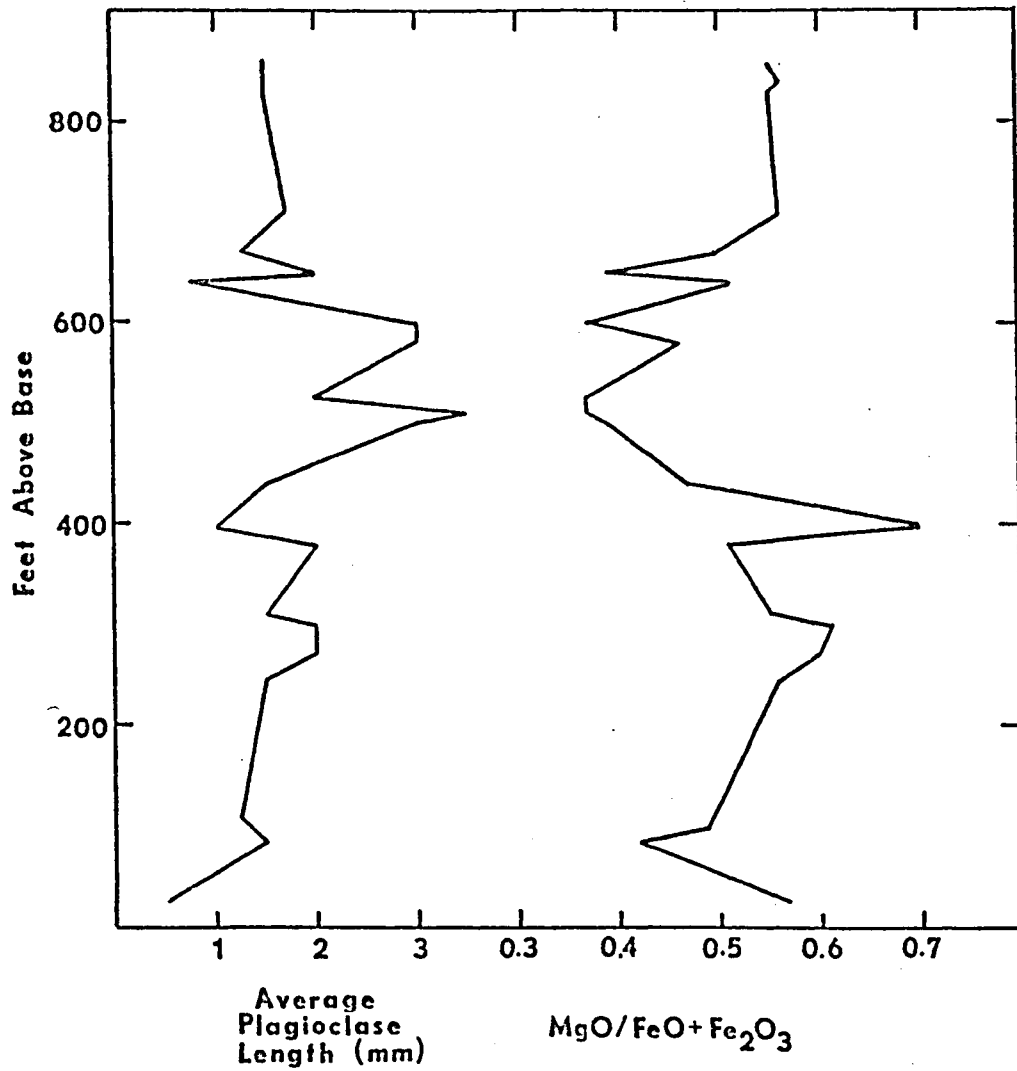


Figure 4. Variations in average plagioclase grain size and the ratio  $\text{MgO}/\text{FeO}+\text{Fe}_2\text{O}_3$  through the Salt River Canyon Complex.

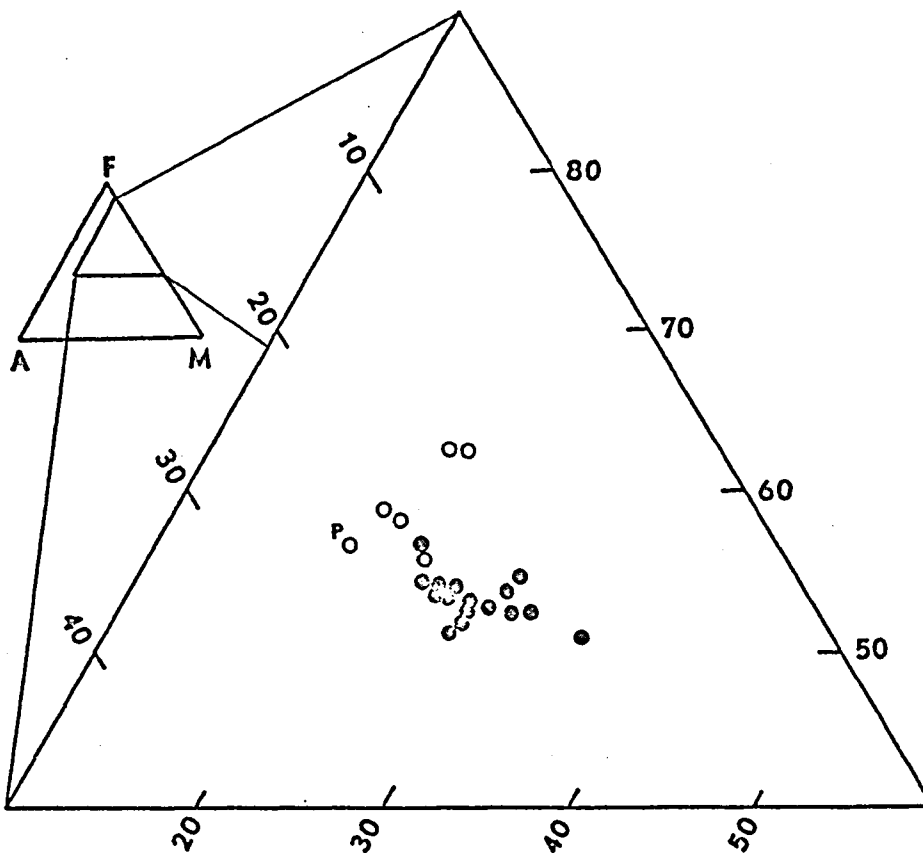


Figure 5. A M F diagram of Salt River Canyon diabases.

Dots: fine- to medium-grained diabase; circles: coarse-grained diabase; P: pegmatitic diabase.

have caused a concentration of more differentiated material in the upper part of the lower unit. Since part of the upper sill has been removed by erosion, little can be said regarding its differentiation history.

The nature of the differentiation process is somewhat obscure. There is no evidence for long range crystal settling although conditions seem to have been favorable. Table 6 shows viscosities and densities calculated according to the methods of Shaw (1972) and Bottinga and Weill (1970), using the analysis of the fine-grained diabase near the base of the complex (SRD-5, Table 3). The water content of the magma is not known, and since water importantly affects both viscosity and density, some realistic value has to be used in the calculations. Yoder and Tilley (1962) concluded that basaltic magma that crystallizes as diabase or gabbro at depth must contain very little water. Moore (1970), from vesicularity and water contents of ocean floor basalts, concluded that these magmas contained between 0.25 and 0.9 per cent water prior to degassing. The nature of the deuteric alteration indicates that some water was present in the Salt River Canyon magmas; thus viscosities and densities were calculated on the bases of 0.5 and 1.0 per cent water.

Magma temperatures during the early to middle stages of crystallization were probably in the 1000<sup>o</sup> to

Table 6. Viscosities and densities calculated from the analyses of sample SRD-5.

Temp. (°C)	H <sub>2</sub> O = 0.5%		H <sub>2</sub> O = 1.0%	
	log η (poises)	Density (g/cc)	log η (poises)	Density (g/cc)
900	3.99	2.69	3.79	2.65
1000	3.35	2.67	3.16	2.64
1100	2.79	2.65	2.62	2.62
1200	2.32	2.64	2.16	2.60

1100°C range. Considering this and the data in Table 6, olivine settling velocities were calculated using a density of 2.65 g/cm<sup>3</sup> and a viscosity of 1000 poises. Olivine was chosen because it appears to have crystallized early and because it is more abundant in the lower and central parts of the lower unit. There is no textural evidence for settling or floating of any other mineral. An olivine crystal with a composition of Fa<sub>20</sub> and a diameter of one millimeter would settle 1913 ft per year (Stokes' Law). Under the same conditions a crystal of the same composition 0.5 mm in diameter would settle 480 ft per year. These calculations indicate that olivine should have settled rapidly. As mentioned above, olivine is more abundant in the lower one half of the lower sill. However, neither the petrography nor the norms indicate any large scale accumulation of olivine. Also, the most olivine-rich rock (SRD-18) is slightly above the center of the sill, not in the lower part. Some short range crystal settling undoubtedly occurred but this appears not to have been a major factor in the crystallization of the diabase.

Hamilton (1965, p. 65) proposed a process called "liquid fractionation" to account for chemical trends observed in a diabase sill in Antarctica. According to this model alkalis, silica, and possibly other elements

become concentrated in the upper parts of the magma in response to pressure and temperature gradients. The trends observed in the Salt River Canyon Complex are not entirely consistent with this model and it is unlikely that significant pressure gradients could have existed in a sheet as thin as the body under consideration.

The existence of the upper sill, that apparently intruded after the lower unit had cooled sufficiently to allow the formation of a chilled zone, suggests that basaltic magma was intruded into the area over a considerable length of time. The dimensions of the complex are not known but it is exposed in both walls of the canyon for a distance of several miles. Considering the magnitude of this sill, or the large volume of magma involved, and the fact that the area was the site of active magmatism for a considerable period of time it is likely that the lower unit does not represent a magma mass that was isolated and quietly crystallized. It probably was emplaced over some time interval, possibly in stages, preventing large scale crystal settling and the development of strongly differentiated phases. The petrographic and chemical data are generally consistent with this interpretation. Figure 4 shows that sample SRD-18 is finer grained and less differentiated than the rocks above and below. It is difficult

to account for this by any mechanism other than separate intrusion.

The coarser grained rocks near the top of the lower unit may represent slightly more differentiated magma that was concentrated in the upper part of the body after emplacement, or they may represent a slightly later intrusion of more differentiated magma. If the later is true, the coarser texture could have resulted from slow cooling because the earlier intrusions had heated up the surrounding rocks and were still hot themselves.

The origin of the albitite dike and its relationship to the diabase is of some interest since the assemblage albite-calcite-chlorite-epidote is common in many spilites. Although the origin of spilites has been debated for years, most authors have stressed the importance of a low temperature sodium-rich liquid or aqueous phase (Gilluly, 1935; Turner and Verhoogen, 1960, p. 270; Amstutz, 1967). Interaction with sea water may be important in the genesis of spilites associated with pillow basalts but this mechanism is not applicable to the Salt River diabase.

Several lines of evidence suggest that the albitite dike formed at low temperatures. The presence of calcite, epidote and chlorite indicate low temperatures since these minerals appear to have formed at the same time as the albite. The "chessboard" twinning seen in the albite is

similar to that described by Crowder and Ross (1973) in hydrothermal albite in California and Nevada. Index of refraction measurements indicate that the albite is very pure which permits the use of x-ray diffraction to estimate the temperature of formation. The separation of the 131 and  $\bar{1}\bar{3}1$  peaks, plotted on the diagram in Barth (1969, p. 131), gives a temperature of 460 degrees.

The chemical and petrographic data for the complex indicate that sodium was concentrated in the residual liquids as crystallization proceeded. Pegmatitic veins show enrichment in sodium relative to other diabase, and the samples showing the most intense deuteric alteration have high sodium contents. Thus, it is likely that the albitite dike formed through the action of a fluid rich in  $\text{Na}_2\text{O}$ ,  $\text{SiO}_2$ ,  $\text{Al}_2\text{O}_3$ , and  $\text{CO}_2$  which moved through a fracture. The absence of replacement textures or relict minerals suggest that the dike represents direct crystallization from this fluid rather than metasomatic replacement. Spilitic rocks may form in this way, at least locally, without the requirement of water or other material from an external source.

## ROOSEVELT DAM SILL

A relatively small sill crops out along the dirt road one quarter mile southwest of Roosevelt Dam. The sill has intruded sedimentary rocks of the Apache Group. The whole area has been tilted such that both the diabase and the enclosing sedimentary rocks strike to the northwest and dip 47 degrees toward the northeast. The sill is essentially parallel to bedding in the sedimentary rocks. Fine-grained, red-brown sandy shale overlies the diabase. Beneath the sill is a pink arkosic sandstone that is slightly coarser grained than the overlying rock. The sill is 185 ft thick in the area where samples were collected. Sample descriptions and locations are listed in Table 7.

### Petrography

The lower one half of the sill is composed almost entirely of plagioclase, augite, and magnetite. Most samples show minor deuteric alteration. Throughout this part of the sill plagioclase averages between 0.5 and 0.8 mm in length. All plagioclase shows some normal zoning with cores ranging between  $An_{52}$  and  $An_{58}$ , except at the lower contact where the plagioclase is  $An_{66}$  in composition.

Table 7. Description and location of samples from the Roosevelt Dam sill.

Sample Number	Rock Type	Distance Above Base
RD-11	Fine-grained, plagioclase-rich diabase.	3'
RD-12	Fine-grained, plagioclase-rich diabase.	6'
RD-10	Fine-grained, plagioclase-rich diabase.	15'
RD-9	Fine-grained, plagioclase-rich diabase. Slightly altered.	60'
RD-8	Fine-grained, plagioclase-rich diabase. Moderate alteration.	80'
RD-7	Medium-grained, altered diabase.	89'
RD-5	Medium-grained olivine diabase.	110'
RD-4	Medium-grained diabase. Distinctly coarser grained than other samples.	164'
RD-3	Fine- to medium-grained diabase. Moderate alteration.	172'
RD-2	Fine-grained diabase. Moderate alteration.	181'
RD-1	Fine-grained, biotite rich diabase.	184'

Augite is pink to tan, biaxial positive with  $2V$ 's of about 50 degrees. The average size of individual grains increases slightly upward in the sill from about 0.6 mm at the base to 1.0 mm just below the center. In some thin sections two or more grains are in optical continuity. Magnetite is moderately abundant although there is some variation from sample to sample. In general, the lower one half of this sill is more homogeneous and richer in plagioclase than is the upper one half.

The upper one half of the Roosevelt Dam sill is much more variable in both texture and mineralogy than the lower part. Except for the uppermost few feet, the grain size is noticeably larger. Slightly above the center of the sill a medium-grained zone contains approximately 15 per cent olivine, in addition to the above minerals. Some biotite and apatite are also present in this zone. Small amounts of olivine are present in other samples from the upper part of the sill. About 20 ft below the top of the sill the rock is the most coarse grained. Plagioclase laths are as large as 4 mm in length and some augite grains are 2 mm across. Apatite is unusually abundant in this zone. Biotite is also abundant while olivine is absent. The uppermost 10 ft of the sill is fine-grained. Biotite is abundant here, and at the upper contact, and is the major mafic mineral.

Plagioclase compositions in the upper part of the sill average  $An_{54}$ , however, at the upper contact they are closer to  $An_{50}$ . Augite is similar to that in the lower part of the sill. Olivine compositions are near  $Fa_{25}$ . The upper one half of the sill contains much more olivine, biotite, and apatite and less plagioclase than the lower one half and locally is coarser grained.

#### Chemistry

Tables 8 and 9 list the analyses for the Roosevelt Dam sill and norms are given in Table 10. In general, the chemistry of this sill is similar to that of the Salt River Canyon Complex. Silica is low and  $TiO_2$ ,  $Al_2O_3$ , and alkalis are high; however, the sodium to potassium ratio is lower than in the Salt River Canyon olivine diabases.

Chemical variations through the sill are shown in Figure 6. Some obvious chemical differences exist between the lower and upper halves of the sill. Silica and  $Al_2O_3$  are more concentrated in the lower one-half, while total iron and  $TiO_2$  are less concentrated than in the upper one-half. This is due to the greater abundance of plagioclase in the lower part. Calcium and MgO are less variable, but MgO is slightly more abundant in the olivine-rich zone (RD-5). Sodium shows little variation except near the two contacts. Potassium and rubidium have nearly identical distributions; both increase in the center and at the

Table 8. Chemical analyses of samples from the Roosevelt Dam sill.

	SiO <sub>2</sub>	TiO <sub>2</sub>	Al <sub>2</sub> O <sub>3</sub>	Fe <sub>2</sub> O <sub>3</sub>	FeO	MnO	MgO	CaO	Na <sub>2</sub> O	K <sub>2</sub> O	Total
RD-11	48.09	2.14	17.27	6.20	6.85	0.19	5.63	8.20	3.12	0.67	98.36
RD-12	47.84	2.12	16.86	3.67	9.55	0.18	6.12	7.82	2.85	1.06	98.07
RD-10	48.10	2.11	16.62	3.93	9.26	0.18	6.10	7.77	2.84	1.03	97.94
RD-9	47.50	1.73	16.64	2.22	8.75	0.16	6.58	8.72	2.54	1.64	96.48
RD-8	48.08	2.08	16.64	3.29	10.26	0.21	6.27	6.79	3.09	1.59	98.30
RD-7	47.61	2.23	16.69	4.39	9.51	0.16	6.18	5.96	3.28	2.69	98.70
RD-5	44.47	3.11	15.94	3.68	10.99	0.20	6.98	8.52	2.97	1.38	98.24
RD-4	45.79	3.56	15.87	3.28	9.66	0.20	3.86	8.88	3.25	2.23	96.58
RD-3	44.70	3.74	15.54	6.27	8.82	0.18	4.89	7.23	2.86	2.71	96.94
RD-2	44.94	3.66	15.51	9.45	6.12	0.23	5.60	8.52	2.82	1.89	98.74
RD-1	49.19	2.34	17.90	10.54	2.24	0.11	1.84	1.66	0.27	11.36	97.45

Table 9. Trace element concentrations and elemental ratios in samples from the Roosevelt Dam sill.

Sample	Cu (ppm)	Sr (ppm)	Rb (ppm)	Rb/Sr	K/Rb	Ca/Sr
RD-11	68	288.4	14.2	0.0491	394	203
RD-12	--	297.8	33.1	0.1112	266	188
RD-10	47	298.0	34.9	0.1171	246	187
RD-9	59	307.9	59.1	0.1919	230	202
RD-8	51	335.2	36.3	0.1084	364	145
RD-7	24	362.5	55.9	0.1542	399	118
RD-5	28	336.8	28.9	0.0859	398	181
RD-4	38	349.9	47.7	0.1363	388	182
RD-3	33	399.0	73.7	0.1847	305	130
RD-2	35	307.2	50.2	0.1634	313	198
RD-1	5	201.1	145.6	0.7239	648	59

Table 10. Norms for samples from the Roosevelt Dam sill.

	RD-11	RD-12	RD-10	RD-9	RD-8	RD-7
Quartz	1.61	--	--	--	--	--
Orthoclase	4.09	6.47	6.30	10.10	9.66	16.25
Albite	28.94	26.46	26.42	23.78	28.54	28.38
Anorthite	32.18	31.11	30.64	30.41	27.62	23.40
Nepheline	--	--	--	--	--	1.04
Wollastonite	3.94	--	--	--	--	--
Diopside	--	7.20	7.44	11.75	5.63	5.47
Hypersthene	19.47	16.55	19.46	6.91	10.08	--
Olivine	--	5.19	2.43	12.12	11.94	17.60
Magnetite	6.69	3.97	4.26	2.42	3.54	4.69
Ilmenite	3.08	3.05	3.05	2.51	2.98	3.18
Hematite	--	--	--	--	--	--
Corundum	--	--	--	--	--	--

	RD-5	RD-4	RD-3	RD-2	RD-1
Quartz	--	--	--	--	--
Orthoclase	8.41	13.93	16.95	11.64	71.17
Albite	21.47	22.84	24.73	26.40	1.21
Anorthite	26.94	23.41	22.84	25.12	8.78
Nepheline	3.64	4.81	1.48	--	0.83
Wollastonite	--	--	--	--	--
Diopside	13.36	18.54	12.11	15.16	--
Hypersthene	--	--	--	3.22	--
Olivine	17.75	7.62	9.42	3.99	4.06
Magnetite	3.97	3.62	6.94	6.85	0.34
Ilmenite	4.47	5.24	5.52	5.32	3.47
Hematite	--	--	--	2.30	7.58
Corundum	--	--	--	--	2.57

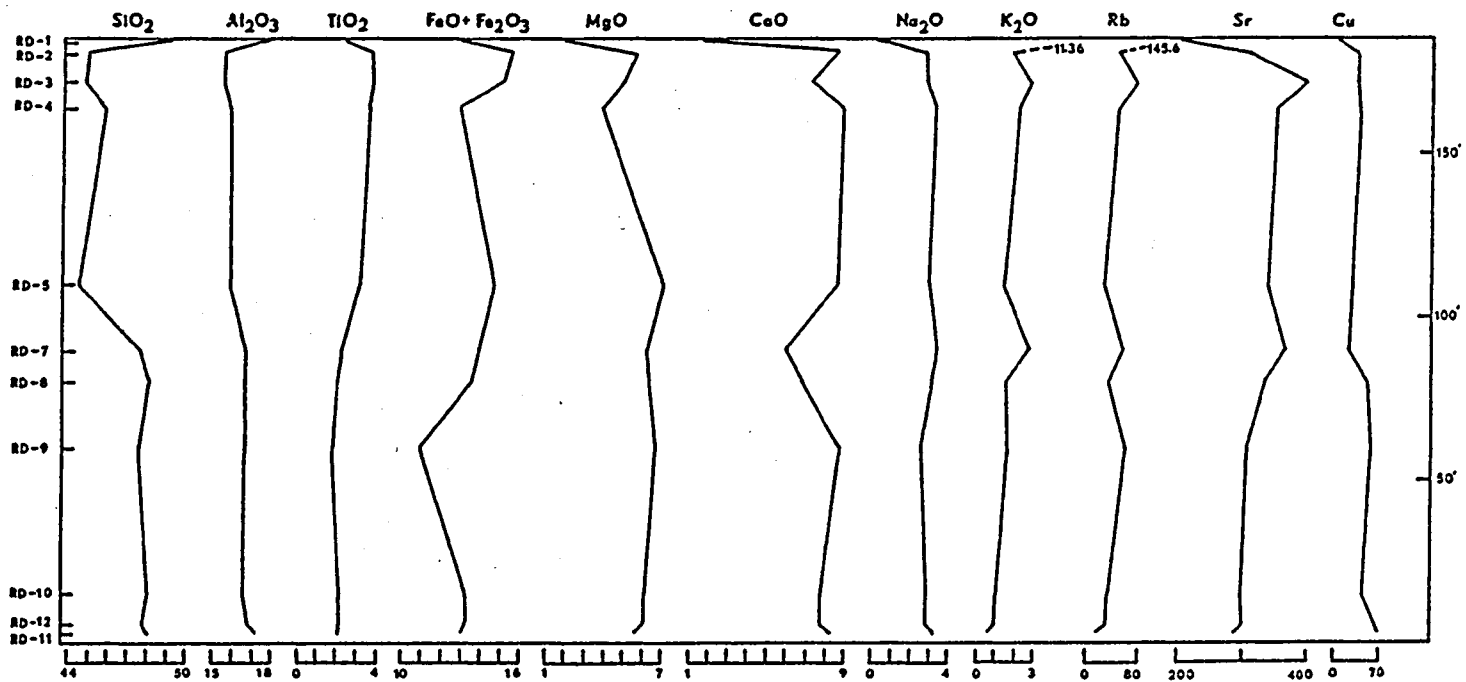


Figure 6. Chemical variations through the Roosevelt Dam sill.  
 Oxides in per cent, trace elements in ppm.

top of the body. Strontium shows little variation except at the top of the sill where it decreases in abundance. Copper is more abundant in the lower part of the sill than in the upper part, but is less abundant overall than in any other bodies investigated. Potassium-rubidium ratios are slightly lower than those in the Salt River Canyon complex while Rb/Sr ratios are higher. Calcium-strontium ratios are similar in the two bodies.

#### Petrogenesis

One of the most notable features of this sill is the extremely high  $K_2O$  content of the fine-grained diabase just below the upper contact. This rock also has unusually high  $SiO_2$ ,  $Al_2O_3$ , and Rb contents and is low in the other major oxides and trace elements when compared to other rocks in this sill. This peculiar chemistry almost certainly results from contamination since those elements most abundant in the overlying sandy shale are most strongly enriched in the diabase. Nehru and Prinz (1970) reported high potassium rocks from the Sierra Ancha complex and concluded that they resulted from the diffusion of fluids from the country rocks into the intrusion.

Chemical and mineralogical differences between the upper and lower parts of the sill suggest that it was emplaced in two stages and is in fact a multiple sill. It is difficult to relate the two parts of the sill by any

differentiation mechanism. The center of the sill is somewhat enriched in  $K_2O$  and Rb (Figure 6, RD-7). This may have resulted from contamination by the overlying sandy shale which would have been in contact with the diabase here if the lower part of the sill represents a separate earlier intrusion. If this interpretation is correct, the upper one-half of the present sill was then emplaced along the contact between the earlier sill and the sandy shale. Variations in other elements are generally consistent with this interpretation.

Fine-grained diabase at the base of the sill (RD-11) is somewhat different from the overlying diabase in its chemistry. Chemical differences here are such that they can not be easily explained by contamination. The standard interpretation that chill zone compositions represent initial magma composition would require that the average composition of the overlying diabase be the same as the chill zone if the magma were emplaced and crystallized as a closed system. This is clearly not the case for the Roosevelt Dam sill (Figure 6). The simplest explanation for the more or less unique composition of the lower fine-grained zone is that the first magma intruded was slightly different in composition from magma intruded later. The sill then crystallized fairly rapidly and underwent no significant differentiation. This is also suggested by

the fine-grained nature of the lower one half of the body. Sometime later more magma was emplaced above this sill forming the upper one half of the present body. This magma apparently cooled more slowly, resulting in coarser textures and permitting olivine crystals to settle giving rise to the olivine rich zone slightly above the center of the present body. Slower cooling would have resulted if the rocks were still hot from the initial intrusion. This might also account for the pronounced interaction between magma and overlying rocks giving rise to the unusually  $K_2O$ -rich upper zone.

## GLOBE COMPLEX

This large mass of diabase is exposed along Arizona Highway 77, 13 miles north of Globe. Fresh rocks are well exposed in road cuts 200 ft south of a small picnic area on the west side of the highway. The relief in the area is relatively small, causing some difficulty in deciphering the exact field relationships. Weathered diabase is exposed at the surface over a large area indicating that the complex is large. The original thickness of the complex is indeterminate since an unknown amount of diabase has been lost through erosion. Field, petrographic, and chemical data all indicate that the complex is a multiple intrusion. A zone of fine-grained diabase approximately 5 ft thick marks the top of a major unit in the complex. This zone dips about 30 degrees toward the north and is overlain by coarser grained diabase which is deeply weathered in most outcrops. The bottom of the complex is in contact with a coarse-grained granite and this contact is roughly parallel to the zone of fine-grained diabase. Samples were collected from the bottom of the sill up to and from the fine-grained zone, a vertical distance of about 100 ft. The complete thickness of this major unit was studied, however, the lower part of the unit may have

been faulted away. This possibility will be discussed in more detail in the following sections.

### Petrography

Eleven samples from the Globe complex were studied in detail. Sample numbers and locations are given in Table 11. This body was selected for study on the basis of petrographic differences between it and other diabases in the same general area. The major differences are the abundances of quartz, orthoclase, and hornblende in this body. The upper fine-grained zone is composed essentially of plagioclase and pyroxene with smaller amounts of magnetite, hornblende, biotite, chlorite, and apatite. Magnetite is unusually abundant and totals approximately 5 per cent of the rock. Some pyroxenes are stained with iron oxides. The texture is subophitic with plagioclase laths averaging 0.6 mm in length. Pyroxenes average about 0.5 mm in diameter and all the magnetite grains are less than 0.2 mm in size.

Sample GD-6 from 10 ft below the top of the fine-grained zone, is slightly more coarse grained. Plagioclase laths average 0.75 mm in length and hornblende, the major mafic mineral, is about 1 mm in diameter. Magnetite is slightly less abundant than in the fine-grained zone, but still is unusually so. Quartz and orthoclase together compose 3 to 5 per cent of the rock and occur in poorly

Table 11. Description and location of samples from the Globe Complex.

Sample Number	Rock Type	Distance Above Base
GD-48	Fine-grained, altered diabase.	1'
GD-47	Fine-grained, altered diabase.	6'
GD-42	Granulated quartz-bearing diabase.	28'
GD-40	Medium-grained quartz-bearing diabase.	40'
GD-14	Medium-grained quartz-bearing diabase. Augite more abundant than in other samples.	50'
GD-11	Fine- to medium-grained quartz-bearing diabase.	55'
GD-9	Fine- to medium-grained quartz-bearing diabase.	65'
GD-8	Medium-grained quartz-bearing diabase.	75'
GD-7	Medium-grained quartz-bearing diabase.	85'
GD-6	Fine-grained quartz-bearing diabase.	90'
GD-5	Fine-grained diabase.	98'

developed micrographic intergrowths. Below sample GD-6 the grain size is larger and shows very little further variation. Plagioclase, augite, and hornblende all average about 1 mm throughout this part of the body. Magnetite remains an important constituent but is not as abundant as in the upper two samples. Most plagioclase is zoned but the average composition is close to  $An_{50}$ . The proportions of hornblende and augite vary but hornblende is much more abundant in most samples.

Pink orthoclase is noticeable in almost all hand samples and occurs as patches up to 2 mm in diameter. In thin section, these patches are rarely pure orthoclase but also contain various amounts of intergrown quartz. In some areas the two minerals are intergrown with a well developed micrographic texture; in other areas the intergrowths are more irregular. Taken together, quartz and orthoclase total between 5 and 10 per cent of each sample from GD-7 through GD-40; the two are usually present in roughly equal amounts.

About 40 ft above the base of the sill the diabase becomes slightly foliated. Rocks in this zone are mineralogically similar to the diabase above but are fractured and granulated. Small fractures are filled with calcite. Below this zone is a gap in exposure of about 20 ft, below which 15 feet of diabase is exposed above the contact with

the granite. This lower zone is homogeneous and different from the diabase above. Quartz and orthoclase are absent and talc, serpentine and chlorite are more abundant than hornblende.

### Chemistry

The chemistry and normative mineralogy of the Globe Complex (Tables 12, 13, and 14) is quite different from that of the Salt River Canyon and Roosevelt Dam diabases. Excluding the two samples from the base of the complex, all samples contain more than 50 per cent  $\text{SiO}_2$ . Titanium falls between 1.50 and 2.00 per cent. All samples are uniformly low in  $\text{Al}_2\text{O}_3$  and relatively high in total iron. Calcium and magnesium are low while alkalis are high compared to the other diabases. No consistent chemical trends are apparent; the most striking feature is the uniformity of the chemistry.

The two samples from near the base of the complex (GD-47 and GD-48) are significantly different from the other samples and are very similar to the Salt River Canyon and Roosevelt Dam rocks. In these two samples  $\text{SiO}_2$  is lower while  $\text{Al}_2\text{O}_3$ ,  $\text{TiO}_2$ , and  $\text{MgO}$  are higher. There are also differences between the trace element contents of these two samples and the rest of the complex. Copper is lower in these rocks than in all other samples except GD-7.

Table 12. Chemical analyses of samples from the Globe Complex.

	SiO <sub>2</sub>	TiO <sub>2</sub>	Al <sub>2</sub> O <sub>3</sub>	Fe <sub>2</sub> O <sub>3</sub>	FeO	MnO	MgO	CaO	Na <sub>2</sub> O	K <sub>2</sub> O	Total
GD-48	46.01	2.94	17.18	6.03	6.85	0.20	5.75	5.81	3.19	1.85	95.81
GD-47	45.69	2.80	17.41	4.61	8.51	0.19	5.96	6.86	3.25	1.25	96.53
GD-42	53.36	1.72	13.31	4.25	8.73	0.14	3.31	5.07	3.94	1.96	95.79
GD-40	52.51	1.70	13.56	3.48	10.19	0.20	4.34	7.38	2.86	1.77	97.99
GD-14	54.51	1.68	13.79	3.23	9.94	0.19	4.19	7.84	2.62	1.54	99.53
GD-11	52.09	1.85	13.67	2.95	11.83	0.21	4.34	7.59	3.06	1.63	99.22
GD-9	53.12	1.82	13.56	5.04	9.20	0.20	4.01	6.89	2.86	1.87	98.57
GD-8	55.46	1.92	13.26	6.86	7.05	0.18	3.10	5.60	3.09	2.56	99.08
GD-7	52.24	1.72	13.40	3.99	10.12	0.21	4.72	6.10	4.69	0.98	98.17
GD-6	52.02	1.80	13.48	5.80	8.88	0.18	4.36	5.98	3.11	1.96	97.57
GD-5	50.82	1.83	13.64	8.48	6.38	0.21	4.51	5.32	5.23	0.37	96.79

Table 13. Trace element concentrations and elemental ratios in samples from the Globe Complex.

Sample	Cu (ppm)	Sr (ppm)	Rb (ppm)	Rb/Sr	K/Rb	Ca/Sr
GD-48	39	458.2	81.7	0.1783	188	91
GD-47	46	532.6	59.5	0.1117	175	92
GD-42	142	169.5	66.5	0.3922	245	214
GD-40	97	189.4	72.8	0.3846	202	279
GD-14	105	174.6	63.1	0.3616	203	321
GD-11	102	177.4	59.6	0.3361	227	306
GD-9	124	226.9	78.1	0.3439	198	217
GD-8	94	210.2	73.8	0.3512	287	190
GD-7	26	193.6	25.2	0.1301	321	225
GD-6	99	192.0	70.9	0.3693	230	223
GD-5	85	98.0	15.2	0.1556	204	388

Table 14. Norms for samples from the Globe Complex.

	GD-48	GD-47	GD-42	GD-40	GD-14	GD-11
Quartz	--	--	5.32	4.56	7.94	1.92
Orthoclase	11.56	7.74	12.34	10.95	9.40	9.97
Albite	30.30	30.58	37.69	26.90	24.32	28.44
Anorthite	28.67	30.64	13.69	19.84	22.05	19.42
Wollastonite	--	--	5.24	7.40	7.26	7.82
Diopside	1.45	4.02	--	--	--	--
Hypersthene	12.53	6.75	18.43	24.06	23.13	26.57
Olivine	4.48	11.13	--	--	--	--
Magnetite	6.67	5.05	4.73	3.81	3.49	3.19
Ilmenite	4.33	4.09	2.55	2.48	2.42	2.67

	GD-9	GD-8	GD-7	GD-6	GD-5
Quartz	7.27	11.61	--	5.81	2.97
Orthoclase	11.55	15.78	5.97	12.20	2.29
Albite	26.85	28.95	43.42	29.42	49.21
Anorthite	19.50	15.40	13.02	17.96	13.27
Wollastonite	6.50	5.44	--	5.32	5.76
Diopside	--	--	14.55	--	--
Hypersthene	20.16	12.55	14.09	20.27	14.54
Olivine	--	--	2.17	--	--
Magnetite	5.51	7.48	4.30	6.39	9.29
Ilmenite	2.65	2.79	2.47	2.64	2.67

Rubidium is approximately the same in both groups of rocks whereas GD-47 and GD-48 are strongly enriched in Sr.

### Petrogenesis

The petrographic and chemical differences between the lower and upper part of the complex reinforce the field evidence for multiple intrusion. It is probable that tectonic movement was involved because of the presence of sheared and granulated rocks. The exact relationships between the two types of diabase can not be determined definitely because of the gap in exposure. The gap results from a small valley that separates two adjacent road cuts and is probably due to more rapid weathering and erosion along the cataclastic zone.

Little can be said regarding the differentiation of this body of diabase. Disregarding the two samples from near the lower contact, the diabase is chemically quite homogeneous. The presence of quartz and orthoclase and the resulting high  $\text{SiO}_2$  and alkali contents indicate that the magma from which these rocks crystallized was much more differentiated than that which gave rise to the Salt River Canyon and Roosevelt Dam rocks. The high total iron values also support a greater degree of differentiation.

## LOOKOUT MOUNTAIN SILLS

Numerous sills and irregular masses of diabase crop out in the northwestern part of the Lookout Mountain Quadrangle. The area has been mapped in detail by Krieger (1968). On Lookout Mountain and in the surrounding area rocks ranging in age from Precambrian to Mississippian are exposed. Older Precambrian Pinal Schist and alaskite are overlain by sedimentary rocks of the Apache Group which, in turn are overlain by Paleozoic sedimentary rocks. The entire area has been faulted and tilted so that the sedimentary rocks generally strike toward the northwest and dip 40 to 50 degrees toward the northeast. Diabase is most abundant in the sedimentary rocks (not differentiated on map), but several sills are present in the alaskite (Figure 7). The best exposures of diabase are in the steep walls of Putnam Wash on the south side of Lookout Mountain. This wash trends nearly normal to the regional strike, exposing a large portion of the geologic section in its walls.

Most of the diabase in the sedimentary rocks is weathered to some extent or is faulted so that relationships are obscured. In the deeper part of the wash, two fresh sills are exposed in the alaskite and these two sills

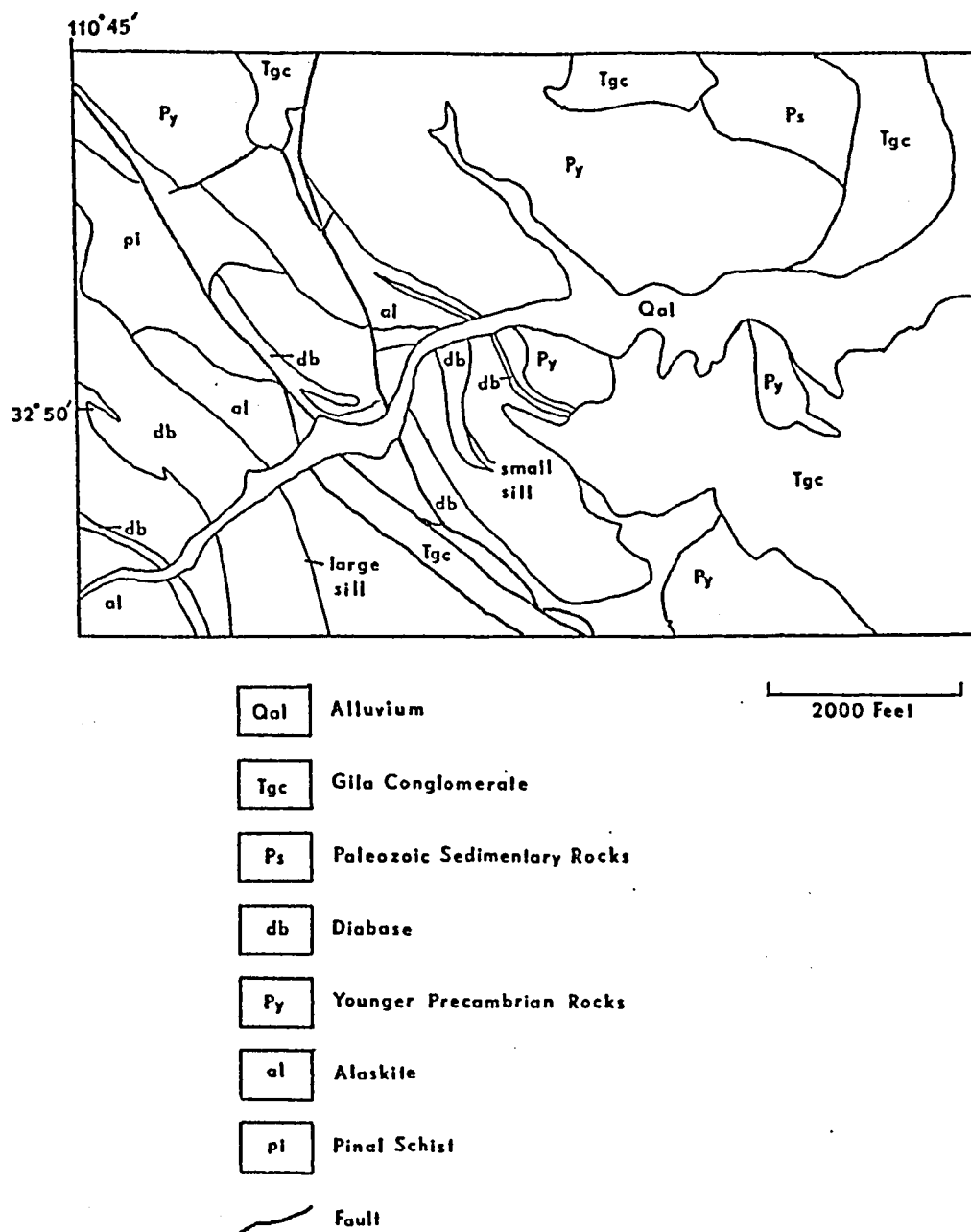


Figure 7. Geologic map of the Lookout Mountain area.

Modified from Krieger, 1968.

were selected for detailed study. The smaller of the two sills crops out 1.3 miles west of the intersection of Aravaipa Creek and the San Pedro River. The sill dips 34 degrees to the east and is 100 ft thick. The larger sill is 2100 ft west of the smaller one, dips 58 degrees to the east, and is 674 ft thick. Both sills have roughly the same orientation as the sedimentary rocks which overlie the alaskite indicating that the sills were probably horizontal at the time of emplacement.

#### Petrography of the Small Sill

Samples collected from this sill are listed in Table 15. All samples from the small sill exhibit a subophitic texture. Plagioclase is the most abundant mineral and ranges in size from about 0.4 mm at the contacts to 1.2 mm near the center of the sill. Most crystals are normally zoned with cores ranging between  $An_{56}$  and  $An_{62}$ . Augite is the next most abundant mineral with a size range similar to plagioclase. In the upper one half of the sill hornblende becomes more abundant at the expense of augite. All samples contain some quartz, orthoclase and magnetite. Small amounts of biotite, chlorite, and apatite are present. Plagioclase and quartz are more abundant in the upper part of the sill.

Table 15. Description and location of samples from the small Lookout Mountain sill.

Sample Number	Rock Type	Distance Above Base
LMD-46	Fine-grained oxidized diabase.	6"
LMD-26	Fine-grained diabase.	1'
LMD-27	Fine-grained diabase.	5'
LMD-28	Fine-grained diabase.	20'
LMD-29	Medium-grained diabase.	40'
LMD-30	Medium-grained diabase.	65'
LMD-31	Fine-grained diabase.	85'
LMD-32	Fine-grained diabase.	97'
LMD-58	Fine-grained diabase.	99'

### Chemistry of the Small Sill

Chemical analyses and norms of nine samples from the small sill are listed in Tables 16, 17, and 18 and chemical variations are plotted in Figure 8. The overall chemistry is somewhat similar to that of the Globe Complex and distinctly different from the Salt River Canyon and Roosevelt Dam diabases. Silica exceeds 50 per cent in all samples, but the alkali content is relatively low. Calcium and MgO are high in most samples while total iron and TiO<sub>2</sub> are low when compared with the diabases previously described. Rubidium is higher in this sill with two samples containing more than 100 parts per million. The high Rb and moderately low K<sub>2</sub>O result in very low K/Rb ratios. Copper values are also higher in these rocks than in most of those discussed previously while Sr values are lower.

Almost all elements show systematic variations with respect to position within the sill (Figure 8). Silica, TiO<sub>2</sub>, K<sub>2</sub>O, Rb, and total iron are more concentrated near the upper and lower contacts of the sill. Conversely, the central part of the sill is enriched in MgO and CaO. Sodium and Al<sub>2</sub>O<sub>3</sub> show little variation from bottom to top. Overall the central part of the sill is more mafic. This sill is very similar to the larger Lookout Mountain sill and the petrogenesis of the two bodies will be discussed together in a later section.

Table 16. Chemical analyses of samples from the small Lookout Mountain sill.

	SiO <sub>2</sub>	TiO <sub>2</sub>	Al <sub>2</sub> O <sub>3</sub>	Fe <sub>2</sub> O <sub>3</sub>	FeO	MnO	MgO	CaO	Na <sub>2</sub> O	K <sub>2</sub> O	Total
LMD-46	53.12	1.34	14.61	6.15	4.70	0.13	4.20	7.94	2.64	1.42	96.22
LMD-26	52.52	1.31	13.70	3.89	7.89	0.17	5.35	8.97	2.43	1.33	97.56
LMD-27	52.72	1.29	13.87	3.73	8.11	0.20	5.69	8.59	2.57	1.53	98.30
LMD-28	52.33	1.26	13.94	3.38	8.12	0.19	6.02	9.83	2.29	1.09	98.45
LMD-29	51.35	1.09	13.87	2.92	7.46	0.20	6.74	10.87	2.66	1.07	98.23
LMD-30	51.56	1.04	13.92	2.62	8.20	0.19	6.42	9.60	2.61	1.19	97.35
LMD-31	51.91	1.26	13.93	3.68	8.25	0.18	5.29	8.82	2.68	1.56	97.56
LMD-32	52.68	1.24	13.94	3.51	8.22	0.20	5.71	8.97	2.42	1.52	98.41
LMD-58	52.92	1.20	13.75	5.77	6.20	0.18	5.29	8.52	2.53	1.73	98.09

Table 17. Trace element concentrations and elemental ratios in samples from the small Lookout Mountain sill.

Sample	Cu (ppm)	Sr (ppm)	Rb (ppm)	Rb/Sr	K/Rb	Ca/Sr
LMD-46	159	164.9	64.6	0.3917	183	344
LMD-26	124	162.3	75.9	0.4675	145	395
LMD-27	114	189.5	101.2	0.5339	125	324
LMD-28	127	161.6	56.8	0.3516	158	435
LMD-29	51	150.3	59.5	0.3962	150	517
LMD-30	119	179.3	66.6	0.3711	149	383
LMD-31	82	189.0	86.0	0.4550	150	334
LMD-32	148	182.4	90.3	0.4950	140	351
LMD-58	117	196.4	111.7	0.5688	129	310

Table 18. Norms for samples from small Lookout Mountain sill.

	LMD-46	LMD-26	LMD-27	LMD-28	LMD-29
Quartz	11.62	6.48	4.90	5.23	0.81
Orthoclase	8.91	8.22	9.36	6.66	6.49
Albite	25.19	22.83	23.90	21.27	24.52
Anorthite	25.33	23.61	22.58	25.40	23.36
Wollastonite	6.62	9.19	8.63	10.02	12.80
Hypersthene	13.52	23.50	24.73	25.95	27.32
Olivine	--	--	--	--	--
Magnetite	6.83	4.26	4.04	3.66	3.13
Ilmenite	6.62	1.91	1.86	1.82	1.56

	LMD-30	LMD-31	LMD-32	LMD-58
Quartz	1.89	3.70	4.93	7.63
Orthoclase	7.30	9.62	9.29	10.64
Albite	24.33	25.11	22.49	23.66
Anorthite	23.63	22.31	23.49	21.94
Wollastonite	10.33	9.34	9.03	8.84
Hypersthene	28.19	24.07	25.18	19.28
Olivine	--	--	--	--
Magnetite	2.84	4.01	3.80	4.07
Ilmenite	1.50	1.83	1.79	1.74

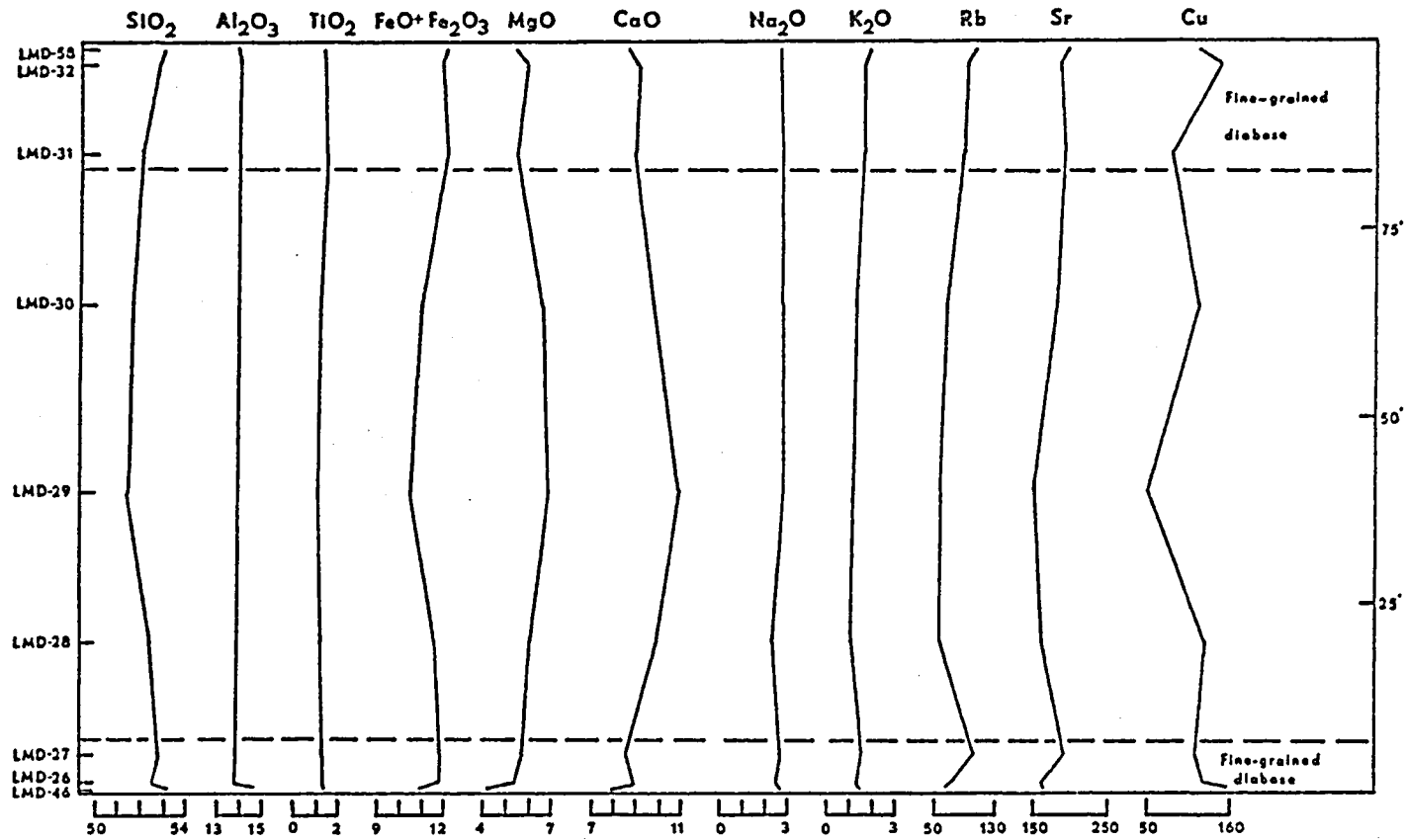


Figure 8. Chemical variations through the small Lookout Mountain sill.

Oxides in per cent, trace elements in ppm.

### Petrography of the Large Sill

The larger sill is petrographically similar to the small sill with two exceptions (Table 19). Exceptions are the presence of a well developed pegmatitic phase approximately 200 ft below the top of the sill, and the presence of orthorhombic pyroxenes. The diabase is fine grained near the contacts and medium grained in the center. Most of the plagioclase is normally zoned with compositions between  $An_{50}$  and  $An_{60}$ . Augite is the most abundant pyroxene in all parts of the sill and is the only pyroxene in samples from near the contacts and near the pegmatitic zone. Because of the more complex mineralogy of this sill, each thin section was point counted in order to better determine mineralogical variations. Modal analyses are listed in Table 20 and variations in mineralogy are shown in Figure 9.

Orthorhombic pyroxenes occur as phenocrysts up to 5 mm in diameter and reach their maximum abundance about 200 ft above the base of the sill. They never compose more than 10 per cent of the rock by volume. Most grains are zoned with rims having higher birefringence; the composition of the center is near  $Fs_{25}$ . The higher birefringence of the rims indicates a higher iron content.

Pegmatitic material occurs in irregular pods just below a 15 ft thick zone of massive diabase pegmatite.

Table 19. Description and location of samples from the large Lookout Mountain sill.

Sample Number	Rock Type	Distance Above Base
LMD-7	Fine-grained diabase.	3'
LMD-8	Fine-grained diabase.	22'
LMD-9	Fine-grained diabase.	45'
LMD-10	Medium-grained diabase.	85'
LMD-11	Medium-grained diabase with sparse hypersthene phenocrysts.	135'
LMD-12	Medium-grained hypersthene diabase.	190'
LMD-13	Medium-grained hypersthene diabase.	265'
LMD-14	Medium-grained hypersthene diabase.	315'
LMD-15	Medium-grained diabase.	380'
LMD-16	Medium-grained diabase.	440'
LMD-17	Diabase pegmatite.	480'
LMD-18	Medium-grained diabase with minor hypersthene.	525'
LMD-19	Medium-grained diabase with minor hypersthene.	580'
LMD-20	Medium-grained diabase.	610'
LMD-21	Medium-grained diabase.	635'
LMD-22	Fine-grained altered diabase.	655'
LMD-23	Fine-grained diabase.....	670'

Table 20. Modal analyses of samples from the large Lookout Mountain sill.

1000 points counted for each sample.

	LMD-7	LMD-8	LMD-9	LMD-10	LMD-11	LMD-12
Plagioclase	46.2	45.9	49.3	47.9	44.4	46.4
Augite	31.6	33.9	39.2	39.3	38.7	32.0
Hypersthene	--	--	trace	--	2.6	9.7
Hornblende	3.7	3.5	1.5	1.1	0.5	1.6
Opaques	4.0	3.1	2.0	2.1	2.3	2.6
Biotite	1.9	1.7	1.1	1.1	1.8	1.3
Orthoclase	7.5	6.1	3.9	4.7	5.6	3.7
Quartz	4.9	5.8	3.0	3.8	4.1	2.7
Others*	0.2	trace	trace	trace	trace	trace
	LMD-13	LMD-14	LMD-15	LMD-16	LMD-17	LMD-18
Plagioclase	46.7	49.2	46.8	42.6	31.6	47.6
Augite	34.6	33.0	34.4	35.0	12.4	35.2
Hypersthene	9.5	5.2	--	--	--	0.8
Hornblende	0.8	1.8	3.2	8.2	17.5	2.8
Opaques	1.5	1.6	4.3	2.0	6.2	3.2
Biotite	1.1	2.0	0.7	2.1	1.7	0.6
Orthoclase	2.6	3.7	6.1	6.5	11.9	5.6
Quartz	3.2	3.5	4.5	3.6	14.0	4.2
Others*	trace	trace	trace	trace	4.7	trace
	LMD-19	LMD-20	LMD-21	LMD-22	LMD-23	
Plagioclase	43.2	47.5	43.0	44.9	46.8	
Augite	31.4	33.8	21.9	15.9	31.2	
Hypersthene	0.7	--	--	--	--	
Hornblende	3.2	8.2	17.5	30.6	0.6	
Opaques	3.2	3.8	4.1	2.3	5.5	
Biotite	1.7	3.3	3.8	1.4	3.3	
Orthoclase	7.3	3.7	4.9	3.1	6.0	
Quartz	7.4	4.4	4.7	1.8	6.6	
Others*	trace	trace	trace	trace	trace	

\*Includes apatite, chlorite, calcite, hematite, and serpentine. In some sections plagioclase is partially altered to sericite, but sericite was not counted separately.

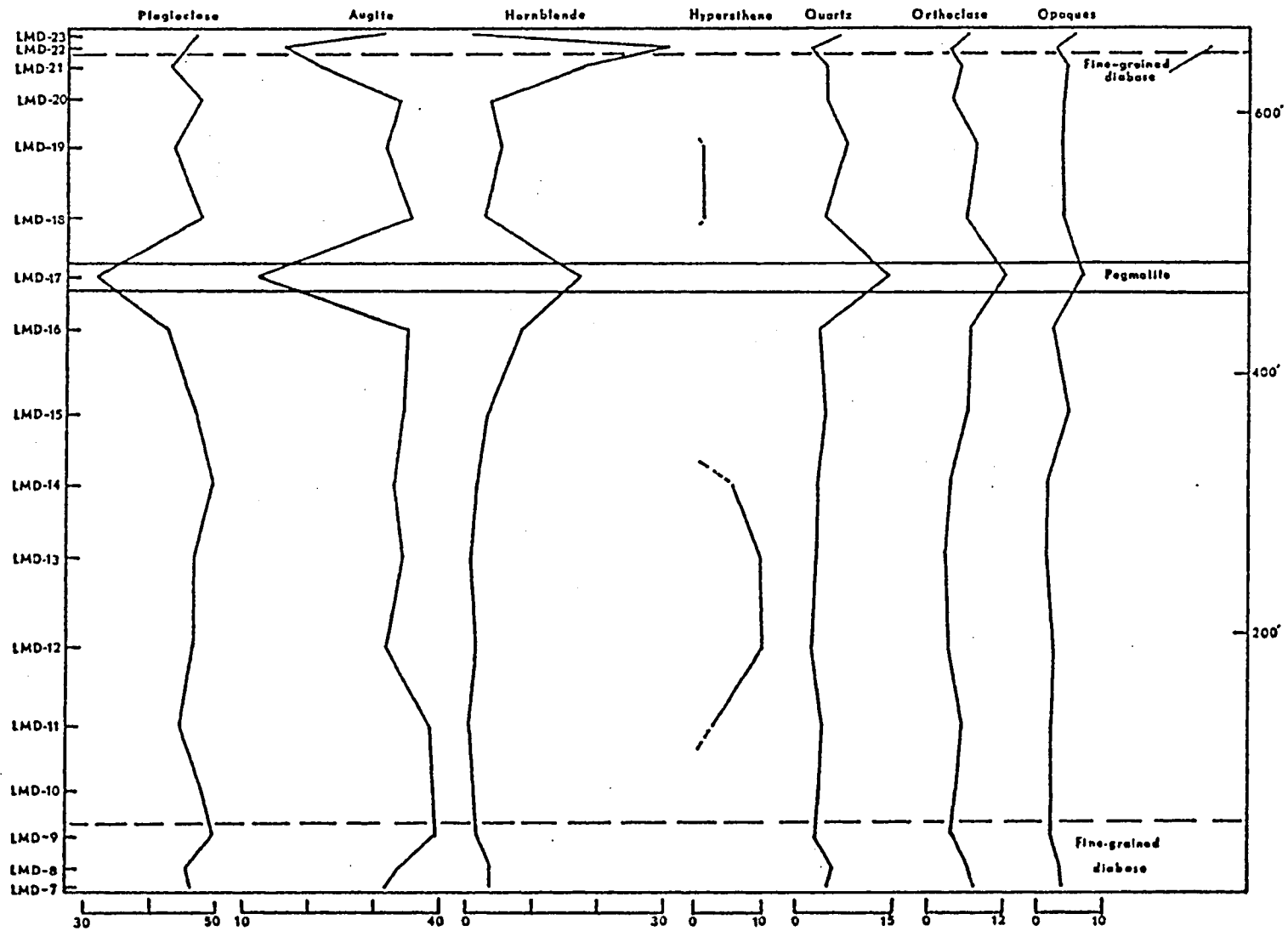


Figure 9. Modal variations through the large Lookout Mountain sill.

The coarse-grained pegmatite is composed largely of plagioclase, augite, and hornblende. Plagioclase is similar to that in the normal diabase but shows strong deuteric alteration to sericite. Augite occurs as elongated curved crystals several millimeters in length. Hornblende surrounds augite and also occurs as discrete crystals. It is strongly pleochroic from pale green to dark blue-green and some crystals are zoned. Quartz and orthoclase occur together in a well developed graphic intergrowth. Opaques are more abundant and more coarse grained than in the normal diabase. Chlorite is rather abundant and often occurs as medium-grained fan-shaped aggregates. Smith (1969) described similar chlorite in diabase pegmatites and concluded that it was a primary mineral. The coarse grain size of the pegmatite causes difficulty in determining the exact mineral percentages. The modal values listed in Table 20 represent 500 points counted in each of two thin sections from the same hand sample.

#### Chemistry of the Large Sill

The chemistry and normative mineralogy of the large sill are very similar to that of the small sill already described (Tables 21, 22, and 23). Overall, the sill is high in  $\text{SiO}_2$  but relatively low in alkalis. All samples contain more than 50 per cent  $\text{SiO}_2$  while  $\text{Na}_2\text{O}+\text{K}_2\text{O}$  ranges between 3 and 4 per cent. Titanium,  $\text{Al}_2\text{O}_3$ , and total iron

Table 21. Chemical analyses of samples from the large Lookout Mountain sill.

	SiO <sub>2</sub>	TiO <sub>2</sub>	Al <sub>2</sub> O <sub>3</sub>	Fe <sub>2</sub> O <sub>3</sub>	FeO	MnO	MgO	CaO	Na <sub>2</sub> O	K <sub>2</sub> O	Total
LMD-7	52.14	1.18	14.00	3.89	7.54	0.19	6.42	9.72	2.42	1.17	98.67
LMD-8	52.16	1.09	14.18	3.17	7.84	0.19	6.67	10.11	2.39	1.18	98.98
LMD-9	51.96	0.99	14.41	2.67	7.55	0.18	7.32	10.79	2.27	0.88	99.02
LMD-10	51.41	1.01	14.27	2.77	7.60	0.18	6.87	10.66	2.27	0.93	97.97
LMD-11	51.56	0.92	14.40	2.37	7.52	0.18	7.36	11.31	2.21	0.78	98.61
LMD-12	51.48	0.92	14.61	2.30	7.48	0.18	7.27	11.18	2.21	0.76	98.39
LMD-13	51.17	0.88	14.02	2.14	7.60	0.18	7.81	10.83	2.18	0.81	97.62
LMD-14	51.85	0.81	14.89	2.23	7.01	0.16	7.68	11.70	2.26	0.83	99.42
LMD-15	52.36	0.97	14.09	1.86	8.77	0.20	6.26	10.10	2.35	0.87	97.83
LMD-16	52.32	1.26	14.08	2.90	9.01	0.20	6.18	9.96	2.36	1.01	99.28
LMD-17	53.41	1.96	13.24	5.12	9.27	0.21	3.90	6.89	2.71	1.87	98.56
LMD-18	52.27	0.99	14.92	2.22	7.97	0.18	6.13	9.82	2.55	1.07	98.12
LMD-19	51.63	1.16	14.08	4.42	6.75	0.19	6.18	9.66	2.40	1.22	97.69
LMD-20	52.10	1.20	14.05	4.58	6.70	0.18	5.80	9.67	2.36	1.16	97.80
LMD-21	51.47	1.33	13.76	4.05	8.07	0.23	5.83	8.86	2.69	1.46	97.75
LMD-22	52.86	1.07	12.77	2.03	9.39	0.21	6.13	9.07	3.34	1.05	98.92
LMD-23	53.12	1.22	13.92	7.14	4.50	0.24	4.86	9.09	2.64	1.35	98.08

Table 22. Trace element concentrations and elemental ratios in samples from the large Lookout Mountain sill.

Sample	Cu (ppm)	Sr (ppm)	Rb (ppm)	Rb/Sr	K/Rb	Ca/Sr
LMD-7	124	149.9	48.9	0.3259	198	464
LMD-8	123	163.3	51.0	0.3125	192	443
LMD-9	131	154.3	35.4	0.2297	206	500
LMD-10	111	162.1	37.4	0.2308	206	470
LMD-11	110	161.4	30.9	0.1917	210	501
LMD-12	113	155.2	28.3	0.1821	223	515
LMD-13	113	150.7	32.7	0.2169	205	514
LMD-14	106	162.7	36.1	0.2220	191	514
LMD-15	142	153.5	32.6	0.2127	221	470
LMD-16	170	159.8	37.6	0.2354	223	446
LMD-17	90	151.2	73.1	0.4832	212	290
LMD-18	117	167.6	41.3	0.2463	215	419
LMD-19	117	177.0	54.3	0.3066	186	390
LMD-20	113	159.8	50.8	0.3179	189	432
LMD-21	135	185.2	75.4	0.4074	160	342
LMD-22	101	123.7	58.2	0.4700	149	525
LMD-23	114	167.0	66.4	0.3975	169	389

Table 23. Norms for samples from the large Lookout Mountain sill.

	LMD-7	LMD-8	LMD-9	LMD-10	LMD-11	LMD-12
Quartz	4.28	2.97	2.47	2.69	1.97	2.10
Orthoclase	7.11	7.13	5.30	5.67	4.71	4.60
Albite	22.36	21.95	20.76	21.02	20.28	20.32
Anorthite	24.59	25.05	27.04	26.83	27.67	28.38
Wollastonite	10.02	10.51	11.00	11.09	11.87	11.37
Hypersthene	25.78	27.45	29.19	28.26	29.67	29.46
Olivine	--	--	--	--	--	--
Magnetite	4.18	3.39	2.84	2.99	2.53	2.46
Ilmenite	1.69	1.55	1.40	1.45	1.31	1.31
	LMD-13	LMD-14	LMD-15	LMD-16	LMD-17	LMD-18
Quartz	1.55	1.00	3.67	3.78	8.70	2.82
Orthoclase	4.93	4.95	5.32	6.12	11.59	6.51
Albite	20.16	20.48	21.85	21.72	25.52	23.57
Anorthite	26.87	28.31	26.24	25.48	19.35	26.88
Wollastonite	11.39	12.11	11.33	10.07	6.60	9.31
Hypersthene	31.54	29.65	29.23	27.93	19.75	27.12
Olivine	--	--	--	--	--	--
Magnetite	2.30	2.35	2.01	3.11	5.61	2.39
Ilmenite	1.26	1.14	1.40	1.80	2.86	1.42
	LMD-19	LMD-20	LMD-21	LMD-22	LMD-23	
Quartz	4.94	6.46	3.14	0.06	10.32	
Orthoclase	7.49	7.14	8.98	6.32	8.33	
Albite	22.41	22.07	25.14	30.56	24.75	
Anorthite	25.01	25.34	22.03	19.86	23.13	
Wollastonite	9.93	9.85	9.49	10.40	9.58	
Hypersthene	23.73	22.41	24.89	29.11	14.32	
Olivine	--	--	--	--	--	
Magnetite	4.80	4.99	4.41	2.16	7.79	
Ilmenite	1.68	1.74	1.93	1.52	1.77	

are low when compared with the Salt River Canyon and Roosevelt Dam rocks. Magnesium and CaO are generally similar to the other rocks but are distinctly higher than in the Globe Complex. Rubidium and copper values are high while Sr is low, resulting in low K/Rb ratios and high Rb/Sr and Ca/Sr ratios.

Figure 10 shows the vertical chemical variation through the sill. Most elements show a systematic variation with position within the sill similar to that noted in the small sill, except for the presence of the pegmatitic zone. The fine-grained diabase at the upper and lower contacts is similar in composition. The most mafic rocks are found in a zone extending from about 50 ft above the lower contact to about 350 ft above the base. Throughout this zone  $\text{SiO}_2$ ,  $\text{TiO}_2$ , Fe,  $\text{Na}_2\text{O}$ ,  $\text{K}_2\text{O}$ , and Rb are relatively low while MgO and CaO are higher. Aluminum is slightly higher in this zone. The maximum concentration of orthorhombic pyroxene occurs within this mafic part of the sill and probably accounts for the higher MgO content. Orthoclase and quartz are less abundant in this part of the sill, consistent with the lower  $\text{SiO}_2$  and alkali values.

The pegmatite zone is enriched in  $\text{SiO}_2$ ,  $\text{TiO}_2$ , Fe,  $\text{Na}_2\text{O}$ ,  $\text{K}_2\text{O}$ , and Rb and depleted in  $\text{Al}_2\text{O}_3$ , MgO, CaO, and Cu. Samples from just below the pegmatite show the same relative enrichments and depletions for most of these elements to a

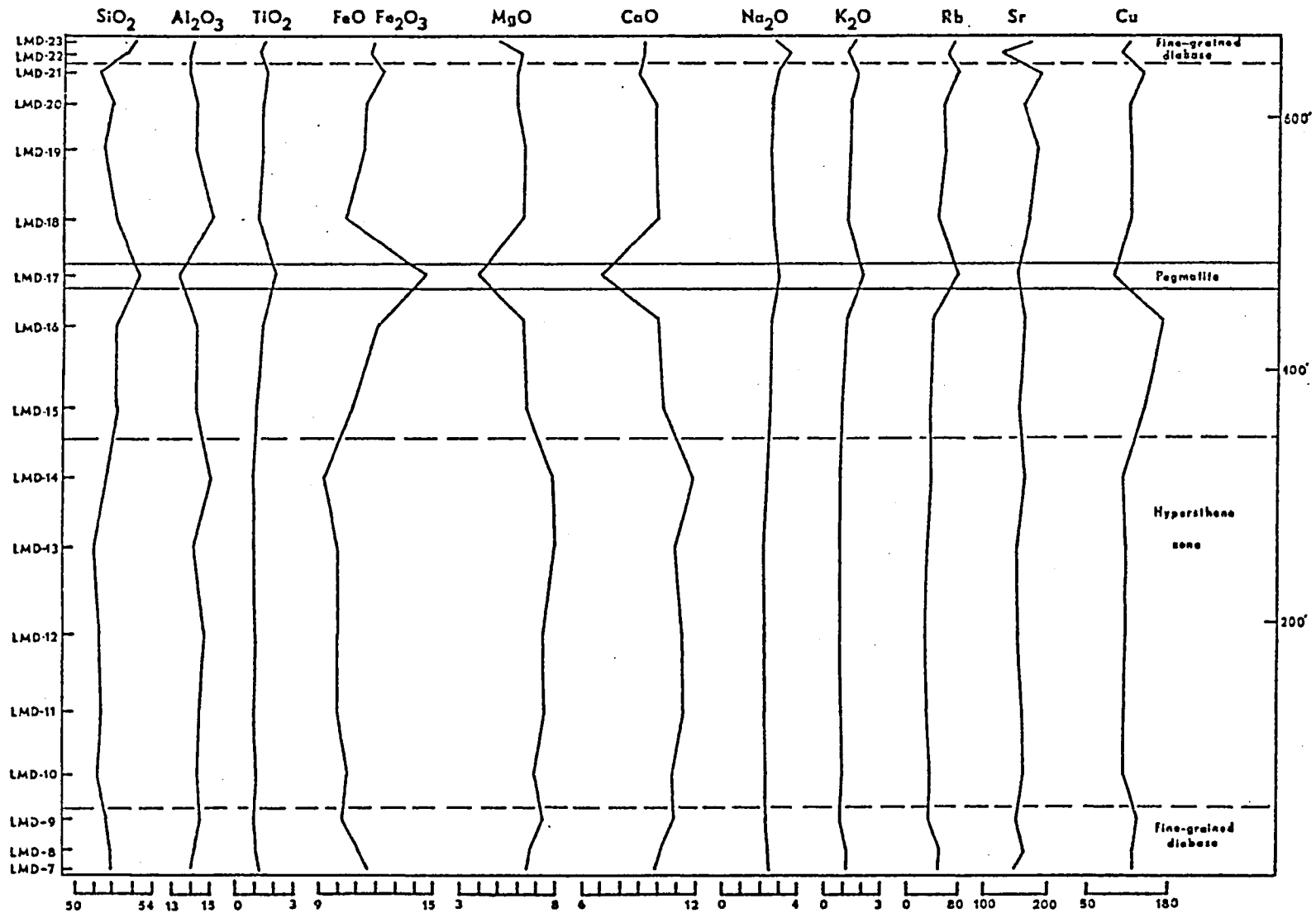


Figure 10. Chemical variations through the large Lookout Mountain sill.

Oxides in per cent, trace elements in ppm.

lesser extent. Copper is the major exception, being more abundant just below the pegmatite but less abundant in the pegmatite. Therefore, a process is suggested which culminated in the crystallization of the pegmatite but was also involved in the crystallization of the diabase immediately underlying the pegmatite.

#### Petrogenesis of the Lookout Mountain Sills

The large sill is remarkably similar to a diabase sill in Victoria Land, Antarctica described by Hamilton (1965). The two sills are approximately the same thickness, both have a central zone more mafic in composition than the fine-grained margins, and both have well developed pegmatitic zones overlying the mafic central zone. The overall chemistry of the two sills is very similar and both contain orthorhombic pyroxenes in their central and lower parts. Hamilton (1965) proposed the process of liquid fractionation to account for these features. According to this theory, after the emplacement of the magma and crystallization of the fine-grained contact zones, concentration gradients developed in the remaining magma in response to temperature and pressure gradients. The most soluble, most volatile, and lowest crystallization temperature components become concentrated in the upper parts of the magma leaving a more mafic magma in the lower and central parts. This more mafic magma crystallizes

to gabbro or diabase while the upper levels crystallize to diabase enriched in  $\text{SiO}_2$  and alkalis, with pegmatite and granophyre forming at the highest level.

Almost all of the features observed in the large Lookout Mountain sill can be satisfactorily explained by the liquid fractionation model if one accepts the basic mechanism. It seems questionable, however, that significant pressure gradients would develop in a sill 674 ft thick. Local temperature gradients might result if heat were lost more rapidly from one contact than from the other. This possibly could occur if large scale crystal settling formed an insulating layer at the base of the sill. However, there is no evidence for such a degree of crystal settling. Even if temperature gradients were established, it does not necessarily follow that they would cause the concentration gradients described by Hamilton in all cases. The liquid fractionation model does not explain the presence of the orthorhombic pyroxene phenocrysts, although their presence does not necessarily conflict with such a process.

The compositional and mineralogical zoning could possibly be due to multiple intrusion; however, this seems unlikely. There are no internal chilled zones and the changes in texture, mineralogy, and chemistry are all gradational.

The process of flow differentiation has recently been proposed to account for features observed in some sills (Simkin, 1967; Bhattacharji, 1967). According to this model, crystals within an intruding magma will tend to be concentrated near the center of the sill during flow. The larger size of the orthopyroxene crystals suggests that they were probably present when the magma was intruded. Flow differentiation and the later superimposed effects of gravity could account for their maximum concentration just below the center of the sill and their absence near the upper and lower contacts. The abundance of orthorhombic pyroxenes can, at least in part, account for the more mafic nature of the lower central part of the sill. Crystallization proceeding inward from both the top and the bottom of the sill, perhaps aided by minor crystal settling, could result in the position of the most differentiated material slightly above the center of the sill. The diabase pegmatite represents the very last portion of the magma to crystallize. The presence of hornblende and chlorite and the deuteric alteration of plagioclase indicate a high concentration of volatiles. Deuteric alteration noted in some samples from the upper part of the sill resulted from upward moving volatiles during the final stages of solidification.

One feature common to both Lookout Mountain sills is an interior zone more mafic in composition than the fine-grained contact zones. In the larger sill this can be attributed, in part, to the presence of orthorhombic pyroxenes in this zone. The smaller sill shows an almost symmetrical increase in MgO and CaO away from the contacts and a similarly symmetrical decrease in SiO<sub>2</sub>, TiO<sub>2</sub>, Fe, and K<sub>2</sub>O. Magnesium and CaO both show a sharp decrease within a few feet of the contacts (Figure 8). Potassium increases rather sharply near both contacts while SiO<sub>2</sub> increases sharply at the lower contact and slightly near the upper contact. Rubidium is concentrated at the upper contact but is only slightly concentrated at the lower contact relative to the center of the sill, but it is considerably less abundant at the contact than a few feet above the contact. Any proposed mechanism of emplacement and differentiation should explain these chemical variations.

The observed chemical variations might result from the mechanics of emplacement if certain conditions existed in a magma chamber before intrusion. It is well known, from studies of fluid flow in a conduit, that velocities are lowest near the walls of the conduit and greatest near the center. If it is assumed that compositional gradients can develop in a large magma chamber with less mafic magma near the chamber top, and that such a magma then intruded

as sills, then the observed chemical variations might be explained. At a given point horizontally along the forming sill, the first magma to arrive would be the least mafic. Magma near the top and bottom of the opening sill would move slowest due to the boundary effects of the conduit and movement would be further retarded if cold country rocks chilled the adjacent magma causing an increase in viscosity. If chilling also caused crystallization, the viscosity would increase greatly. Magma would still move freely near the center of the opening sill and, if emplacement covered some significant time period, more mafic magma from deeper within the magma chamber could occupy the central part of the sill. After emplacement of the large sill was completed, the magma underwent some differentiation in place to form the pegmatite and the slightly differentiated material beneath it. The small sill apparently crystallized too rapidly for this to occur.

Figure 11 shows that the small sill is slightly more differentiated than most parts of the large one. This can be explained if it crystallized from magma removed earlier from the top of the stratified magma chamber. Magma removed from a lower level would be more mafic and could give rise to the large sill. Orthorhombic pyroxenes that had crystallized and sunk to deeper levels in the chamber were carried by this magma when it was emplaced.

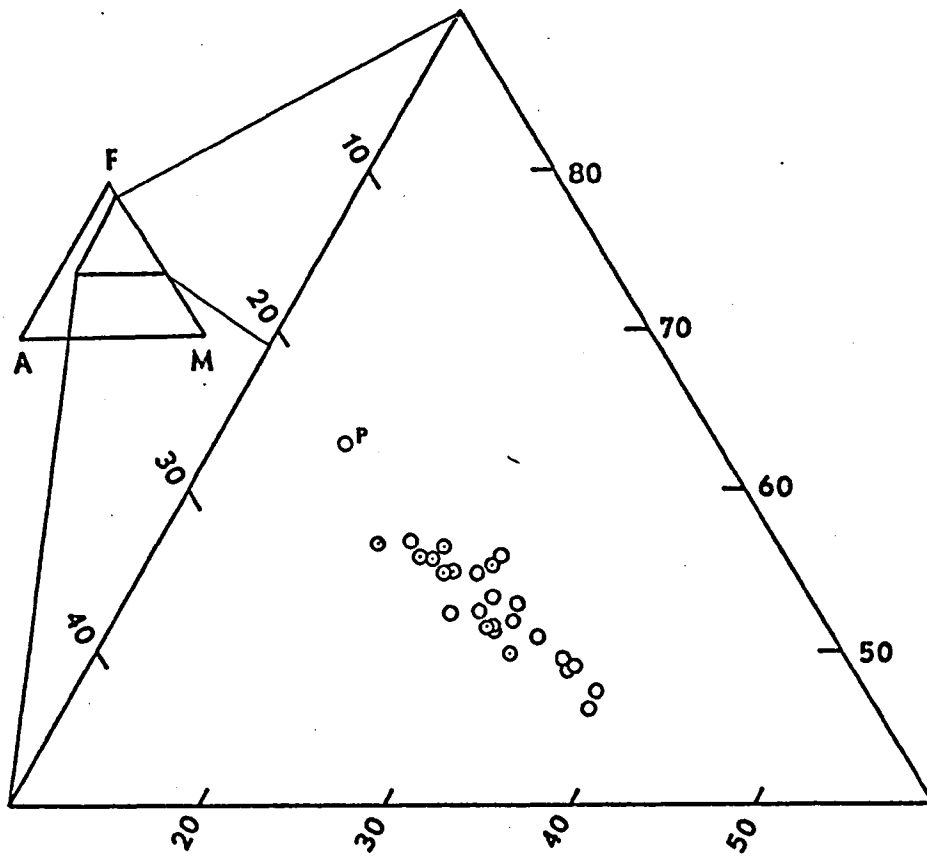


Figure 11, A M F diagram of the Lookout Mountain diabases.

Circles: large sill; circles with dots: small sill; P: diabase pegmatite.

Both sills show the same differentiation trend (Figure 11). This supports the derivation of the two sills from the same parent magma.

This proposed mechanism requires some special conditions which may or may not be realistic. The major requirement is a stratified initial magma chamber. A chamber of fairly large vertical dimensions would have greater pressure and temperature gradients than a thin sheet, possibly resulting in chemical gradients. A second requirement is that magma is removed first from that part of the chamber where the magma is less mafic, presumably near the top. Also, intrusion rates are thought to be rapid which might prevent the border chilling suggested. Finally, large volumes of magma would have to be removed. The abundance of diabase in the Lookout Mountain area indicates that this latter requirement could be satisfied.

Another possible explanation of the noted chemical variations is that the contact zones have been contaminated with material from the alaskite which is rich in  $\text{SiO}_2$  and alkalis. The strong enrichment in  $\text{K}_2\text{O}$  and Rb in the upper few inches of the Roosevelt Dam sill almost certainly resulted from contamination, and suggests that the same thing could happen on a smaller scale in other sills. This possibility will be discussed in more detail below.

### Petrography and Chemistry of the Alaskite

In order to better evaluate the possibility of contamination, six samples of alaskite were collected. Two of these were obtained well away from any diabase, three are from within 3 in of the diabase contact, and one is a xenolith from the upper part of the large sill. These samples were examined in thin section and chemically analysed.

The normal alaskite away from the diabase is medium grained with a pinkish red color. Mineralogically the rock is composed of plagioclase (24.5 per cent), quartz (36.1 per cent), orthoclase (37.8 per cent), and biotite (1.5 per cent). Plagioclase is slightly sericitized and biotite is partially replaced by chlorite. Orthoclase is mostly unaltered but contains abundant very fine-grained hematite which is responsible for the pink color of the rock. Some of the larger plagioclase grains are slightly granulated along their margins and most of the larger quartz grains are strained.

Alaskite at the contacts is very similar to that just described. In sample A-3, quartz and orthoclase are finer grained near the contact while plagioclase remains unchanged. Orthoclase contains fewer inclusions, but hematite is concentrated at grain boundaries. Orthoclase is complexly twinned in this rock in contrast to the other

samples in which it is untwinned. Biotite is a deep red-brown and chlorite is absent. The other two contact samples also contain clearer orthoclase than the two samples away from the diabase but are otherwise similar. Sample A-6 is a xenolith 5 in in diameter from near the top of the large sill and is the only xenolith seen in any of the sills examined. It has a fine-grained interlocking texture commonly seen in rocks that have undergone recrystallization. Chlorite is much more abundant than in the other samples and is the only mafic mineral present.

Chemical analyses of the six alaskite samples are listed in Table 24 and shown graphically in Figure 12. With the exception of A-5 there are consistent chemical differences between the contact samples and the other samples. A-5 was obtained from the lower contact of the sill while the other samples are from the upper contact. In general, the contact samples are enriched in  $\text{Al}_2\text{O}_3$ ,  $\text{TiO}_2$ , Fe, MgO, CaO,  $\text{Na}_2\text{O}$ , and Sr, and depleted in  $\text{SiO}_2$ ,  $\text{K}_2\text{O}$ , and Rb relative to the normal alaskite. Overall, the tendency is toward enrichment in those elements more abundant in diabase than alaskite and depletion in those elements relatively more abundant in the alaskite. Sodium is the major exception to this tendency and is higher in the contact samples than in the normal alaskite; however, the  $\text{Na}_2\text{O}$  content of the normal alaskite is only slightly

Table 24. Chemical analyses of alaskite.

A-1, A-2, representative alaskite. A-3, A-4, A-5, within 3 in of diabase contact. A-6, xenolith in diabase.

	A-1	A-2	A-3	A-4	A-5	A-6
SiO <sub>2</sub>	76.29	73.82	71.78	72.09	77.69	67.57
TiO <sub>2</sub>	0.24	0.30	0.30	0.33	0.30	0.51
Al <sub>2</sub> O <sub>3</sub>	11.90	12.74	13.61	12.96	11.49	15.30
Fe <sub>2</sub> O <sub>3</sub>	0.91	1.09	1.23	0.99	0.88	0.77
FeO	0.74	0.74	2.77	1.30	0.54	4.35
MnO	0.04	0.05	0.06	0.07	0.03	0.11
MgO	0.33	0.44	1.02	0.53	0.17	1.57
CaO	0.36	0.35	0.74	1.00	0.57	1.33
Na <sub>2</sub> O	2.85	3.17	5.67	2.97	3.44	4.95
K <sub>2</sub> O	5.06	5.02	1.04	5.14	3.24	1.64
Total	98.72	97.72	98.22	97.38	98.35	98.10
Rb	239	266	49	306	132	72
Sr	109	98	68	120	125	196

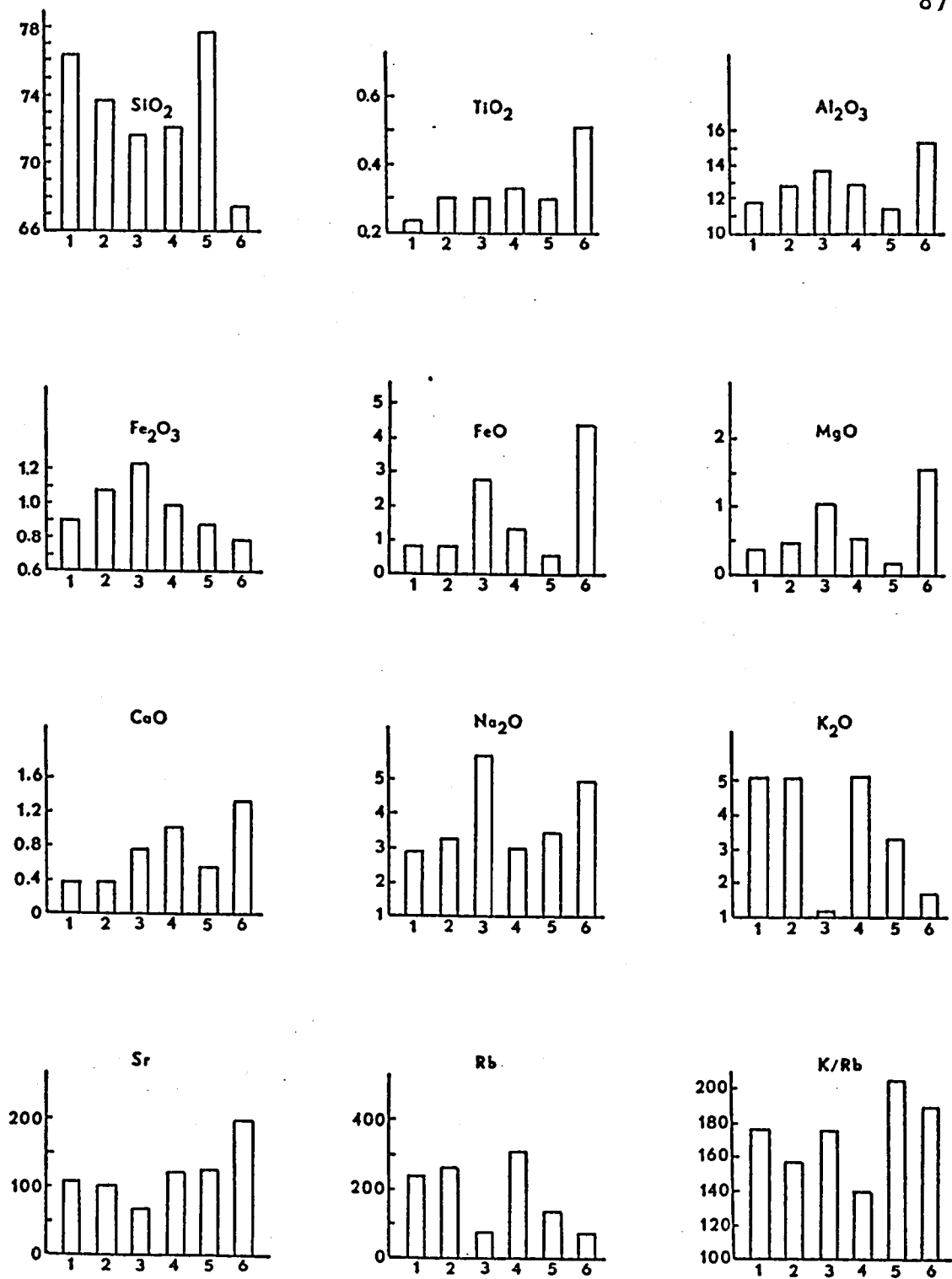


Figure 12. Chemical analyses of alaskite shown as bar graphs.

1 and 2: representative alaskite; 3, 4, and 5: alaskite at diabase contact; 6: alaskite xenolith.

greater than that of the diabase. Potassium-rubidium ratios are generally higher in the contact samples than in the normal alaskite while rubidium-strontium ratios are lower. It is interesting that the xenolith (A-6) shows the most extreme chemical differences.

The two most obvious mechanisms that might lead to contamination of the diabase with material from the alaskite are partial melting of alaskite at the contact and the movement of heated groundwater into the diabase. The work of Piwinskii and Wyllie (1968) indicates that melting begins at grain boundaries and that orthoclase and quartz are the first minerals to completely melt. Melting of these two minerals would deplete the remaining rock in  $K_2O$ ,  $Al_2O_3$ , and  $SiO_2$ ; and the diabase would be enriched in these elements. The contact alaskite samples are depleted in  $SiO_2$  and  $K_2O$  but are enriched in  $Al_2O_3$ . Diabase is enriched in  $K_2O$  and  $SiO_2$  near the contacts, but it is also enriched in Fe and  $TiO_2$ . The  $TiO_2$  enrichment is very slight and may not be significant. It is likely that if melting did occur it would be a very small scale feature and would, at most, lead to contamination of the diabase over a very narrow zone at the contact. Chemical changes in alaskite extend only a few inches from the contact while the less mafic zones of diabase extend several feet into the sill. Therefore, there is insufficient evidence to support large

scale contamination by melting. In addition, no evidence of melting was observed in the field or in thin section.

Recent studies of oxygen and hydrogen isotopes in igneous rocks have led some investigators to propose that heated ground water may move into shallow intrusions from the surrounding country rocks (Taylor and Epstein, 1968; Taylor and Forester, 1971). If this occurs, the water could remove some of the more soluble elements from the heated rocks near the contact, leading to contamination of the marginal zones of the intrusive rock. Most of the contact alaskite samples are depleted in  $\text{SiO}_2$ ,  $\text{K}_2\text{O}$ , and Rb. Ellis and Mahon (1967) reacted volcanic rocks with hot water and determined the concentrations of some elements in the water. Concentrations varied somewhat with rock type, but all contained significant amounts of Si, Na, K, and Rb as well as some Ca and Mg. The potassium-rubidium ratio of the solution was low indicating that Rb is more readily removed from the rock than K. All of these observations are consistent with the transport of these elements from alaskite to the margins of the sill.

Trends for some other elements are not so easily explained by this mechanism. Sodium is enriched in alaskite near the contact and slightly enriched in the margins of the diabase. The work of Ellis and Mahon (1967) indicates that Na should be more mobile than K, suggesting that a

similar distribution pattern for the two elements should occur. Similarly,  $\text{TiO}_2$  and Fe are enriched in both diabase and alaskite in the contact zones. The  $\text{TiO}_2$  enrichment, however, is very slight and considering the small amount present probably is not significant. These observations suggest that contamination by inward moving ground-water probably cannot account for all of the variations noted in the Lookout Mountain sills. The process may occur locally, and may account for features like the abrupt increase in  $\text{K}_2\text{O}$ ,  $\text{SiO}_2$ , and Rb at the extreme margins of the small sill. The emplacement mechanism discussed earlier is a more likely explanation of the chemical variations, but changes resulting from contamination probably occurred locally. The potassium-rich contact zone in the Roosevelt Dam sill almost certainly resulted from contamination with material from the overlying sandy shale.

## SANTA CATALINA MOUNTAINS SILL

A small sill, exposed on the northwest side of the Santa Catalina Mountains north of Tucson, was sampled in order to have a representative from the southern part of the Province. Several other sills in the Santa Catalina Mountains were examined and all were altered to some degree. The one selected for study is much less altered than any of the others examined. This sill is exposed in the northwest wall of Peppersauce Canyon 1.1 miles west of the Peppersauce picnic area on the dirt road from Oracle to Mount Lemmon. The sill is approximately 70 ft thick where sampled and intrudes the Dripping Springs Quartzite.

### Petrography

Most of the samples collected are so intensely altered that they were not studied in detail. Three samples, however, were relatively fresh. Samples SCD-39, SCD-39A, and SCD-44 are from 8, 16, and 45 ft below the top of the sill respectively. All three samples are petrographically similar. Plagioclase is the most abundant mineral, occurring as stubby laths about 1 mm in length. Almost all grains show slight sericitic alteration. The second most abundant mineral is augite which is similar in size to plagioclase.

Hornblende, chlorite, and calcite are alteration products of augite and, together, are more abundant than augite in samples SCD-39 and SCD-44. Magnetite is always partially replaced by hematite. Quartz and orthoclase commonly occur together in graphic intergrowths and together make up between 5 and 10 per cent of the rock. Minor amounts of biotite and apatite are also present. Samples SCD-39A contains trace amounts of pyrite.

In the more intensely altered samples plagioclase is almost completely replaced by sericite. Augite is completely replaced by calcite with minor amounts of chlorite and iron oxide. The alteration is probably hydrothermal in nature and may be related to small copper deposits in the area.

#### Chemistry

Five samples are analysed, but two were so rich in calcite that the chemistry is quite different from the other three samples. Analyses are listed in Tables 25 and 26. All three rocks contain more than 50 per cent  $\text{SiO}_2$  and are chemically similar to the Globe and Lookout Mountain diabases. The high  $\text{Fe}_2\text{O}_3/\text{FeO}$  ratios result from partial oxidation of magnetite to hematite. Minor element concentrations are also similar to the Globe and Lookout Mountain rocks. Copper and Rb values are relatively high, while Sr is low. Rubidium-strontium ratios are high while

Table 25. Chemical analyses and norms for samples from the Santa Catalina Mountains sill.

	SCD-44	SCD-39A	SCD-39
SiO <sub>2</sub>	52.64	53.48	53.09
TiO <sub>2</sub>	1.18	1.37	2.12
Al <sub>2</sub> O <sub>3</sub>	13.37	13.74	12.95
Fe <sub>2</sub> O <sub>3</sub>	6.89	5.56	7.35
FeO	4.84	6.76	6.90
MnO	0.18	0.19	0.19
MgO	6.37	5.54	4.07
CaO	6.65	6.78	4.66
Na <sub>2</sub> O	2.02	2.37	2.46
K <sub>2</sub> O	1.81	1.62	1.40
Total	95.95	97.41	95.19
Quartz	11.85	10.39	16.79
Orthoclase	11.39	10.06	9.03
Albite	19.32	22.37	24.12
Anorthite	23.52	23.21	22.03
Wollastonite	4.65	4.86	1.29
Hypersthene	19.85	21.00	15.12
Magnetite	7.67	6.11	8.39
Ilmenite	1.75	2.01	3.23

Table 26. Trace element concentrations and elemental ratios in samples from the Santa Catalina Mountains sill.

Sample	Cu (ppm)	Sr (ppm)	Rb (ppm)	Rb/Sr	K/Rb	Ca/Sr
SCD-44	140	246.6	60.5	0.2454	248	193
SCD-39A	127	189.9	58.7	0.3093	228	255
SCD-39	123	158.4	39.5	0.2494	294	256

K/Rb ratios are low. Because of the poor sampling, little can be said regarding chemical variations within the body.

## PETROGRAPHIC TYPES IN THE DIABASE PROVINCE

The six diabase sills described above can be divided into two distinct petrographic types. Some samples from both the Salt River Canyon and Roosevelt Dam bodies contain olivine; quartz and potassium feldspar are absent, even in the most highly differentiated phases. In the other four bodies, quartz and orthoclase are present in almost all samples while olivine is absent. Hornblende is more abundant in the Globe complex than in any of the others. This raises the question of whether or not other diabases in the province fit into this two-fold classification and, if so, what is the geographic distribution of each type.

The Sierra Ancha Sill is composed mostly of olivine diabase (Smith, 1969; Nehru and Prinz, 1970), although Smith (1969) noted the local presence of quartz near the top of the sill and suggested it may have resulted from contamination with overlying sedimentary rocks. Neuerburg and Granger (1960) gave a brief petrographic description of diabases related to uranium deposits, mostly in the Sierra Ancha region of Gila County. They described the unaltered rocks as being composed mostly of plagioclase, augite, and olivine and do not mention any quartz-bearing varieties. Ransome (1903, 1919) described diabase in the Globe area

as being composed essentially of plagioclase, augite, and olivine, but noted the occasional presence of quartz in some coarser grained differentiates. Schmidt (1971) described quartz-bearing diabases in the Tortilla Mountains, a short distance north of the Lookout Mountain sills described in this study.

In the absence of more detailed studies it is difficult to draw conclusions regarding the distribution of the two types of diabase. Based on the present research and the references cited above, it seems that most diabase in the Sierra Ancha, Salt River Canyon, and Globe area contains olivine with quartz occurring only in minor, highly differentiated or contaminated phases. The Globe diabase described here is an obvious exception to this general statement. Other than the four quartz-bearing sills described here, the diabase studied by Schmidt (1971) is the only described occurrence in which quartz is an important constituent throughout a sill. With one exception, all of these sills are located in the central or southern parts of the diabase province. Although more study is obviously needed before solid conclusions can be made, the present data suggest that olivine-bearing diabase is dominant in the northern part of the province, while quartz-bearing varieties may be more numerous in the southern portion.

## DIABASIC MAGMA TYPES

Students of basaltic rocks have, for many years, recognized the existence of two more or less distinct magma types. Kennedy (1933) applied the names tholeiite and plateau basalt to the two types. The term tholeiite is still retained, but plateau basalt has been largely replaced by the more descriptive term alkali olivine basalt. Although the distinction between the two types initially was largely petrographic, most investigators now use chemistry directly or indirectly, as reflected by the normative mineralogy, to classify basaltic rocks. This method has the obvious advantage of being applicable to glassy rocks as well as to holocrystalline rocks and is less dependent on the particular crystallizing characteristics of individual rock bodies.

MacDonald and Katsura (1964) and Kuno (1967) have used a simple alkali-silica diagram to distinguish tholeiitic and alkali olivine basalts in Hawaii and Japan respectively. Figure 13 is such a diagram for the rocks examined in this study. Since it is difficult to determine which samples represent the original magma composition for each sill, all samples except obviously fractionated or contaminated ones are plotted. The

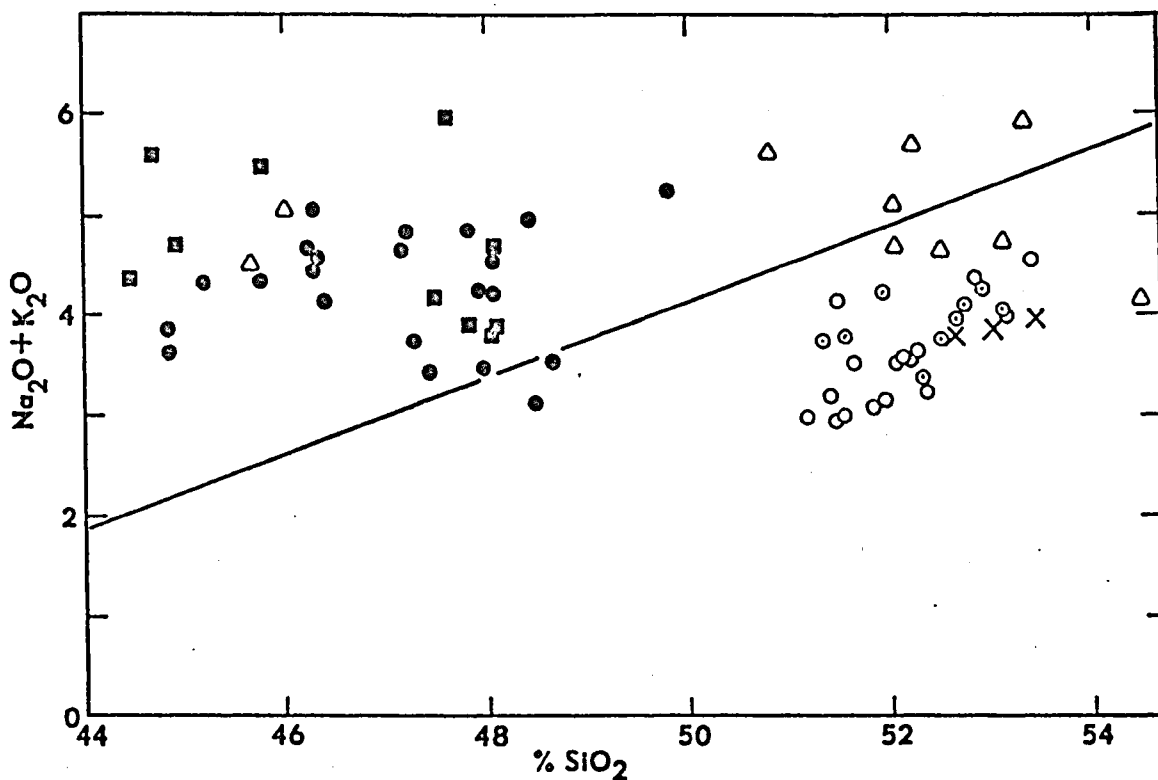


Figure 13. Relationship between SiO<sub>2</sub> and alkalis for the analysed rocks.

Solid symbols are samples from olivine-bearing sills; open symbols are samples from quartz-bearing sills. Large dots: Salt River Canyon diabase; squares: Roosevelt Dam diabase; triangles: Globe diabase; circles: large Lookout Mountain sill; circles with dots: small Lookout Mountain sill; X: Santa Catalina Mountains diabase.

diagonal line separating the two types is from MacDonald and Katsura (1964) and is almost identical to the boundary used by Kuno (1967). All of the Lookout Mountain and Santa Catalina Mountains samples plot in the tholeiite field while all of the Roosevelt Dam samples and the great majority of the Salt River Canyon samples fall within the alkali olivine basalt field. Quartz-bearing samples from the Globe complex plot near the boundary, with about an equal number of samples falling on either side. The separation is more a result of differences in  $\text{SiO}_2$  content than in alkalis. Alkalis are generally more concentrated in the lower silica rocks, but there is considerable overlap. MacDonald and Katsura (1964, p. 86), however, pointed out that the amount of alkalis must be considered in relation to the amount of silica.

MacDonald and Katsura (1964, p. 105) noted that  $\text{TiO}_2$  is more abundant in the alkali olivine basalts from Hawaii. Manson's (1967, p. 227) compilation of basalt analyses also indicate that alkali olivine basalts contain more  $\text{TiO}_2$  than tholeiites. As will be discussed later, the Roosevelt Dam and Salt River Canyon rocks contain much more  $\text{TiO}_2$  than the Lookout Mountain samples. The Globe samples are intermediate in their  $\text{TiO}_2$  content while the Santa Catalina Mountains rocks are more similar to those from Lookout Mountain. Thus, based on their alkali,

silica, and titanium contents, the olivine-bearing sills can be classified as alkali olivine basalts and the Lookout Mountain and Santa Catalina Mountains sills as tholeiites. The quartz-bearing samples from the Globe complex are intermediate between the two types.

Yoder and Tilley (1962, p. 352) and Green and Ringwood (1967, p. 106) have used normative mineralogy to classify basaltic rocks. These two classifications are very similar and essentially separate tholeiites and alkali basalts on the basis of whether or not hypersthene is present in the norm. Hypersthene-normative basalts are considered tholeiites while basalts with normative olivine but no hypersthene are alkali olivine basalts. Modifying terms are used according to whether quartz or nepheline are present in the norm.

All samples from the Lookout Mountain and Santa Catalina Mountains sills contain normative hypersthene and quartz, and according to the above classifications, they are quartz tholeiites. All of the quartz-bearing samples from the Globe Complex with one exception contain normative hypersthene and quartz and are quartz tholeiites. The one exception contains olivine along with hypersthene in the norm; it is an olivine tholeiite. The two samples from near the base of this complex which contain no quartz are also olivine tholeiites according to this classification,

although they would be considered alkali olivine basalts on the basis of their alkali,  $\text{SiO}_2$ , and  $\text{TiO}_2$  contents.

Samples from the Roosevelt Dam sill are more variable in their normative mineralogy. One sample contains normative quartz and four contain nepheline. The remaining five samples contain normative hypersthene and olivine. These samples would be quartz tholeiite, alkali basalt, and olivine tholeiite respectively. Four samples from the Salt River Canyon complex contain normative nepheline; three of these being from the upper unit. Normative hypersthene and olivine are present in the other samples; thus, they are olivine tholeiites.

Kuno (1960) defines what he considered to be a third fundamental magma type: high-alumina basalts. Rocks belonging to this group contain more than about 15 per cent  $\text{Al}_2\text{O}_3$  and intermediate amounts of alkalis and silica. Figure 14 is a plot of  $\text{SiO}_2$  versus  $\text{Al}_2\text{O}_3$  for the Arizona diabases. This plot shows the separation of the olivine-bearing diabases (high  $\text{Al}_2\text{O}_3$ , low  $\text{SiO}_2$ ) and the quartz-bearing diabases (low  $\text{Al}_2\text{O}_3$ , high  $\text{SiO}_2$ ) and indicates that some of the olivine-bearing rocks may be high-alumina basalts. In Figure 15 Kuno's diagram is reproduced for rocks containing between 47.51 and 50.00 per cent  $\text{SiO}_2$ . Plotted on this diagram are Arizona diabases in this  $\text{SiO}_2$  range which contain more than 15 per cent  $\text{Al}_2\text{O}_3$ . Rocks

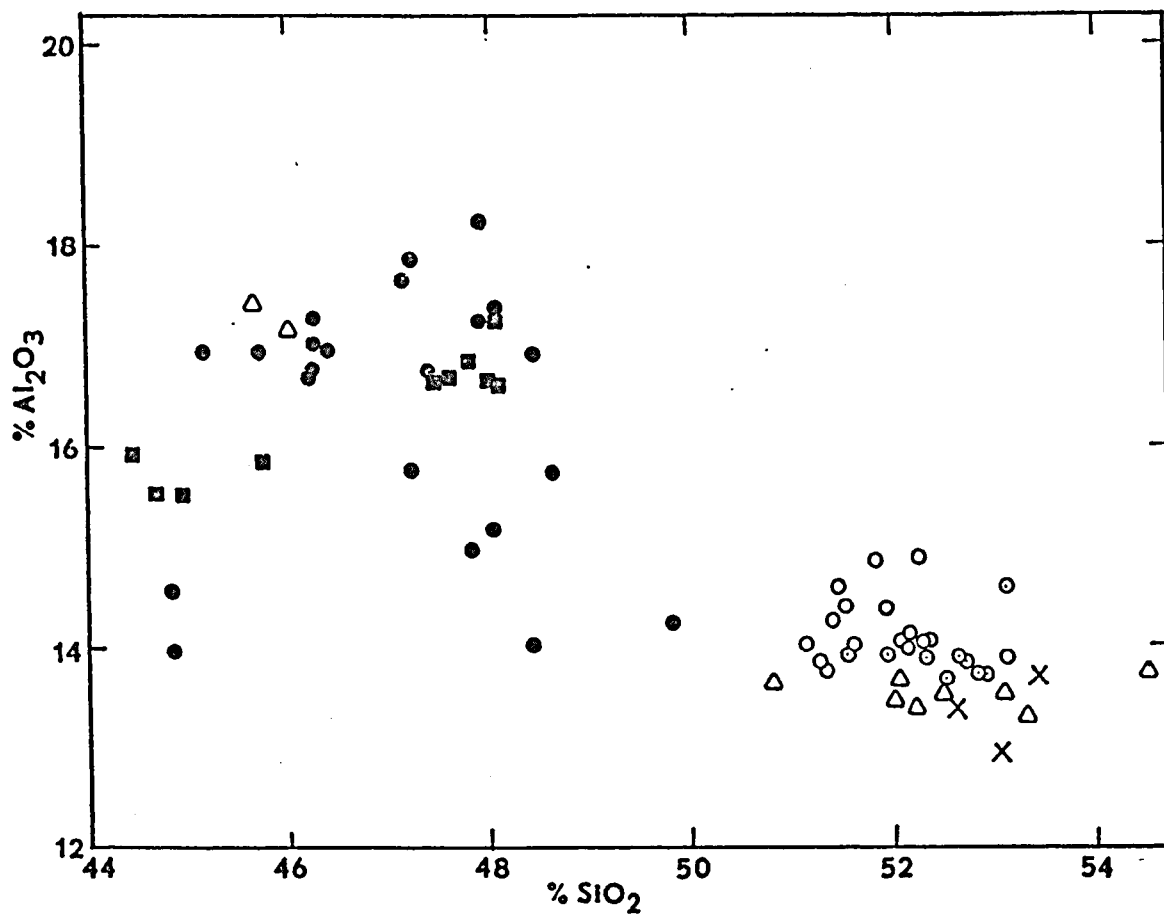


Figure 14. Relationship between Al<sub>2</sub>O<sub>3</sub> and SiO<sub>2</sub> for the analysed rocks.

Solid symbols are samples from olivine-bearing sills; open symbols are samples from quartz-bearing sills. Symbols are same as in Figure 13.

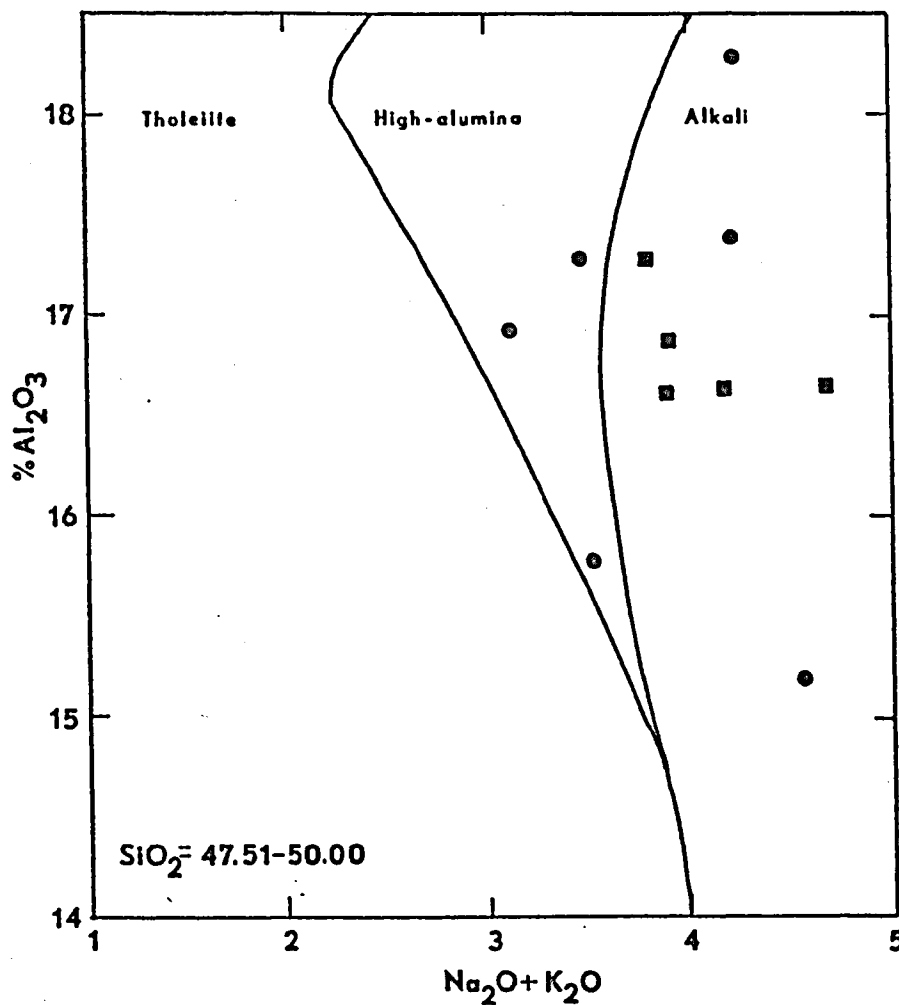


Figure 15. Relationship between Al<sub>2</sub>O<sub>3</sub> and alkalis for rocks containing more than 15 per cent Al<sub>2</sub>O<sub>3</sub> and between 47.51 and 50.00 per cent SiO<sub>2</sub>.

Large dots: Salt River Canyon diabase; squares: Roosevelt Dam diabase.

containing less  $\text{Al}_2\text{O}_3$  obviously can not be high-alumina basalts and were not plotted. Three samples fall within the high-alumina basalt field. The fine-grained diabase from the base of the Salt River Canyon sill falls within this group indicating a high-alumina affinity for the magmas involved if this sample accurately represents the composition of the initial magma. Other samples containing more than 15 per cent  $\text{Al}_2\text{O}_3$  and 45.00 to 47.50 per cent  $\text{SiO}_2$  were plotted on Kuno's diagram for rocks within this  $\text{SiO}_2$  range, however, none fell within the high-alumina field.

In summary, the Lookout Mountain and Santa Catalina Mountains diabases are clearly quartz tholeiites. Based on their normative mineralogy, the Globe quartz-bearing diabases fall within this group. The Roosevelt Dam diabases are olivine tholeiites or alkali-olivine basalts, depending upon the method of classification. Most of the Salt River Canyon rocks are olivine tholeiites or alkali olivine basalts; however, a few rocks, including those in the fine-grained basal zone, are high-alumina basalts. It should be emphasized again that it is difficult to determine which samples best represent the composition of the original magma. As will be discussed later, the quartz-bearing rocks from the Globe complex are probably more differentiated than most of the other diabases.

Table 27 lists the chemistry of tholeiitic basalts from some different provinces. The values listed for the Lookout Mountain diabases are averages of analyses listed earlier excluding possibly contaminated rocks. Lookout Mountain rocks are similar to most of the continental tholeiites but have slightly higher alkali contents and are lower in CaO and MgO. Oceanic tholeiites are distinctly different from all of the continental rocks listed. Average values for the Salt River Canyon and Roosevelt Dam diabases are listed in Table 28 along with some other alkali and high-alumina basalts. The Arizona rocks are more similar to alkali basalts than high-alumina basalts.

Table 27. Comparison of Arizona quartz tholeiites with some other tholeiites.

A, average Lookout Mountain diabase. B, average Karroo dolerite (Barth, 1962). C, average Palisade chilled basalt (Barth, 1962). D, hypersthene tholeiite, Antarctica (Compston, MacDougall and Heier, 1968). E, Tasmanian dolerite (Compston and others, 1968). F, Precambrian Wyoming diabases (Condie, Barsky and Mueller, 1969). G, Oceanic tholeiite (Compston and others, 1968).

	A	B	C	D	E	F	G
SiO <sub>2</sub>	52.05	52.5	52.2	53.75	53.18	49.0	49.34
TiO <sub>2</sub>	1.14	1.0	1.2	0.70	0.65	1.44	1.49
Al <sub>2</sub> O <sub>3</sub>	14.08	15.4	15.4	14.23	15.37	12.7	17.04
Fe <sub>2</sub> O <sub>3</sub> *	11.94	11.5	11.3	10.69	10.02	15.0	9.57
MnO	0.19	0.2	0.1	0.18	0.15	0.15	0.17
MgO	6.30	7.1	7.3	6.64	6.71	7.07	7.19
CaO	9.83	10.3	10.0	10.60	11.04	9.43	11.72
Na <sub>2</sub> O	2.46	2.1	2.4	1.83	1.65	2.18	2.73
K <sub>2</sub> O	1.14	0.8	0.8	0.81	1.03	0.95	0.16
Sr	164	--	--	125	130	186	115
Rb	55	--	--	31	33	45	1

\*Total iron expressed as Fe<sub>2</sub>O<sub>3</sub>.

Table 28. Comparison of Arizona alkali basalts with some other alkali and high-alumina basalts.

A, average Salt River Canyon and Roosevelt Dam diabases. B, alkali basalts (Condie and others, 1969). C, alkali basalt, Japan (Kuno, 1967). D, alkali basalt, Hawaii (MacDonald and Katsura, 1964). E, high-alumina basalt from chilled zone of Skaergaard intrusion (Kuno, 1967).

	A	B	C	D	E
SiO <sub>2</sub>	46.99	49.5	47.95	46.46	48.08
TiO <sub>2</sub>	2.31	2.49	1.09	3.01	1.17
Al <sub>2</sub> O <sub>3</sub>	16.34	15.6	16.46	14.64	17.22
Fe <sub>2</sub> O <sub>3</sub> *	14.22	13.1	10.90	13.39	10.70
Mno	0.19	0.13	0.21	0.14	0.16
MgO	6.22	5.92	8.99	8.19	8.62
CaO	7.94	8.68	10.46	10.33	11.38
Na <sub>2</sub> O	3.06	3.47	2.72	2.92	2.37
K <sub>2</sub> O	1.34	1.4	1.09	0.84	0.25
Sr	396	761	--	--	--
Rb	31	51	--	--	--

\*Total iron expressed as Fe<sub>2</sub>O<sub>3</sub>.

## CHEMISTRY OF THE DIABASE PROVINCE

The overall chemistry of the six sills studied will now be discussed and compared. Based on their chemistry, the rocks analysed can be divided into two distinct groups; this distinction will be emphasized.

Silica and alumina relationships were shown in Figure 14. The Salt River Canyon and Roosevelt Dam sills contain much more  $\text{Al}_2\text{O}_3$  and less  $\text{SiO}_2$  than the other diabases. Two samples from the base of the Globe complex also plot with these rocks. Four quartz-bearing sills show a tight clustering of points.

Samples from near the upper part of the lower Salt River Canyon sill show enrichment in  $\text{SiO}_2$  and depletion in  $\text{Al}_2\text{O}_3$ . This same trend can be seen among the quartz-bearing rocks. Starting with the large Lookout Mountain sill, there is a regular increase in  $\text{SiO}_2$  and decrease in  $\text{Al}_2\text{O}_3$  through the small Lookout Mountain sill, the Globe quartz-bearing diabases, and the Santa Catalina Mountains sill. The Roosevelt Dam sill is an exception to this trend since samples from the upper part of the sill are low in both  $\text{SiO}_2$  and  $\text{Al}_2\text{O}_3$ .

There are some systematic variations in MgO, CaO, and Fe among the six sills but they are not as distinct as

the  $\text{SiO}_2$  and  $\text{Al}_2\text{O}_3$  variations. Samples from the Lookout Mountain sills contain between 5 and 8 per cent MgO. The central part of the larger sill shows the highest MgO values. Samples from the Roosevelt Dam sill average about 6 per cent MgO while those from the Salt River Canyon sill are mostly between 6 and 8 per cent. With the exception of two samples from near the base, no samples from the Globe sill contain as much as 5 per cent MgO. Three samples from the Santa Catalina Mountains sill contain between 4 and 6.50 per cent MgO. Allowing for variations within each sill, there are no differences in the MgO contents of five of the six sills examined. Quartz-bearing samples from the Globe sill contain significantly less MgO than all of the other samples.

Calcium values show considerable variation from sill to sill and within each sill but, in general, are higher in the two Lookout Mountain sills and the Salt River Canyon sill. The highest values occur near the center of the large Lookout Mountain Sill. The Globe sill generally has a lower CaO content than the other five sills.

Iron is generally more concentrated in the quartz-bearing samples from the Globe complex, although a few samples from the Salt River Canyon and Roosevelt Dam sills have similarly high values. Much of the variation in iron is related to differentiation, which will be discussed later.

Samples from the Globe sill are generally higher in total alkalis than the other samples, while the Salt River Canyon rocks have the highest  $\text{Na}_2\text{O}/\text{K}_2\text{O}$  ratios. Potassium, sodium, and calcium are plotted on a triangular diagram in Figure 16. The Lookout Mountain samples show a very regular trend of alkali enrichment while the other samples are more scattered. Most of the Salt River Canyon samples and some samples from the Globe complex plot below the main trend showing the enrichment of these bodies in  $\text{Na}_2\text{O}$ .

Olivine- and quartz-bearing diabases have distinctly different  $\text{TiO}_2$  contents.  $\text{TiO}_2$  values are low and very consistent in the Lookout Mountain sills. Quartz-bearing diabase from the Globe complex contain slightly more  $\text{TiO}_2$ .  $\text{TiO}_2$  is more variable in the Salt River Canyon and Roosevelt Dam samples but much more concentrated than in the quartz-bearing samples from the other sills. Figure 17 is a plot of  $\text{TiO}_2$  versus  $\text{Rb}/\text{Sr}$  showing the separation of the two types of diabase on the basis of these elements.

Strontium varies markedly among the six sills. The highest values occur in the Salt River Canyon complex where concentrations exceed 500 ppm in several samples. The Roosevelt Dam samples average around 300 ppm. Quartz-bearing diabases almost all contain between 150 and 200 ppm Sr. In Figure 18  $\text{Ca}/\text{Sr}$  is plotted against K. The quartz-bearing diabases all have fairly high  $\text{Ca}/\text{Sr}$  ratios

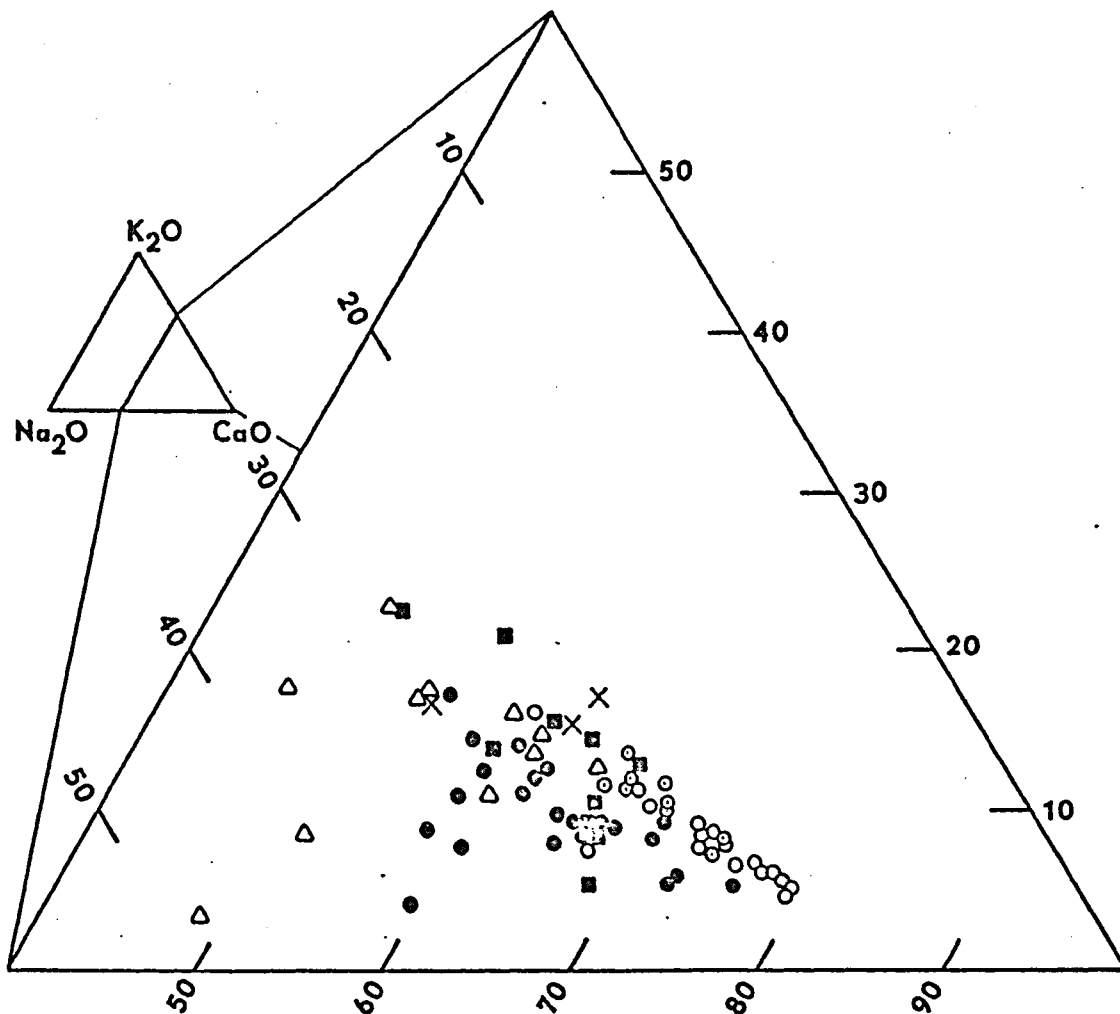


Figure 16. Relationship between  $K_2O$ ,  $Na_2O$ , and  $CaO$  for the analysed rocks.

Solid symbols are samples from olivine-bearing sills; open symbols are samples from quartz-bearing sills. Symbols are same as in Figure 13.

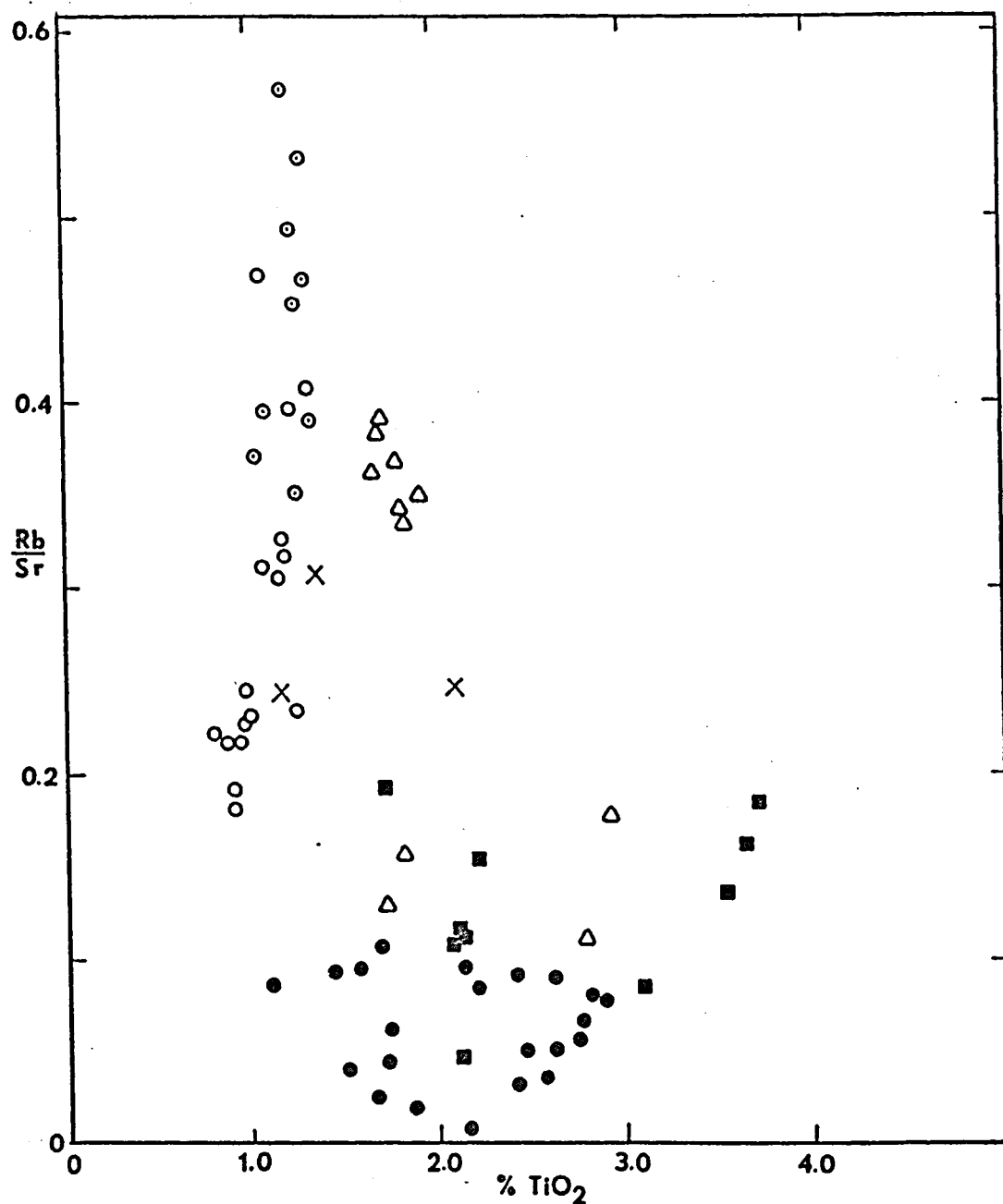


Figure 17. Relationship between TiO<sub>2</sub> and the ratio Rb/Sr for the analysed rocks.

Solid symbols are samples from olivine-bearing sills; open symbols are samples from quartz-bearing sills. Symbols are same as in Figure 13.

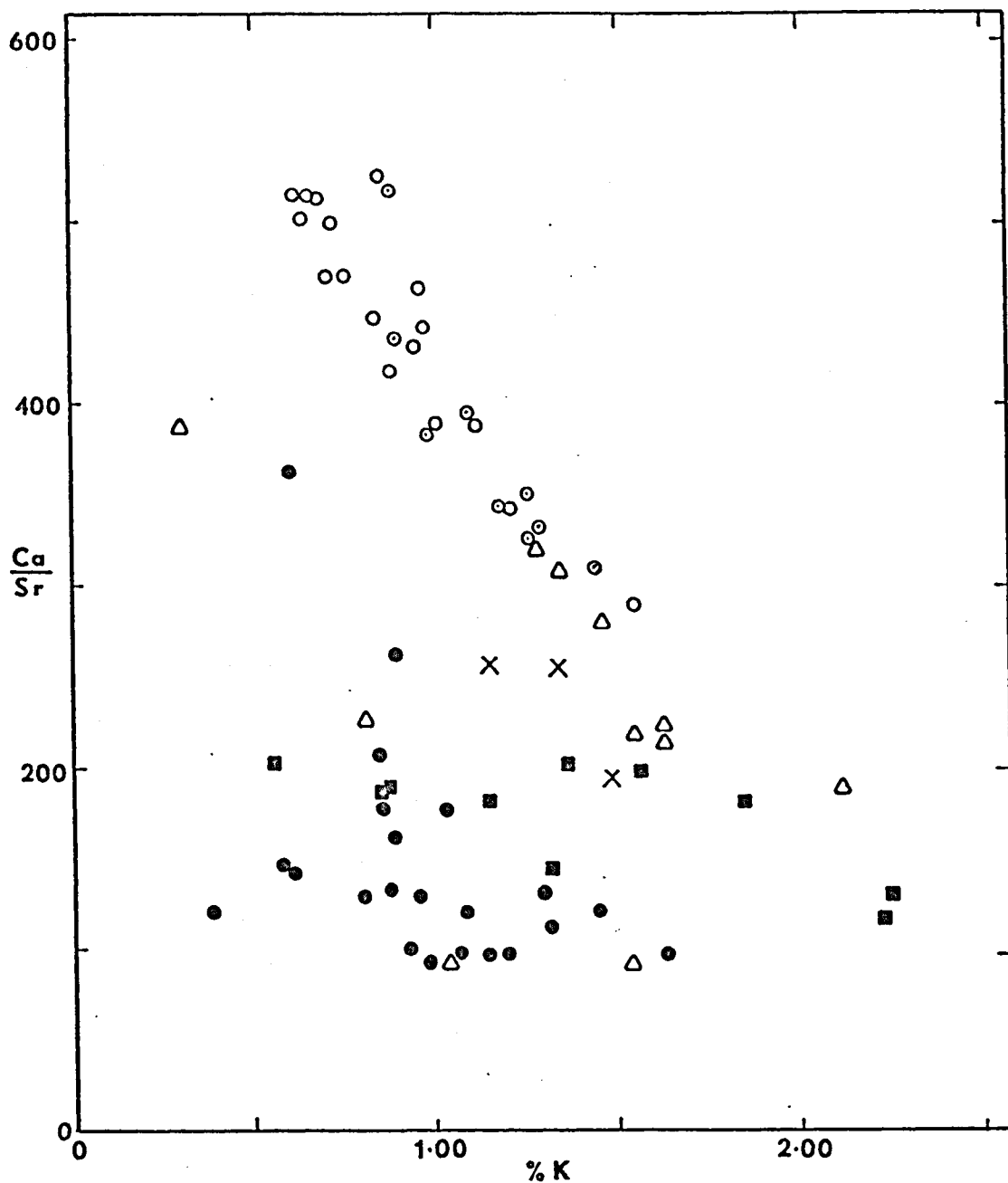


Figure 18. Relationship between K and the ratio Ca/Sr for the analysed rocks.

Solid symbols are samples from olivine-bearing sills; open symbols are samples from quartz-bearing sills. Symbols are same as in Figure 13.

which decrease very regularly with increasing K content. The two olivine-bearing sills have lower Ca/Sr ratios and show little systematic variation with potassium.

Rubidium is more abundant in the quartz-bearing diabases and Rb/Sr ratios are much higher in these rocks. Figure 19 is a plot of Rb versus Sr showing the separation of the two groups of diabases. Figure 20 is a plot of Rb versus the ratio Rb/Sr. Both groups show a systematic increase in the Rb/Sr ratio with increasing Rb.

The Lookout Mountain samples have very low K/Rb ratios and show a regular decrease in this ratio with increasing K (Figure 21). The Globe samples also have low ratios, but the ratio generally increases with K content. The olivine-bearing samples have much higher K/Rb ratios. Samples from the Roosevelt Dam sill show little change in the ratio with changes in K while the Salt River Canyon samples show a fairly regular decrease.

Copper is more concentrated in the quartz-bearing sills. There is a rather systematic increase in Cu with increasing  $\text{SiO}_2$  content (Figure 22) throughout the range of compositions, however, the two varieties of diabase tend to be separated. A few samples from the Salt River Canyon sill are anomalously enriched in Cu relative to the other samples. Several samples from this body contain sulfide minerals which may account for these erratic values.

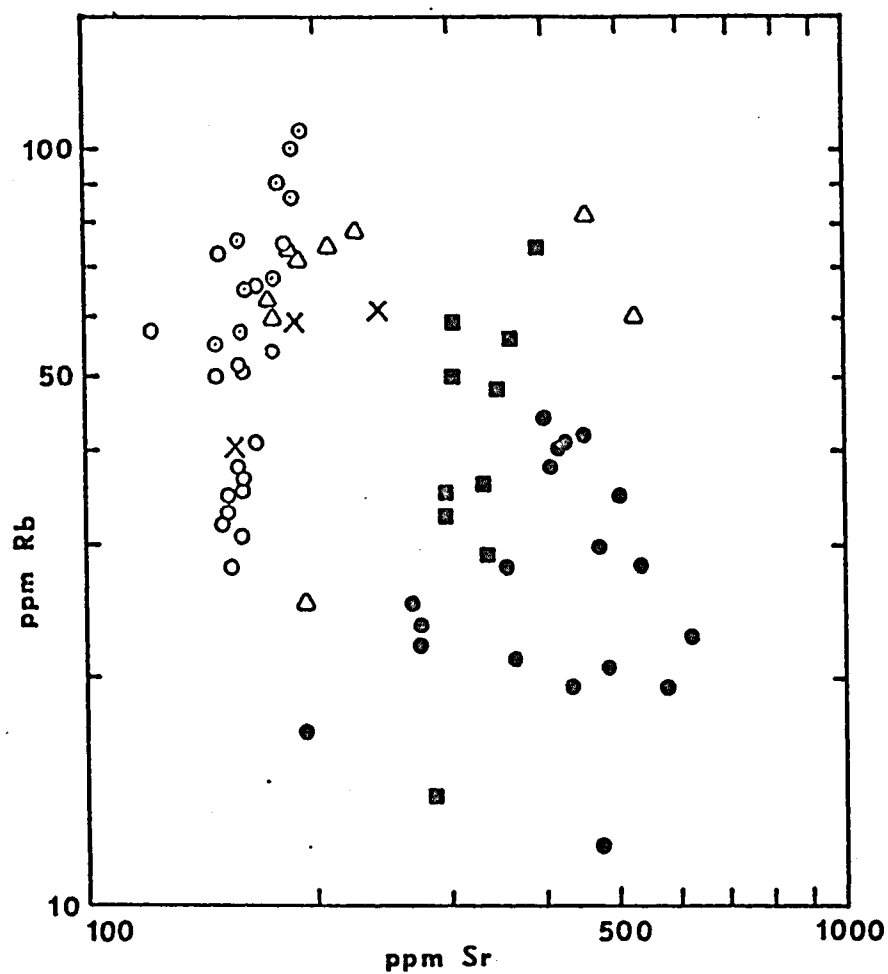


Figure 19. Relationship between Rb and Sr for the analysed rocks.

Solid symbols are samples from olivine-bearing sills; open symbols are samples from quartz-bearing sills. Symbols are same as in Figure 13.

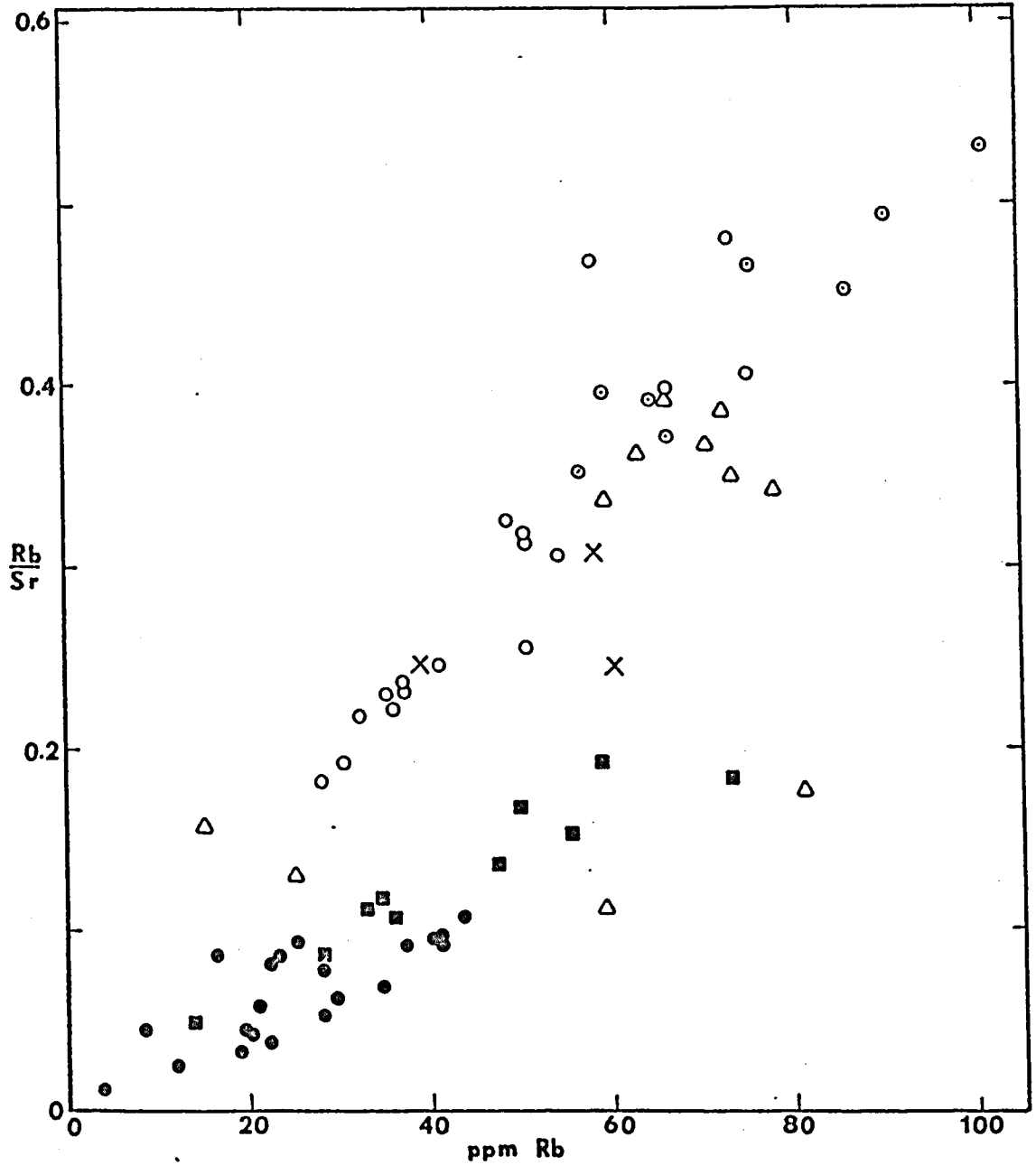


Figure 20. Diagram of Rb versus the ratio Rb/Sr.

Solid symbols are samples from olivine-bearing sills; open symbols are samples from quartz-bearing sills. Symbols are same as in Figure 13.

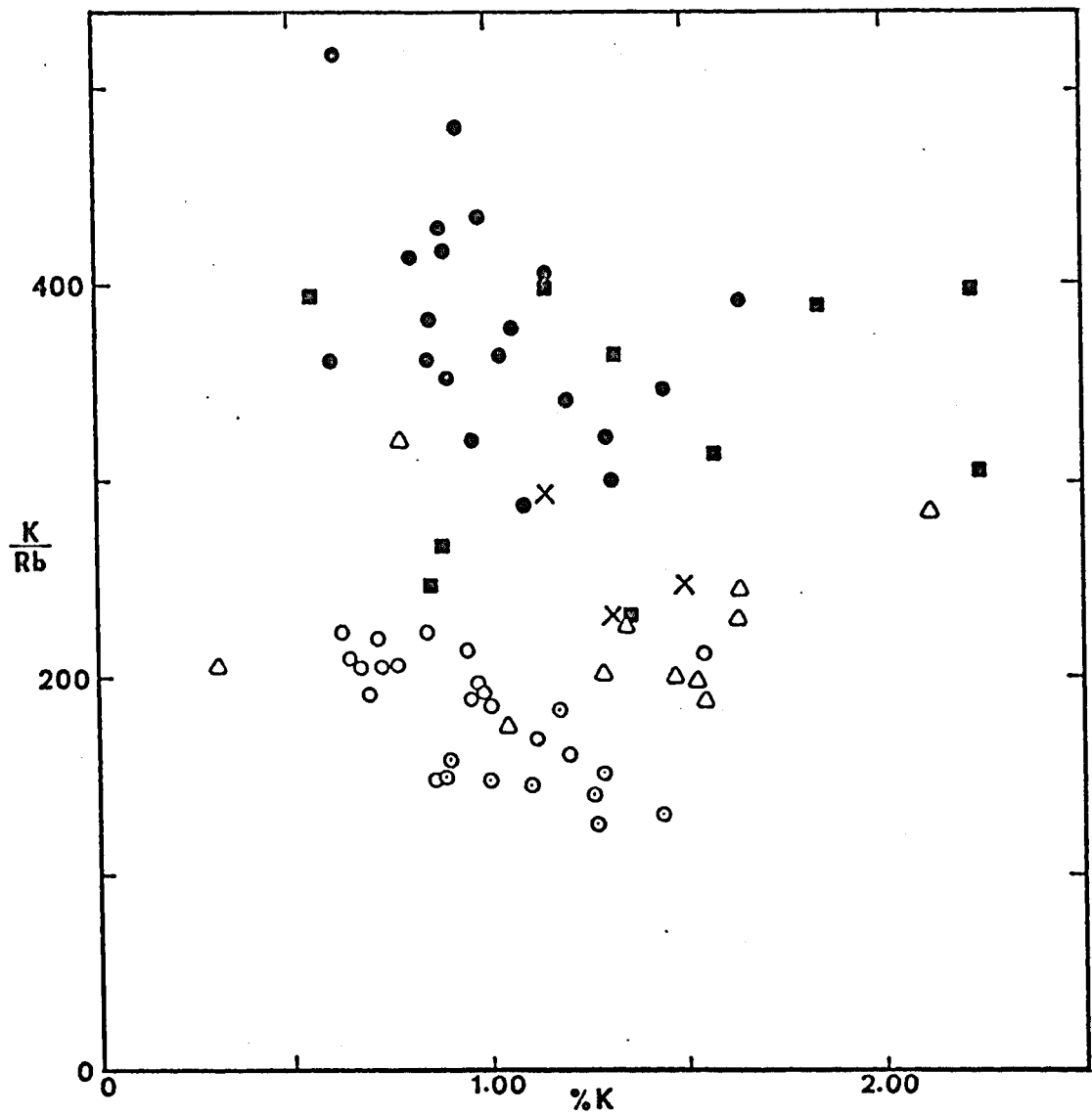


Figure 21. Relationship between K and the ratio  $K/Rb$  for the analysed rocks.

Solid symbols are samples from olivine-bearing sills; open symbols are samples from quartz-bearing sills. Symbols are same as in Figure 13.

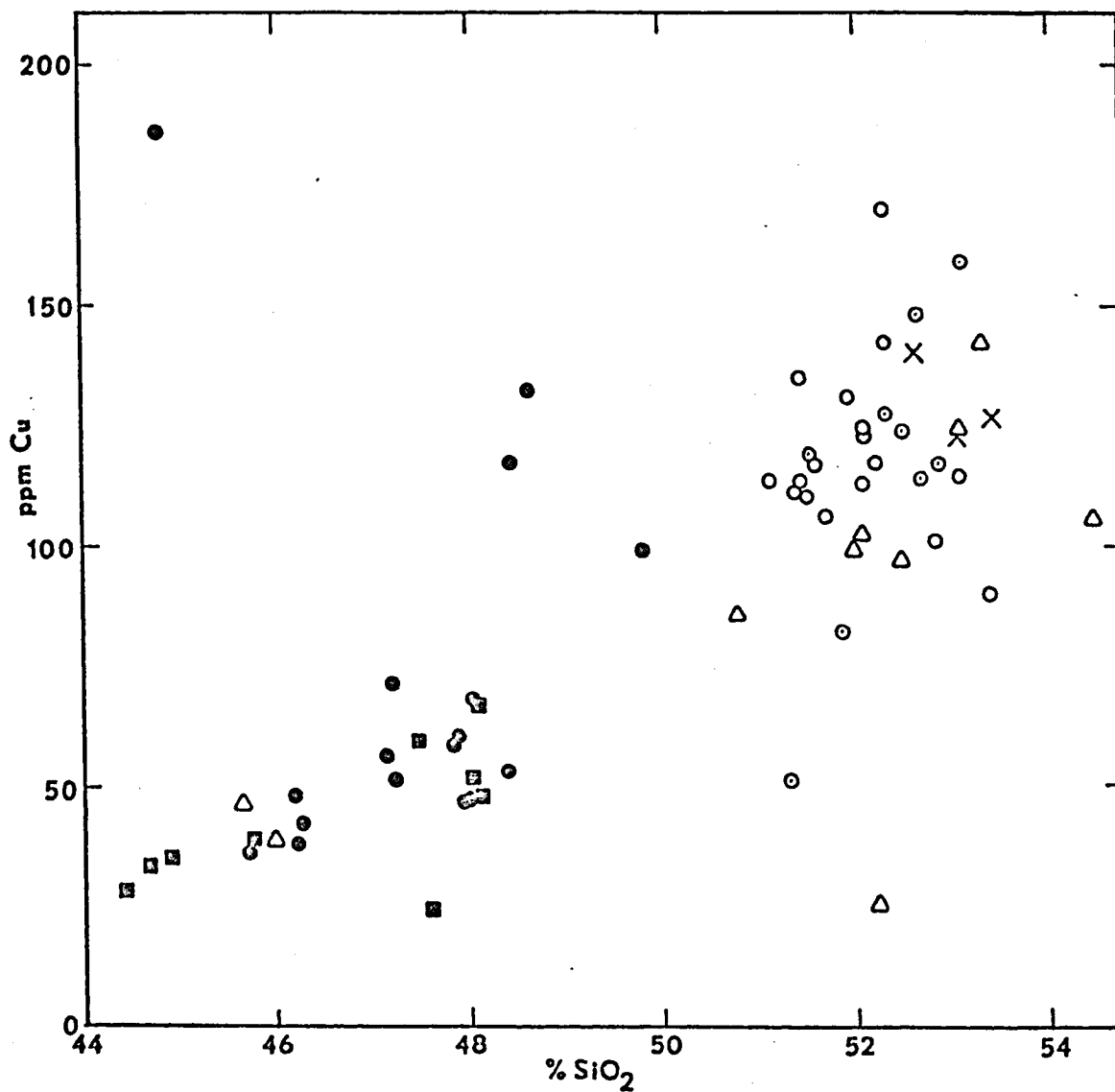


Figure 22. Relationship between SiO<sub>2</sub> and Cu for the analysed rocks.

Solid symbols are samples from olivine-bearing sills; open symbols are samples from quartz-bearing sills. Symbols are same as in Figure 13.

In summary, there are distinct chemical differences between olivine-bearing and quartz-bearing diabases. The olivine-bearing rocks are enriched in  $\text{Al}_2\text{O}_3$ ,  $\text{TiO}_2$ ,  $\text{Na}_2\text{O}$  and Sr and depleted in  $\text{SiO}_2$ , Rb, and Cu relative to quartz-bearing rocks. Other oxides have similar concentrations in the two groups. Olivine-bearing sills have higher K/Rb ratios and lower Rb/Sr and Ca/Sr ratios than do quartz-bearing varieties.

## DISCUSSION OF THE TRACE ELEMENT DATA

In recent years there has been an increased interest in the trace element content of basaltic rocks. This has resulted, in part, from improved analytical techniques which allow accurate determination of these elements. More importantly, it has been recognized that certain trace elements and elemental ratios may be more useful petrogenetic indicators than major elements alone. Copper, strontium, and rubidium concentrations in the Arizona diabases have been listed and diagrammed in various ways previously. The geochemistry of the three elements will now be discussed in more detail,

### Copper

The behavior of Cu during the crystallization of a basaltic magma is not well known. Its behavior is largely dependent upon whether or not a sulfide phase forms, which is in turn dependent on the sulfur content of the magma. Copper is partitioned into the sulfide phase when one forms (Wager, Vincent and Smales, 1957). In the absence of a sulfide phase, Cu is incorporated into the structures of the mafic minerals. Wager and Mitchell (1951) showed that Cu concentration increased in the Skaergaard liquid until

the magma was 90 per cent crystallized and then decreased rapidly. Correspondingly, they show that the Cu content increases in non-sulfide minerals with increased fractionation. The same general trend appears in the diagram of Cu versus  $\text{SiO}_2$  (Figure 22) for the Arizona diabases. In the large Lookout Mountain sill Cu generally increases with  $\text{SiO}_2$ , except in the pegmatitic zone where Cu decreases. This probably corresponds to the strong depletion of Cu in the late stage granophyric zone in the Skaergaard intrusion (Wager and Mitchell, 1951).

Prinz's (1967) compilation shows that tholeiites have significantly higher Cu values than do alkali basalts. This agrees well with the findings of the present study where the Lookout Mountain and Santa Catalina Mountains rocks (quartz tholeiites) contain much more Cu than the Salt River Canyon and Roosevelt Dam diabases (similar to alkali basalts). The Globe diabases generally have intermediate Cu contents, but are more similar to the quartz tholeiites.

The south central Arizona diabase province roughly corresponds to the Arizona copper province and diabase is abundant in the vicinity of several copper deposits. Krauskopf (1971) has suggested that the Arizona Copper Province may be an area of general copper enrichment. The present study does not bear this out with respect to the

diabase province. Comparison with the compilations of Prinz (1967) shows that the Cu values reported here are about average for these rock types.

### Strontium

Strontium abundance in basaltic rocks is highly variable, making it difficult to determine a meaningful average value. The data of Prinz (1967) show that many tholeiites contain between 0 and 400 ppm Sr while most alkali basalts contain between 200 and 1000 ppm. Alkali basalts in general contain much more Sr than tholeiites. The same trend is evident in the Arizona diabases but the values are somewhat lower. Most samples from the Salt River Canyon and Roosevelt Dam sills contain between 300 and 600 ppm Sr while the quartz-bearing diabases average about 175 ppm and show little variation.

Turekian and Kulp (1956) concluded that the dispersion in Sr values for most basaltic provinces is small. The Arizona diabase province apparently is an exception to this tendency since the olivine-bearing rocks are enriched by a factor of 2 relative to quartz-bearing varieties.

The behavior of Sr during the crystallization of basaltic magma is complicated since Sr is incorporated to differing degrees into several Ca-bearing minerals (feldspar, clinopyroxenes, apatite). Wager and Mitchell (1951) showed

that during the early stages of crystallization of the Skaergaard magma Sr increased in the liquid, reached a maximum concentration when the magma was about 60 per cent crystallized, and then decreased. Early formed plagioclases preferentially incorporated Ca in their structures causing an increase in Sr in the liquid until the middle stages of crystallization, after which more Sr was taken into crystallizing plagioclase. If this mechanism is operative there should be a decrease in the whole rock Ca/Sr ratio with fractionation. It was shown earlier (Figure 18) that the Lookout Mountain sills and the quartz-bearing sample from the Globe Complex show a very regular decrease in Ca/Sr with increasing K content. Since K normally increases with fractionation, the above mechanism explains the trend in Ca/Sr ratios very well. Samples from the Salt River Canyon sill also show a less regular, but obvious, decrease in Ca/Sr ratios with increasing K. The trend is not as clear in the Roosevelt Dam sill; however, the two samples with the highest K content also have the lowest Ca/Sr ratios.

#### Rubidium

Rubidium is chemically very similar to potassium, the major difference being the larger size of the rubidium atom. Because of the similarity and the fact that Rb forms

no minerals of its own, K and Rb would be expected to show a close covariance. This covariance has been shown to exist in rocks of all compositions (Shaw, 1968), however, some differences in the K/Rb ratio have been noted for different rock types. For these reasons it is useful to consider not only the absolute amounts of Rb but also the K/Rb ratio.

The compilation of Prinz (1967) shows that alkali basalts have higher average Rb contents than do tholeiites (51 and 30 ppm respectively). In the present study quartz tholeiites contain significantly more Rb than do the more alkali-like diabases. The potassium content of the olivine-bearing basalts is not greatly different from that of the quartz tholeiites. Hence, K/Rb ratios are lower in this latter group.

There has been much debate as to whether the K/Rb ratio decreases, increases, or remains constant with increasing K content (Shaw, 1968). All three cases have been reported, however, most studies of basaltic rocks show a general decrease in K/Rb with increasing K (Taubeneck, 1965). This would be expected from crystal chemical considerations since, while both elements are generally concentrated in the liquid phase during magmatic crystallization, Rb is more strongly concentrated because of its larger

atomic radius. A general decrease in the K/Rb ratio results as crystallization proceeds.

As was shown earlier (Figure 21), the two Lookout Mountain sills show a very regular decrease in K/Rb with increasing K contents. The Salt River Canyon complex shows a less regular but distinct decrease although the values of the ratios are greater. Potassium/rubidium ratios in the quartz-bearing rocks from the Globe Complex generally increase with increasing K, while the Roosevelt Dam sill shows little or no change. There are too few samples from the Santa Catalina Mountains sill to show a pattern. Therefore, all three types of behavior are present within the six sills studied. When all samples are considered together no obvious trend emerges.

Potassium and rubidium abundances have been determined in several other diabasic provinces and several provinces have rather low K/Rb ratios when compared with other basaltic rocks. Average K/Rb ratios for some provinces are: Antarctic, 240 (Gunn, 1965); Tasmanian, 208 (Heier, Compston and MacDougall, 1965); Wyoming Precambrian, 213 (Condie and others, 1969). All are similar to the values found in the Arizona quartz-bearing samples. Diabases with higher K/Rb ratios are the Karroo dolerites of South Africa with an average ratio of 453 (Erlank and Hofmeyer, 1966) and Triassic diabase from North Carolina

with an average ratio of approximately 500 (Ragland, Rogers and Justus, 1968). The North Carolina diabases have extremely low Rb (2.6 ppm average) and K (0.20 per cent average) contents.

Among other basaltic groups the oceanic tholeiites consistently have the highest K/Rb ratios. These range from slightly over 500 for the Hawaiian tholeiites (Lessing, Decker and Reynolds, 1963) to almost 1500 for some ridge crest tholeiites (Tatsumoto, Hedge and Engel, 1965). All of these rocks have extremely low K and Rb contents.

Figure 23 shows K/Rb versus K for some basaltic rocks from the Western United States. Precambrian tholeiitic diabases from Wyoming have K/Rb ratios similar to the Arizona quartz tholeiites; three of the 45 Wyoming samples have ratios between 400 and 500 and fall above the area shown in Figure 23. Younger extrusive basalts have K/Rb ratios distinctly higher than the Wyoming and Arizona Precambrian diabases. These rocks are all Cenozoic or younger and are from the northwestern United States, the Basin and Range (mostly Nevada), and Mount Taylor, New Mexico. These differences in K/Rb ratio may reflect changes in the composition of the upper mantle through geologic time or they may be due to other processes such as different depths of magma generation.

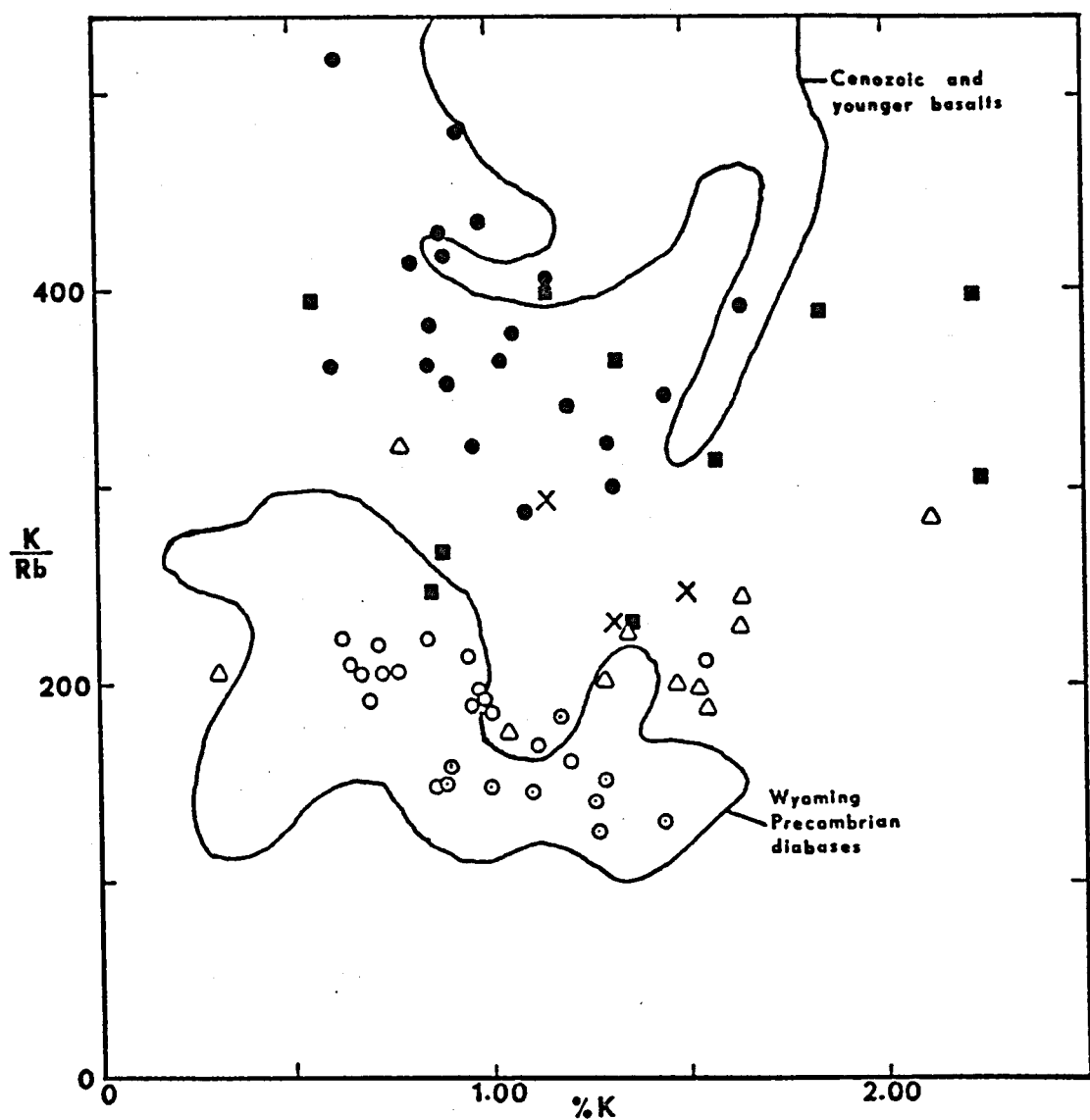


Figure 23. Comparison of K/Rb ratio in the Arizona diabases with those in some other basaltic rocks in the western United States.

Data from Condie, Barsky, and Mueller (1969), Baker and Ridley (1970), Hedge, Hildreth, and Henderson (1970), and Leeman (1970).

It was mentioned earlier that diabasic rocks from several areas have low K/Rb ratios. The same tendency is shown in the Western United States (Figure 23) in which diabasic rocks have lower ratios than extrusive basalts. This suggests that lower K/Rb ratios may be related to the intrusive origin of diabases. It was shown earlier that both K and Rb are depleted in alaskite in contact with the Lookout Mountain sill. The contact samples had higher K/Rb ratios than unaltered alaskite indicating that Rb is more mobile in the metasomatic environment. It seems unlikely that this type of interaction with country rock could drastically lower the K/Rb ratio in diabases except on a very local scale, but the possibility cannot be definitely ruled out.

Prinz (1967) stated that alkali basalts have lower Rb/Sr ratios than do tholeiites. However, a comparison of his average Rb and Sr values for the two types shows that the Rb/Sr ratios are very similar. Arizona quartz tholeiites have higher ratios than do alkali basalts (Figure 20). Most of the Salt River Canyon samples have ratios less than 0.1, and the Roosevelt Dam samples have ratios between 0.1 and 0.2. Almost all of the quartz diabases have Rb/Sr ratios greater than 0.2. In each group of diabase there is a regular increase in the Rb/Sr ratio with increasing fractionation (increasing Rb).

## DIFFERENTIATION TRENDS

No highly differentiated phases were found in any of the sills examined in this study. Smith (1969) described potassium-rich granophyres in the Sierra Ancha sill, but concluded that they resulted from interaction with country rocks. Pegmatitic material occurs as veins, pods, and irregular zones in the large Lookout Mountain sill and in the Salt River Canyon Complex. These are, by far, the two thickest sills examined and could be expected to have undergone more extreme fractionation than the smaller sills.

Standard A M F plots were presented earlier for the Salt River Canyon and Lookout Mountain rocks. All rocks are plotted on a similar diagram in Figure 24. The resulting trend is one of moderately strong iron enrichment. There is considerable overlap and olivine-bearing and quartz-bearing diabases show no distinct separation. Quartz-bearing diabases from the Globe Complex are the most highly differentiated rocks.

Figure 25 shows differentiation trends for Hawaiian tholeiites, alkali basalts, and the calc-alkaline trend. Arizona diabases fall between the two Hawaiian trends and are very different from the calc-alkaline trend.

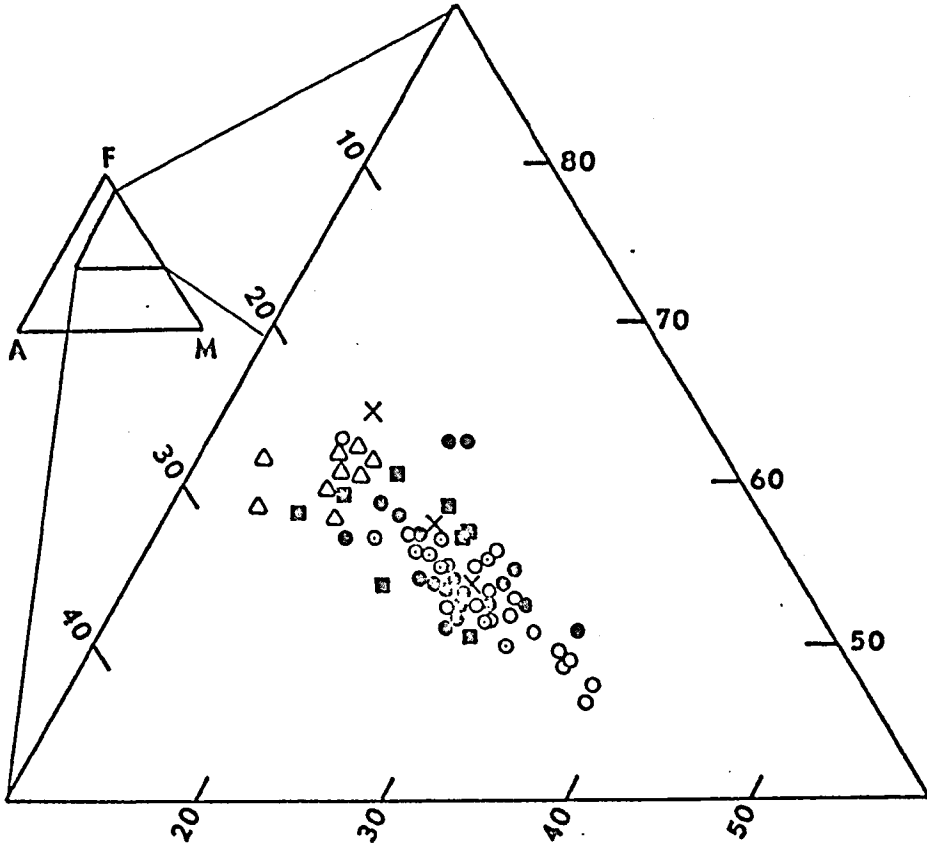


Figure 24, A M F diagram for the Arizona diabbases.

Solid symbols are samples from olivine-bearing sills; open symbols are samples from quartz-bearing sills. Symbols are same as in Figure 13.

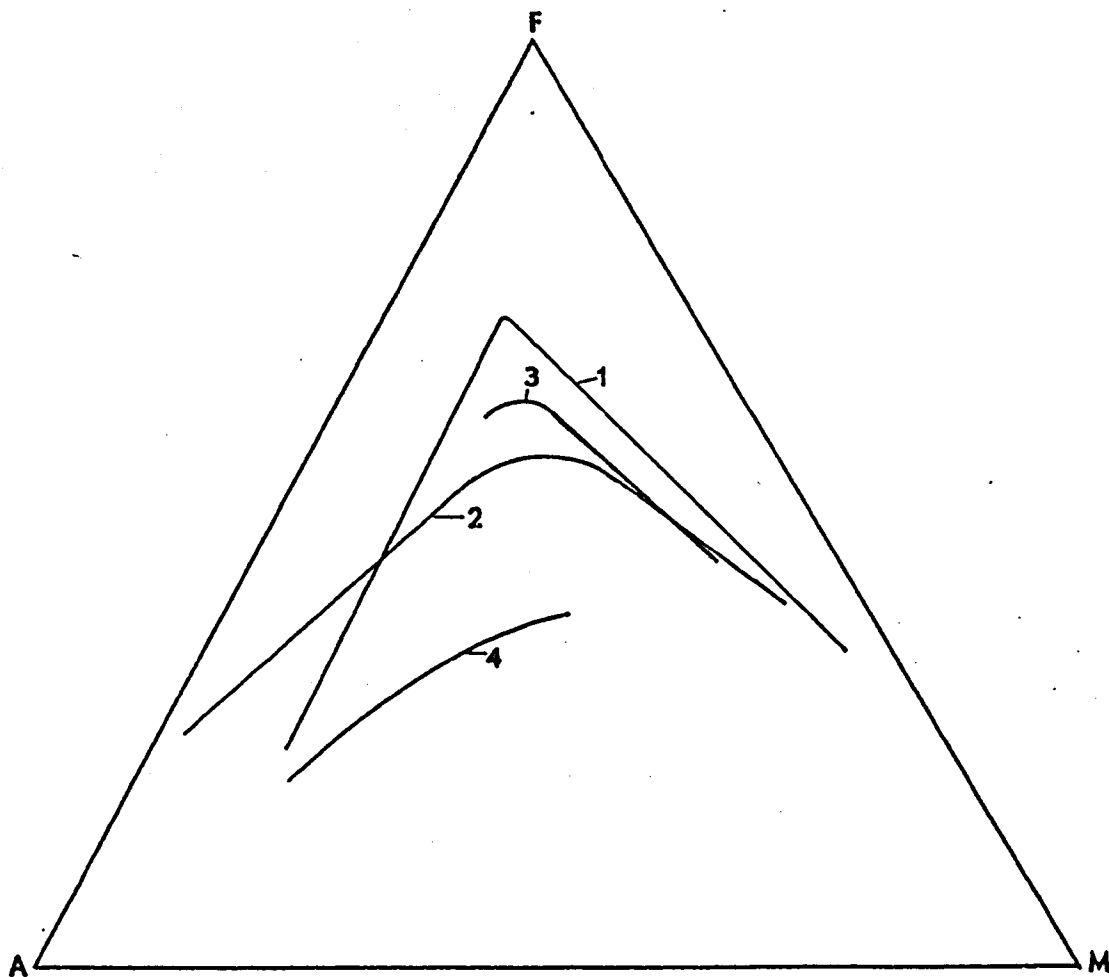


Figure 25. A M F diagram showing trends for some basaltic rocks.

- 1: Hawaiian tholeiites (MacDonald and Katsura, 1964).
- 2: Hawaiian alkali basalts (MacDonald and Katsura, 1964).
- 3: Arizona diabases. 4: Calc-alkaline trend (Yoder and Tilley, 1962).

Osborn (1959) proposed that oxygen fugacity plays a large part in determining whether an iron enrichment or silica enrichment trend develops. Diagrams of  $\text{FeO}+\text{Fe}_2\text{O}_3/\text{FeO}+\text{Fe}_2\text{O}_3+\text{MgO}$  versus  $\text{SiO}_2$  gave three distinct trends when mixtures were fractionally crystallized under the conditions of constant total composition (decreasing oxygen pressure), constant oxygen pressure, and increasing oxygen pressure. Figure 26 is a similar plot for the Arizona diabases. The two Lookout Mountain sills show a well developed trend similar to the constant total composition trend of Osborn. The quartz-bearing Globe diabases define a trend similar to Osborn's constant oxygen pressure trend. The upper and lower parts of the Roosevelt Dam sill form two separate trends, both similar to the constant composition trend. No well defined trend is present in the Salt River Canyon diabases.

Recent work has indicated that the open versus closed system crystallization proposed by Osborn may not be valid (Nordlie, personal communication). Therefore, the above conclusions are questionable. The Lookout Mountain sills, however, do show a well-defined trend somewhat different from the other sills which may indicate some differences in the conditions under which these bodies crystallized.

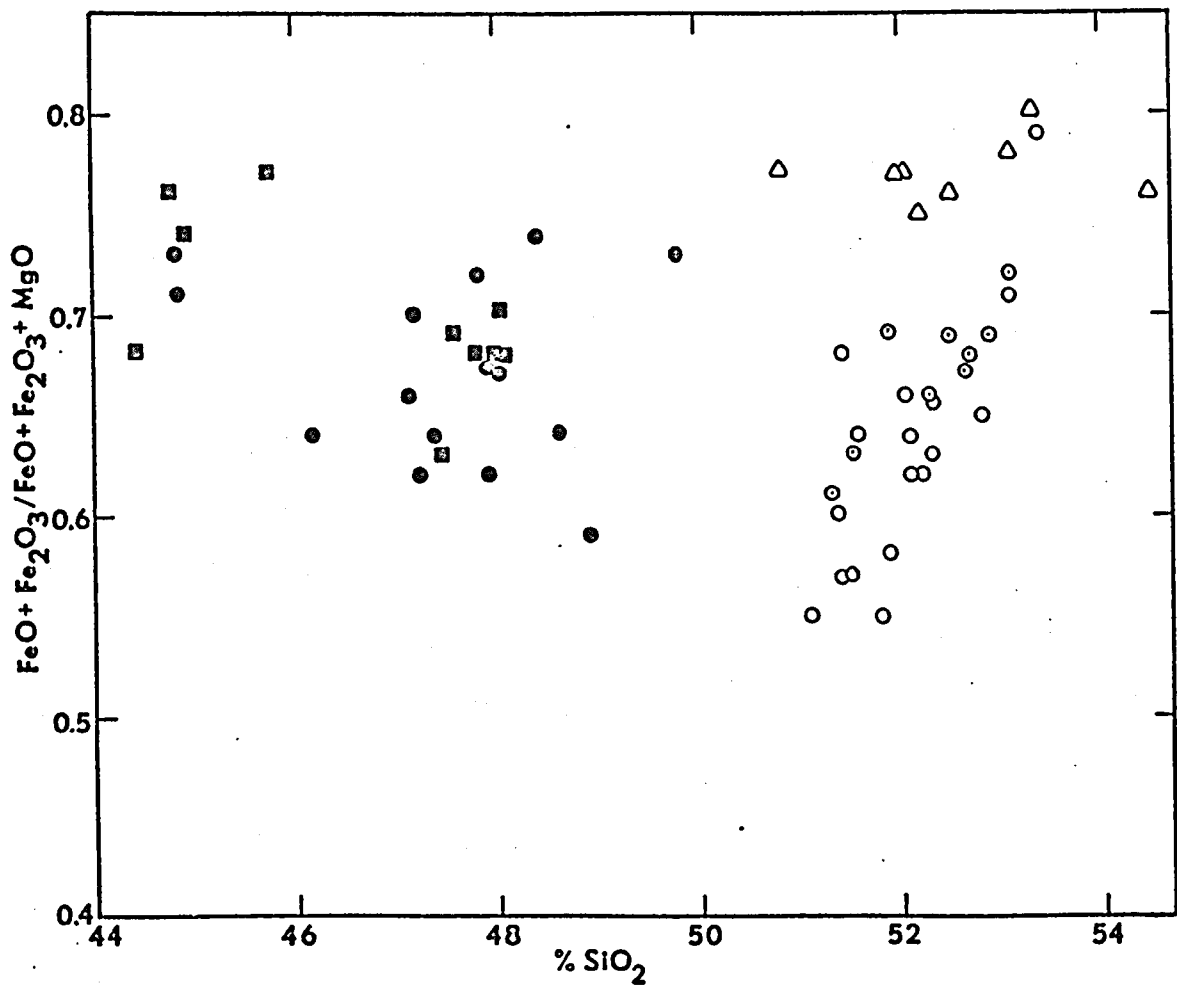


Figure 26. Diagram of SiO<sub>2</sub> versus the ratio FeO+Fe<sub>2</sub>O<sub>3</sub>/FeO+Fe<sub>2</sub>O<sub>3</sub>+MgO.

Symbols are same as in Figure 13.

## GENESIS OF THE DIABASE

It has been pointed out that the six sills described here can be divided into two rather distinct groups. One group contains modal quartz and is generally similar to typical continental quartz tholeiites. The other group is undersaturated with respect to silica and is more similar to alkali olivine basalts or high-alumina olivine tholeiites. Any model for the origin of the diabases must explain the existence of these two types of rocks.

The chemistries of the two groups are sufficiently different that they can not be related by a continuous differentiation trend from one type to the other. Future work in the province may prove the existence of intermediate types but at the present time none are known. The Sierra Ancha sill, the only other well studied occurrence, is chemically very similar to the Salt River Canyon and Roosevelt Dam sills (Smith, 1969; Nehru and Prinz, 1970).

Kuno (1967) has related different basalt types in Japan to different depths of magma generation along a subduction zone underneath the Japanese islands. A similar mechanism is possible for the Arizona diabases but there is no evidence that such an environment existed in the late

Precambrian. It is more reasonable to assume that the central Arizona diabases originated from one common parental magma that was subsequently modified to produce the two types of diabase observed.

Experimental work reported by Green and Ringwood (1967) provides a framework for basalt genesis which appears to explain the Arizona diabases. According to these investigators, fractionation of olivine tholeiite magma, at depths of approximately 30 km, leads to derivative liquids with relatively constant  $\text{SiO}_2$  contents (47 to 49 per cent), increasingly high  $\text{Al}_2\text{O}_3$  contents (15 to 17 per cent) with normative olivine and hypersthene (5 to 15 per cent olivine).

The  $\text{SiO}_2$  and  $\text{Al}_2\text{O}_3$  contents as well as the normative mineralogy of the Salt River Canyon and Roosevelt Dam diabases are very similar to this. Green and Ringwood (1967) showed that low pressure fractionation leads to convergence of the low-alumina and high-alumina tholeiites toward quartz tholeiite liquids with more than 50 per cent  $\text{SiO}_2$ , 12 to 14 per cent  $\text{Al}_2\text{O}_3$ , and showing some enrichment in iron and alkalis, i.e., rocks similar to the quartz bearing diabases of central Arizona. According to this model, the olivine-bearing diabases in the northern part of the province resulted from an olivine rich tholeiite parent magma that underwent fractionation at about 30 km and was then

emplaced. Some magma was not directly emplaced but, rather, moved to shallower depths, fractionated, reacted with the wall rocks, and gave rise to quartz tholeiite liquids which were emplaced to form the quartz-bearing diabases in the central and southern parts of the province.

Trace element data presented earlier is consistent with this proposed origin. Green and Ringwood (1967) have suggested that at higher pressures Sr behaves as an "incompatible element" and would be enriched in a liquid through a process of wall rock reaction. The olivine-bearing Arizona diabases are relatively rich in Sr, supporting the idea that they represent magma fractionated at higher pressures. At lower pressures Sr behaves as a compatible element because of the stability of plagioclase. The quartz-bearing Arizona diabases are low in Sr and are consistent with a history of low pressure fractionation as proposed. Green and Ringwood (1967) further suggested that titanium may behave in a similar manner. As discussed, the olivine-bearing Arizona diabases contain much more  $\text{TiO}_2$  than do the quartz-bearing diabases. Finally, Green and Ringwood proposed that rocks enriched in incompatible elements at low pressures should be characterized by rapid increases in the Rb/Sr ratio, while basalts enriched in incompatible elements at high pressures should show relatively small changes in the Rb/Sr ratio through

large variations in overall incompatible elements abundances. The quartz-bearing Arizona diabases have Rb/Sr ratios increasing from slightly less than 0.2 to 0.5 whereas the olivine-bearing rocks range from 0.01 to 0.2 (Figure 20).

The quartz-bearing Arizona diabases have chemistries generally similar to Mesozoic dolerites from Antarctica and Tasmania (Compston and others, 1968), especially with regard to their K, Rb, and Sr contents and their K/Rb ratios. These authors have suggested that the high K and Rb and low Sr contents and K/Rb ratios observed in those rocks resulted from contamination with crustal material while the magma was undergoing fractionation at shallow depths. A similar history is suggested for the Arizona quartz-bearing diabases.

## SUMMARY AND CONCLUSIONS

Both quartz- and olivine-bearing diabase are present in the central Arizona province. Olivine-bearing diabase occurs in the northern part of the province while quartz-bearing varieties are present in the central and southern parts. Future work may show that the two types are not restricted to these areas.

The olivine-bearing diabases have chemistries similar to alkali olivine basalts or olivine tholeiites while the quartz-bearing rocks are quartz tholeiites. The former are enriched in  $\text{Al}_2\text{O}_3$ ,  $\text{TiO}_2$ ,  $\text{Na}_2\text{O}$  and Sr relative to the latter. The quartz-bearing diabases have lower K/Rb ratios and higher Rb/Sr and Ca/Sr than do the olivine bearing varieties. Quartz-bearing diabase is chemically similar to Precambrian diabase from Wyoming and Mesozoic diabase from Antarctica and Tasmania. All of these rocks have lower K/Rb ratios than do most basalts. Cenozoic and younger basalts in the western United States have higher K/Rb ratios than the Arizona diabases.

The parental magma of the Arizona diabases was probably an olivine-rich tholeiite. The quartz-bearing varieties crystallized from magma that underwent lower

pressure fractionation and wall rock reaction. Superimposed on these processes is local differentiation which follows an iron-enrichment trend. Relationships between the  $\text{SiO}_2$  content and the ratio  $\text{FeO}+\text{Fe}_2\text{O}_3/\text{FeO}+\text{Fe}_2\text{O}_3+\text{MgO}$  indicates that the Lookout Mountain, Roosevelt Dam, and possibly the Salt River Canyon sills crystallized under conditions of decreasing oxygen pressure. The quartz-bearing Globe rocks may have crystallized with constant or increasing oxygen pressure.

The Salt River Canyon complex contains a small dike consisting of a typical spilitic mineral assemblage. Mineralogical and field evidence indicate that this formed from a late, low-temperature fluid phase.

The Arizona diabases crystallized from magmas having low viscosities. This probably accounts for the great lateral persistence of many of the sills and the absence of structural disruptions in the host rocks.

Visible contact metamorphic effects are generally absent; however, there are fairly consistent chemical differences between alaskite at one diabase contact and alaskite some distance from the contact. Alaskite at the contact is enriched in those elements more abundant in the diabase (Fe, Mg, Ca and possibly Ti) and depleted in elements less abundant in diabase (Si, K, Rb). Slight

increases in the  $K_2O$ , and Rb content of the diabase near the alaskite contact may result from contamination and suggests that chilled zones may not be reliable indicators of initial magma chemistry in some cases.

## APPENDIX I

### ANALYTICAL METHODS

#### Atomic Absorption Analyses

Major element and copper concentrations were determined using a lithium metaborate fusion technique similar to that described by Medlin, Suhr and Bodkin (1969) and a Perkins-Elmer Model 403 atomic absorption spectrophotometer. One tenth gram of the powdered rock is mixed with a half gram of reagent grade anhydrous  $\text{LiBO}_2$ . This mixture is placed in a clean pre-ignited graphite fusion crucible which is then inserted into a furnace at  $1000^\circ\text{C}$  for 15 minutes. The molten sample is then poured into a plastic beaker containing 40 ml of 3 per cent  $\text{HNO}_3$  and gently stirred with a magnetic stirring unit until solution is complete. Any beads remaining in the graphite crucible are removed after their solidification and added to the  $\text{HNO}_3$ . Solution is usually complete after about 5 minutes. If large beads remain in the graphite crucible more time is required for the solution.

Two ml of the above solution are diluted with 40 ml of distilled metal-free  $\text{H}_2\text{O}$  (1:20 dilution) for  $\text{Na}_2\text{O}$

and  $K_2O$  analyses. For the alaskites a 1:40 dilution was used. Five ml of the  $HNO_3$  solution was added to 30 ml of a 1 per cent lanthanum solution (1:6 dilution) for analyses for  $SiO_2$ ,  $Al_2O_3$ ,  $CaO$ ,  $MnO$ ,  $MgO$ , and total Fe.  $TiO_2$  and Cu were determined by analysing the undiluted  $HNO_3$  solution.

$SiO_2$ ,  $Al_2O_3$ , and  $TiO_2$  require the use of nitrous oxide while the other elements can be satisfactorily determined by using air as an oxidant. Acetylene is used as the fuel for all elements. Instrument settings are those recommended by the Manufacturer's handbook.

Few problems were encountered in the analyses of elements using the air-acetylene combination. A single slot 4 inch burner head was used for all analyses employing air as an oxidant.  $MgO$  in the concentration range encountered was more effectively determined with the burner head perpendicular to the beam. Some workers (Medlin and others, 1969) have suggested a similar arrangement for Fe analyses, however, no significant differences were observed with this arrangement so most of the Fe analyses were done with the burner head parallel to the beam.

Great care is required in the cleaning and handling of glassware used for sodium analyses. Serious contamination can result from touching a rubber stopper or any other equipment. Extreme Ca contamination was found in new

glassware that had been carefully rinsed with metal-free water; thus, all new glassware required special cleaning. The most effective cleaning solution was found to be a mixture of  $K_2Cr_2O_7$  and concentrated  $H_2SO_4$ . This solution can be prepared or the commercial product, "Chromerge," can be added to concentrated  $H_2SO_4$ . Cleaning can also be accomplished by submerging the glassware in hot concentrated  $HNO_3$ , however, this process is somewhat slower. Pipettes must be kept very clean to assure consistent delivery as well as to avoid contamination.

Determination of  $SiO_2$ ,  $Al_2O_3$ , and  $TiO_2$  presented more problems. The major problem was instrument drift. Use of the  $NO_2$ -acetylene combination results in a slow buildup of deposits along the lips of the burner head and causes a decrease in absorbance units when the deposit becomes large. This, however, caused no great problems because the formation of the deposit can be easily observed and the burner head can be cleaned before the deposit becomes large. Normally, cleaning was required after about 30 minutes.

$SiO_2$  analyses presented the most problems. Under the most ideal conditions, the absorbance units-concentration ratio is fairly low so that any drift or fluctuations can cause serious errors. Therefore, great care is necessary to insure that the maximum number of absorbance units and

the greatest stability are obtained. This requires very careful burner alignment, optimum fuel:oxidant mixture, and aspiration rate. A standard was run after every two or three samples to monitor any instrument drift that might have occurred.

Standards used for the major element analyses of the diabase were: diabase (W-1), peridotite (PCC-1), andesite (AGV-1) and two basalts (BCR-1 and BR). BR was obtained from the Centre de Recherches Petrographiques et Geochimiques, Nancy, France; the other standards were prepared by the United States Geological Survey. The choice of the best values for each standard is of fundamental importance. It is somewhat disturbing to see the fairly large range of values obtained by different analysts. The most recent compilation of values available when this work was begun was that of Abbey (1970) and his preferred values were used for PCC-1, BCR-1, and AGV-1. Fleischer's (1969) preferred values were used for W-1. Flanagan's (1973) compilation of preferred values for all international standards was published after much of the work was completed. However, Flanagan's values agreed very well with those of Abbey in most cases so it was felt that nothing would be gained by reinterpreting the previous analyses in light of the new data. The most significant difference noted in the 1973 compilation was that of  $\text{Al}_2\text{O}_3$

in W-1. Fleischer (1969) proposed a value of 14.85 per cent while Flanagan (1973) proposed 15.00 per cent. The later value agrees more closely with values obtained during this investigation. The values used for the basalt BR were those proposed by Roubault, LaRoche and Govindaraju (1970).

For the alaskite analyses the following standards were used: United States Geological Survey analysed andesite (AGV-1), granodiorite (GSP-1), granite (G-2), and the French granites GA and GH. Values used for these rocks are from Abbey (1970). Precision and accuracy of the analyses are given in Table 29.

#### Ferrous Iron Analyses

Ferrous iron concentrations were determined by wet chemical techniques involving titration with a  $K_2MnO_4$  solution. Approximately 0.15 grams of the powdered sample is accurately weighed and placed in a Teflon crucible. A small amount of reagent grade  $CaCO_3$  is also placed in the crucible. An acid solution is prepared by mixing 5 ml  $H_2O$ , 5 ml HF, and 5 ml  $H_2SO_4$  in that order in a plastic beaker. This is then poured into the crucible containing the sample and  $CaCO_3$ . The solution is quickly brought to boil on a hot plate and boiled for 10 minutes. The crucible should be kept tightly covered while boiling as  $CO_2$  being evolved precludes oxidation of the ferrous iron. While the acid mix is boiling, a second solution consisting of 10 ml

Table 29. Compilation of replicate analyses of BCR-1.

	Number	Standard Deviation	Mean	Preferred	
SiO <sub>2</sub>	14	.315	54.44	54.36 <sup>1</sup>	54.50 <sup>2</sup>
TiO <sub>2</sub>	12	.043	2.18	2.24	2.20
Al <sub>2</sub> O <sub>3</sub>	15	.155	13.47	13.56	13.61
Fe <sub>2</sub> O <sub>3</sub> -T	15	.133	13.38	13.40	13.40
MnO	4	.008	0.18	0.19	0.18
MgO	13	.037	3.51	3.46	3.46
CaO	14	.197	6.98	6.94	6.92
Na <sub>2</sub> O	14	.051	3.28	3.26	3.27
K <sub>2</sub> O	13	.030	1.69	1.67	1.70

1. Abbey, 1970.

2. Flanagan, 1973.

of 1:1  $\text{H}_2\text{O}:\text{H}_2\text{SO}_4$ , 50 ml of 5 per cent  $\text{H}_3\text{BO}_3$  and enough  $\text{H}_2\text{O}$  to give a total volume of about 200 ml is prepared in a glass beaker. After boiling for 10 minutes the Teflon crucible and its contents are quickly immersed in this solution and titrated with the  $\text{KMnO}_4$  solution. The first pink color which persists beyond 15 seconds marks the end point of the titration. A blank is titrated with each group. The ferrous iron content of the sample is then calculated by using the following relationship:

$$\% \text{FeO} = \frac{(N_{\text{KMnO}_4}) (V_{\text{KMnO}_4}) (7.185)}{(\text{Wt. rock in grams})}$$

where  $N_{\text{KMnO}_4}$  is the normality and  $V_{\text{KMnO}_4}$  is the volume in mls.

The normality of the  $\text{KMnO}_4$  solutions used varied from 0.027 to 0.043. More dilute solutions are useful for rocks containing small amounts of FeO as the volume required is increased and the relative errors involved in reading the meniscus and recognizing the end point of the titration are decreased. Rocks containing higher concentrations of FeO can be satisfactorily titrated with a more concentrated  $\text{KMnO}_4$  solution thus conserving the solution. However, more concentrated solutions take on a very dark color which increases the difficulty of reading the meniscus accurately.

The preparation and handling of the  $\text{KMnO}_4$  solutions is important if good results are to be attained. A solution with a normality of about 0.0273 results from dissolving 1.6 gms  $\text{KMnO}_4$  and diluting to 2 liters. After the solution is prepared it is brought to a boil and kept hot for one hour, covered, and cooled overnight. The solution is then force filtered through a clean sintered glass crucible and stored in a bottle covered with aluminum foil as extended exposure to light will cause the normality to decrease more rapidly than usual.

The normality of the  $\text{KMnO}_4$  solutions is determined by titrating a sodium oxylate solution prepared by dissolving about 0.04 gm of sodium oxylate which had been dried for at least one hour at a temperature of about  $105^\circ\text{C}$  and then cooled in a dessicator before weighing in 30 ml of 6N  $\text{H}_2\text{SO}_4$  and diluting with  $\text{H}_2\text{O}$  to give approximately 200 ml of solution. This is then heated to a temperature between  $60^\circ\text{C}$  and  $90^\circ\text{C}$  and quickly titrated. The normality of the  $\text{KMnO}_4$  solution is calculated using the following expression:

$$N_{\text{KMnO}_4} = \frac{\text{Wt. in grams sodium oxylate}}{(V_{\text{KMnO}_4}) (0.067)}$$

where  $V_{\text{KMnO}_4}$  is the volume in mls.

The normality of new  $\text{KMnO}_4$  solutions was established by performing 3 or 4 titrations. The normality decreases slightly with time and should be checked periodically. Precision and accuracy of the iron analyses are given in Table 30.

#### X-Ray Fluorescence Analyses

Rubidium and strontium concentrations were determined by x-ray fluorescence spectrometry using a method similar to that described by Livingston (1969, p. 58). The powdered rocks were pressed into discs approximately 4 mm in thickness. Boric acid was used to form a back and rim around the discs.

Analyses were done using a Siemens unit, molybdenum x-ray tube,  $\text{LiF}_{220}$  crystal, and a scintillation counter. The x-ray tube was operated at 55 kilovolts and 46 milliamperes and the scintillation counter was operated at 1050 volts. Measurements were made of the molybdenum Compton-scattered, Rb  $K_\alpha$ , Sr  $K_\alpha$  peaks, and one background intensity. Each measurement consisted of two one-minute counting intervals. Computer programs prepared by Dr. D. E. Livingston were used for data reduction.

The U. S. Geological Survey analysed rocks listed earlier in this appendix were used as standards. Repeated analyses of these rocks indicate errors of  $\pm 0.7$  per cent

Table 30. Compilation of replicate analyses of W-1.

Number of Analyses	Standard Deviation	Mean Value	Preferred <sup>1</sup>
6	.071	8.70	8.72

1. Flanagan, 1973.

for Sr in the 200-400 ppm range and  $\pm 4.0$  per cent for Rb in the 20 ppm range (Livingston, personal communication).

## REFERENCES

- Abbey, S., 1970, U. S. Geological Survey Standards. A critical study of published analytical data: *Can. Spectrosc.*, 15, p. 10-16.
- Amstutz, G. C., 1967, Spilites and spilitic rocks, in A. Poldervaart, ed., *Basalts*, 2: New York, John Wiley and Sons, Inc., p. 737-753.
- Baker, I., and W. I. Ridley, 1970, Field evidence and K, Rb, Sr data bearing on the origin of the Mount Taylor volcanic field, New Mexico, USA: *Earth and Planetary Sci. Letters*, 10, p. 106-114.
- Balla, J. C., 1972, The relationship of Laramide stocks to regional structure in central Arizona: Unpublished Ph. D. Dissertation, University of Arizona, 132 p.
- Banks, N. G., H. R. Cornwall, and R. F. Marvin, 1972, Chronology of intrusion and ore deposition at Ray, Arizona: Part I, K-Ar ages: *Econ. Geol.*, 67, p. 864-878.
- Barth, T. F. W., 1962, *Theoretical Petrology*: New York, John Wiley and Sons, Inc., 416 p.
- Barth, T. F. W., 1969, *Feldspars*: New York, Wiley-Interscience, 261 p.
- Bhattacharji, S., 1967, Scale model experiments on flowage differentiation in sills, in P. J. Wyllie, ed., *Ultramafic and Related Rocks*: New York, John Wiley and Sons, Inc., p. 69-70.
- Bottinga, Y., and D. F. Weill, 1970, Densities of liquid silicate systems calculated from partial molar volumes of oxide components: *Amer. Jour. Sci.*, 269, p. 169-182.

- Compston, W., I. MacDougall, and K. S. Heier, 1968, Geochemical comparison of Mesozoic basaltic rocks of Antarctica, South Africa, South America, and Tasmania: *Geochim. et Cosmochim. Acta*, 32, p. 129-149.
- Condie, K. C., C. K. Barsky, and P. A. Mueller, 1969, Geochemistry of Precambrian diabase dikes from Wyoming: *Geochim. et Cosmochim. Acta*, 33, p. 1371-1388.
- Creasey, S. C., 1965, Geology of the San Manuel area Pinal County, Arizona: U. S. Geol. Survey Prof. Paper 471, 64 p.
- Creasey, S. C., 1967, General geology of the Mammoth Quadrangle Pinal County, Arizona: U. S. Geol. Survey Bull. 1218, 95 p.
- Crowder, D. F., and D. C. Ross, 1973, Petrography of some granitic bodies in the northern white Mountains, California-Nevada: U. S. Geol. Survey Prof. Paper 775, 28 p.
- Damon, P. E., D. E. Livingston, and R. C. Erickson, 1962, New K-Ar dates for the Precambrian of Pinal, Gila, Yavapai, and Coconino Counties, Arizona: 13th Field Conference, Mogollon Rim Region. New Mexico Geol. Soc. Guidebook Ann. Field Conference.
- Darton, N. H., 1925, A resume of Arizona geology: Arizona Bur. Mines Bull. 119, 298 p.
- Ellis, A. J., and W. A. J. Mahon, 1967, Natural hydrothermal systems and experimental hot water/rock interactions, Part II: *Geochim. et Cosmochim. Acta*, 31, p. 519-538.
- Erlank, A. J., and P. K. Hofmeyer, 1966, K/Rb and K/Cs ratios in Karroo dolerites from South Africa: *Jour. Geophys. Res.*, 71, p. 5439-5445.
- Flanagan, F. J., 1973, 1972 values for international geochemical reference samples: *Geochim. et Cosmochim. Acta*, 37, p. 1189-1200.
- Fleischer, M., 1969, U. S. Geological Survey Standards-I. Additional data on rocks G-1 and W-1, 1965-1967: *Geochim. et Cosmochim. Acta*, 33, p. 65-79.

- Gilluly, J., 1935, Keratophyres of eastern Oregon and the spilite problem: *Amer. Jour. Sci.*, 29, p. 225-252.
- Granger, H. C., and R. B. Raup, 1969, Geology of uranium deposits in the Dripping Springs Quartzite, Gila County, Arizona: U. S. Geol. Survey Prof. Paper 595, 108 p.
- Green, D. H., and A. E. Ringwood, 1967, The genesis of basaltic magmas: *Contr. Mineral. and Petrol.*, 15, p. 103-190.
- Gunn, B. M., 1965, K/Rb and K/Ba ratios in Antarctic and New Zealand tholeiites and alkali basalts: *Jour. Geophys. Res.*, 70, p. 6241-6247.
- Hamilton, W., 1965, Diabase sheets of the Taylor Glacier Region Victoria Land, Antarctica: U. S. Geol. Survey Prof. Paper 456-B, 71 p.
- Hedge, C. E., R. A. Hildreth, and W. T. Henderson, 1970, Strontium isotopes in some Cenozoic lavas from Oregon and Washington: *Earth and Planetary Science Letters*, 8, p. 434-438.
- Heier, K. S., W. Compston, and I. MacDougall, 1965, Thorium and uranium concentrations and the isotopic composition of strontium in the differentiated Tasmanian dolerites: *Geochim. et Cosmochim. Acta*, 29, p. 643-659.
- Kennedy, W. Q., 1933, Trends of differentiation in basaltic magmas: *Amer. Jour. Sci.*, 25, p. 239-256.
- Krauskopf, K. B., 1971, The source of ore metals: *Geochim. et Cosmochim. Acta*, 35, p. 643-659.
- Krieger, M. H., 1968, Geologic map of the Lookout Mountain Quadrangle, Pinal County, Arizona: U. S. Geol. Survey Geologic Quadrangle Maps of the United States, GQ-670.
- Kuno, H., 1960, High-alumina basalts: *Jour. Petrol.*, 1, p. 121-145.
- Kuno, H., 1967, Differentiation of basalt magma, in A. Poldervaart, ed., *Basalts*, 2: New York, John Wiley and Sons, Inc., p. 623-688.

- Leeman, W. P., 1970, The isotopic composition of strontium in Late-Cenozoic basalts from the Basin-Range province, western United States: *Geochim. et Cosmochim. Acta*, 34, p. 857-872.
- Lessing, P., R. W. Decker, and R. C. Reynolds, 1963, Potassium and rubidium distribution in Hawaiian lavas: *Jour. Geophys. Res.*, 68, p. 5851-5855.
- Livingston, D. E., 1969, Geochronology of Older Precambrian rocks in Gila County, Arizona: Unpublished Ph. D. Dissertation, University of Arizona, 224 p.
- MacDonald, G. A., and T. Katsura, 1964, Chemical composition of Hawaiian lavas: *Jour. Petrol.*, 5, p. 82-133.
- Manson, V., 1967, Geochemistry of basaltic rocks: major elements, in A. Poldervaart, ed., *Basalts*, 2: New York, John Wiley and Sons, Inc., p. 215-269.
- Medlin, J. H., N. H. Suhr, and J. B. Bodkin, 1969, Atomic absorption analysis of silicates employing  $\text{LiBO}_2$  fusion: *Atomic Abs. Newsletter*, 8, p. 25-29.
- Moore, J. G., 1970, Water content of basalt erupted on the ocean floor: *Contr. Mineral. and Petrol.*, 28, p. 272-279.
- Nehru, C. E., and M. Prinz, 1970, Petrologic study of the Sierra Ancha sill complex, Arizona: *Geol. Soc. Amer. Bull.*, 81, p. 1733-1766.
- Neuerburg, G. J., and H. C. Granger, 1960, A geochemical test of diabase as an ore source for the uranium deposits of the Dripping Springs district, Arizona: *Neues Jahrb. Mineralogie Abh.*, 94, p. 759-797.
- Osborn, E. F., 1959, Role of oxygen pressure in the crystallization and differentiation of basaltic magma: *Amer. Jour. Sci.*, 257, p. 609-647.
- Peterson, N. P., C. M. Gilbert, and G. L. Quick, 1951, Geology and ore deposits of the Castle Dome area, Gila County, Arizona: *U. S. Geol. Survey Bull.* 971, 134 p.
- Piwinskii, A. J., and P. J. Wyllie, 1968, Experimental studies of igneous rock series: A zoned pluton in the Wallowa batholith, Oregon: *Jour. Geol.*, 76, p. 205-234.

- Prinz, M., 1967, Geochemistry of basaltic rocks: trace elements, in A. Poldervaart, ed., Basalts, 2: New York, John Wiley and Sons, Inc., p. 271-323.
- Ragland, P. C., J. J. W. Rogers, and P. S. Justus, 1968, Origin and differentiation of Triassic dolerite magmas, North Carolina, USA: *Contr. Mineral. and Petrol.*, 20, p. 57-80.
- Ransome, F. L., 1903, Geology of the Globe copper district, Arizona: U. S. Geol. Survey Prof. Paper 12, 168 p.
- Ransome, F. L., 1919, The copper deposits of Ray and Miami, Arizona: U. S. Geol. Survey Prof. Paper 115, 192 p.
- Roubault, M., H. LaRoche, and K. Govindaraju, 1970, Etat actuel (1970) des etudes cooperatives sur les standards geochemiques du Centre de Recherches Petrographiques et Geochemiques: *Sci. de la Terre*, 15, p. 351-393.
- Schmidt, E. A., 1971, A structural investigation of the northern Tortilla Mountains, Pinal County, Arizona: unpublished Ph. D. Dissertation, University of Arizona, 248 p.
- Sharp, B. J., 1956, Preliminary report on a uranium occurrence and regional geology in the Cherry Creek area, Gila County, Arizona: U. S. Atomic Energy Comm. RME-2036, 16 p.
- Shaw, D. M., 1968, A review of K-Rb fractionation trends by covariance analysis: *Geochim. et Cosmochim. Acta*, 32, p. 573-601.
- Shaw, H. R., 1972, Viscosities of magmatic silicate liquids: an empirical method of prediction: *Amer. Jour. Sci.*, 272, p. 870-893.
- Shride, A. F., 1967, Younger Precambrian geology in southern Arizona: U. S. Geol. Survey Prof. Paper 566, 89 p.
- Silver, L. T., 1960, Age determinations on Precambrian diabase differentiates in Sierra Ancha, Gila County, Arizona (abs): *Geol. Soc. Amer. Bull.*, 71, p. 1973-1974.

- Simkin, T., 1967, Flow differentiation in the picrite sills of North Skye, in P. J. Wyllie, ed., Ultramafic and Related Rocks: New York, John Wiley and Sons, Inc., p. 64-69.
- Smith, D., 1969, Mineralogy and petrology of an olivine diabase sill complex and associated unusually potassic granophyres, Sierra Ancha, Central Arizona: Ph. D. Dissertation, California Institute of Technology, 314 p.
- Smith, D., 1970, Mineralogy and petrology of the diabase rocks in a differentiated olivine diabase sill complex, Sierra Ancha, Arizona: *Contr. Miner. and Petrol.*, 27, p. 95-113.
- Tatsumoto, M., C. E. Hedge, and A. E. J. Engel, 1965, Potassium, rubidium, strontium, thorium, uranium, and the ratio of Sr-87 to Sr-86 in oceanic tholeiitic basalts: *Sci.*, 150, p. 886-888.
- Taubeneck, W. H., 1965, An appraisal of some potassium-rubidium ratios in igneous rocks: *Jour. Geophys. Res.*, 70, p. 475-478.
- Taylor, H. P., and S. Epstein, 1968, Hydrogen isotope evidence for influx of meteoric ground water into shallow igneous intrusions: *Geol. Soc. Amer. Spec. Paper* 121, p. 294.
- Taylor, H. P., and R. W. Forester, 1971, Low  $O^{18}$  igneous rocks from the intrusive complexes of Skye, Mull, and Ardnamurchan, western Scotland: *Jour. Petrol.*, 12, p. 465-497.
- Turekian, K. K., and J. L. Kulp, 1956, The geochemistry of strontium: *Geochim. et Cosmochim. Acta*, 10, p. 245-296.
- Turner, F. J., and J. Verhoogen, 1960, Igneous and Metamorphic Petrology: New York, McGraw-Hill, 694 p.
- Wager, L. R., and R. L. Mitchell, 1951, The distribution of trace elements during strong fractionation of basic magma--a further study of the Skaergaard intrusion, East Greenland: *Geochim. et Cosmochim. Acta*, 1, p. 129-208.

- Wager, L. R., E. A. Vincent, and A. A. Smales, 1957, Sulfides in the Skaergaard intrusion, East Greenland: *Econ. Geol.*, 52, p. 855-903.
- Williams, F. J., 1957, Structural control of uranium deposits, Sierra Ancha region, Gila County, Arizona: U. S. Atomic Energy Comm. Report RME-3152, 117 p.
- Yoder, H. S., and C. E. Tilley, 1962, Origin of basalt magmas: an experimental study of natural and synthetic rock systems: *Jour. Petrol.*, 3, p. 342-532.

... ..  
... ..  
... ..

... ..  
... ..  
... ..

... ..  
... ..  
... ..